12-2018

Influence of Loss of Function of the Fatty Acid Desaturase 7 Gene on Photosynthetic Activity and Foliar Redox Status

Janithri Savindya Wickramanayake
University of Arkansas, Fayetteville

Influence of Loss of Function of the *Fatty Acid Desaturase 7* Gene on Photosynthetic Activity and Foliar Redox Status

A dissertation submitted in partial fulfillment
of the requirements for the degree of
Doctor of Philosophy in Entomology

by

Janithri Wickramanayake
University of New England
Bachelor of Science in Biological Sciences, 2014

December 2018
University of Arkansas

This dissertation is approved for recommendation to the Graduate Council.

_____
Fiona L. Goggin, Ph.D.
Dissertation Director

_____
Robert Wiedenmann, Ph.D.
Committee Member

_____
Donn Johnson, Ph.D.
Committee Member

_____
Vibha Srivastava, Ph.D.
Committee Member

_____
Kenneth Korth, Ph.D.
Committee Member

Abstract

Fatty Acid Desaturase7 (FAD7) is a chloroplast-localized enzyme that converts 16 and 18 carbon dienoic fatty acids to trienoic fatty acids. The *suppressor of prosystemin-mediated response2* (*spr2*) mutant in tomato (*Solanum lycopersicum*) and the *fad7-1* mutant in Arabidopsis (*Arabidopsis thaliana*) result in the loss of function of FAD7, which alter the fatty acid profiles of chloroplast membranes and enhance resistance against aphids. This research contributes toward the long-term goal of identifying factors that determine aphid resistance in FAD7 mutants. Previous data suggested constitutive differences between *spr2* and WT including increased expression of genes associated with photosynthesis and differences in redox status in chloroplasts suggested by lipid profiles. The objective of this study was to validate these previous data. This study reports that the *spr2* mutant enhances photosynthetic efficiency constitutively compared to wild-type (WT) plants. While no constitutive differences in intermediates and products of photosynthesis were detected, the *spr2* mutants showed increased growth, suggesting increased photosynthesis may be translated in to growth. Moreover, glutamate levels were constitutively higher in *spr2* compared to WT and could be important in defense signaling for aphid resistance. Also, the *spr2* mutants were able to maintain the enhanced photosynthesis under potato aphid (*Macrosiphum lycopersicum*) pressure. One-day after aphid infestation, aphids triggered a short-term increase in the energy directed towards photosynthesis. The enhanced photosynthesis could also be channeling energy towards defense compound production for the resistance mechanism or could be the plant adapting to adverse environmental stress, indicative of tolerance. Furthermore, to study the redox status in chloroplasts, Arabidopsis *fad7-1* lines containing *roGFP2* transgene were developed as a useful tool. Preliminary results indicated the *fad7-1* mutant is as or more reduced than WT (Col-0), but further studies are

needed to confirm this. The redox status depends on the relative balance between reactive oxygen species (ROS) and antioxidants. The plants could potentially have more ROS due to enhanced photosynthesis, but they could also have more antioxidants. Further work is necessary to detect individual ROS species. This study aids in identifying potential links between primary metabolism and plant defenses against insects.

Acknowledgements

First, I would like to express my sincere gratitude to my dissertation advisor, Dr. Fiona Goggin, who paved my way for a successful completion of my research and dissertation. Without her guidance, academic and financial support, completion of my Ph.D. studies and the dissertation at University of Arkansas would not have been possible. Appreciation is also due to my committee members, Dr. Robert Wiedenmann, Dr. Donn Johnson, Dr. Ken Korth and Dr. Vibha Srivastava for their guidance, which helped me to improve my research focus and critical thinking skills. I also appreciate the help I received from Dr. Jung Ae Lee in completion of the statistical analyses related to my dissertation work, and Jessica Kivett for her help with the maintenance of the greenhouse and growth chambers. In addition, I would like to thank my wonderful lab members Dr. Aravind Galla, Dr. Jiamei Li, Dr. Junhuan Xu, Dr. Min Woo Lee, Hillary Fischer, Dhaval Shah, Mali Sirisena and Abeer Muhammedali Jasim Al-Nasrawi for their help in completing my research. Also, I would like to acknowledge the academic and financial support I received from the Department of Entomology and the Division of Agriculture during the past four years.

Special thanks go to Dr. Ursula Roese for providing me the research experience in her lab and for recognizing my potential to continue my education beyond my undergraduate studies at University of New England. Also, I would like to thank my friends Hillary, Rose, Tara, Zach, Liese and Kyle for standing by me through the good times and bad. I am grateful to fellow graduate students and faculty of the Department of Entomology for the camaraderie and providing me a supportive learning environment. I should also mention my fiancé, Dinuka Gunasekara and my aunt, Darshana Udayanganie for all of their support, humor and words of encouragement that helped me to get through the past years.

Finally, I would like to thank my family. My father and brother lived thousands of miles away from me in the past eight years, but they did not stop believing in me and supported me in every possible way. Special acknowledgement goes to my late mother. Her courage in accomplishing her life goals inspired me throughout my life and her words of encouragement still echoes in my mind.

Dedication

This dissertation is dedicated to my aunt, Dr. Darshana Udayanganie, for her unconditional love and endless support.

Table of Contents

Chapter I: Introduction **1**

Importance of aphids as crop pests 1

Importance of understanding plant aphid interactions 3

Aphids and photosynthesis 6

Aphids and ROS 13

Fatty acid desaturases and plant resistance to stress 16

Research questions 20

References **24**

Chapter II: Enhanced photosynthetic efficiency in tomato with loss of function of FATTY ACID DESATURASE 7 ..... **34**

Abstract 34

Introduction 35

Materials and Methods 37

Results 41

Discussion 43

References **50**

Chapter III: Effects of *suppressor of prosystemin-mediated response2* on primary metabolism and photosynthetic responses to aphids **53**

Abstract 53

Introduction 54

Materials and methods 56

Results 60

Discussion 63

References **74**

Chapter IV: Development of transgenic lines containing *roGFP2* reporter gene to study the overall redox status of Arabidopsis plants with impaired *FAD7-1* function..... 77
Abstract 77
Introduction 78
Methods and materials 81
Results 86
Discussion 90
References 101

Chapter V: Conclusion 104
References 107

Chapter I

Introduction

Studies of plant interactions with insects have tended to focus on secondary metabolism because of the importance of specialized metabolites in defense. However, an emerging body of evidence shows that insects can affect primary metabolism and these effects can mediate damages that insects inflict. Furthermore, it is important because primary metabolism can influence levels of susceptibility or resistance. An interesting question in biology right now is to what extent the aspects of primary metabolism influences biotic interactions. We are using fatty acid metabolism and its influence on aphids as a system to explore this interaction of primary metabolism and defense.

Importance of aphids as crop pests

Impact of aphids on crops

Aphids (Hemiptera: Aphididae) are a group of phloem-feeding insects that attack most major crops. Nearly 450 aphid species have been recorded from crops and about 100 species are considered as economically important agricultural pests (Morrison and Peairs, 1998). Aphids cause substantial yield losses in different crops. It was reported that the introduction of Russian wheat aphid (*Diuraphis noxia*) in North America has caused US$893 million loss in cereal crops between 1987 and 1993 (Morrison and Peairs, 1998). A field study conducted in South Dakota showed that one soybean aphid (*Aphis glycines*) introduced at vegetative growth stage V5 increased to 4627 aphids per plant and has reduced the yield by 38% (1400 kg/ha) (Beckendorf et al., 2008), and Song et al. (2006) predicted that if left untreated, economic loss due to soybean

aphid damage could be over $2.4 billion, annually. Such substantial economic damage on agricultural crops confirms the importance of developing effective control of aphid infestations.

Aphids are phloem feeders that remove photoassimilates by tapping their stylets into the sieve-elements of the phloem and creating artificial sinks in plants (Louis et al., 2012). Aphid feeding can induce a variety of effects, directly (by probing and extracting phloem sap) and indirectly (by pathogen transmission), on their host plants. Their direct effects can include chlorosis, necrosis, impact on photosynthesis, wilting, stunted growth and decreases in growth rate, which ultimately lead to reduction in crop yields (Goggin, 2007; Beckendorf et al., 2008). However, these effects vary depending upon the aphid species and host plants as well as the magnitude of the infestation and the growth stage of the plant. It is crucial to note that even when aphids do not cause visible symptoms, they can still cause yield losses by withdrawing photoassimilates and altering the physiology of the host plant (Goggin et al., 2017). The effects of aphids on photosynthesis are discussed later in this chapter.

Aphids can also indirectly decrease the rate of photosynthesis of the host plant by excreting honeydew on the leaves and promoting the growth of black sooty mold (Kaakeh et al., 1992). In addition, aphids are known to transmit plant viruses that result in substantial damage to crops and it is reported that 50% of insect-vectored viruses are transmitted by aphids (reviewed in Ng and Perry, 2004). For example, the green peach aphid, *Myzus persicae*, is a widespread pest that transmits over 100 plant viruses including Potato leaf roll virus (PLRV) and cucumber mosaic virus (Morrison and Peairs, 1998). The magnitude and diversity of aphid damage on crops emphasizes the need to manage aphid populations.

Importance of understanding plant aphid interactions

Current aphid management practices rely on chemical and biological control as well as host-plant resistance in some crops. However, there are limitations to chemical and biological control. Chemical control using insecticides such as pyrethroids and neonicotinoids is one of the major tactics used for aphid control on crops (Dewar, 2007). For example, the management of soybean aphid – the most economically damaging insect of soybean in the United States – heavily depends on foliar-applied broad-spectrum insecticides (Hodgson et al., 2012; Koch et al., 2018). These pesticide applications can lead to reductions of beneficial insects that naturally control aphid populations and development of resistance against insecticides (Bass et al., 2014; Foster et al., 2017). However, many of these pesticides are being withdrawn from the market or categorized as restricted use such as carbofuran and aldicarb due to environmental impacts, and this reduces options for chemical control (Dooley, 2009). Also, pesticides are a high cost to growers, have negative impact on non-target species, raise safety concerns for worker and consumer safety, contaminate groundwater, contribute to secondary pest outbreaks (Damalas and Eleftherohorinos, 2011; Pimentel and Burgess, 2014; Carvalho, 2017).

Another common tactic of managing aphids is biological control using natural enemies such as ladybeetles, parasitoid wasps and green lacewings. One practical limitation of biological control is maintaining the efficiency of the natural enemies since they are easily affected by variable abiotic conditions such as temperature and weather (Powell and Pell, 2007). It is essential that biological control agents are released at the right time. When using predators and parasitoids, it is important to know their biology, specifically at what life-cycle stage of the pest they prefer. It is important that predators are able to maintain predator-prey dynamics in order to maintain their own population (Rutledge et al., 2004). Growers can choose biological control as

a control measure either by artificially releasing the biological control agents or by providing conditions that are conserve biological control agents, such as providing food sources. Also, it is important to make sure their chemical control measures are compatible with biological control agents. More biological control is used in the greenhouses due to its confined and controlled conditions. Also, the greenhouse crops are mostly high value crops; therefore, the growers are able to afford to keep releasing biological control agents. (Parrella, 2008; Boivin et al., 2012).

Host plant resistance is another important management tactic, which uses plant's ability to resist or tolerate damaging insects. However, this tactic is deployed only in some crops. There are different types of host-plant resistance. Host plants can affect insects' settling behavior by having characteristics that are unappealing to the pest such presence of waxy leaves (antixenosis), and their survival and fecundity (antibiosis). Also, some plants can withstand the insect damage (tolerance) (Emden, 2017). There are several possible sources of resistance. One is dependent upon differences in the concentration of certain of allele chemicals such as glucosinolates and DIMBOA. A study showed higher fecundity of green peach and cabbage aphids on Arabidopsis mutants that contained lower amount of glucosinolates (Mewis et al., 2005). Moreover, Arabidopsis leaves infiltrated with aphid salivary secretions have shown an increased expression of glucosinolate biosynthesis-related genes (De Vos and Jander, 2009). Mechanical resistance such as cuticular waxes is another source of resistance, although it is not common in aphid resistance literature. It has been shown that glossy pea varieties are resistant to pea aphids (White and Eigenbrode, 2000). Another important source of resistance is the use of resistance genes (R genes) that are involved in perception and recognition of the pest then trigger induced defense responses. Resistant crop cultivars have been developed by selecting for or engineering cultivars that contain host-plant defenses. Aphid resistant crop varieties are used in

commercial agricultural production. For example, *Mi1.2* in tomato, *Rag1* resistance gene in soybean cultivars and in some cereal crops to control Russian what aphid (e.g. *Dn* genes) (Rossi et al., 1998; Hill et al., 2006; Li et al., 2006; Khan et al., 2009; Pallipparambil et al., 2010; Hill et al., 2017). Also, few lettuce cultivars containing an *Nr* gene that confer resistance against *Nasonovia ribisnigri* are commercially available (Tatchell et al., 2017). This tactic can be particularly useful in cases where aphids cause leaf rolling, which provides them protection from insecticide contact and biological control agents (Haile et al., 1999). This approach is more cost effective because such resistant crops would result a higher yield and could cut costs on pesticides used in aphid control. It is also environmentally friendly because it is less hazardous. However, relatively little is known about the physiological factors that regulate resistance or tolerance to aphids. Also, it is important to identify more resistant genes, specifically the ones that can be applied to many crop plants.

These studies show that there are different physiological mechanisms of resistance involving different secondary metabolites and genetic variation in levels of resistance to aphids. However, an interesting question in biology is how primary metabolism influences resistance too. It's important to understand how the aphids interact with the plant's physiology and primary metabolism, so we can understand what results in susceptibility, resistance and tolerance, and what traits need to be enhanced. To achieve this, it is essential that we understand the interaction with photosynthesis and reactive oxygen species (ROS), which may contribute to enhanced defense responses.

Aphids and photosynthesis

Aphids have been reported to influence carbon assimilation, a measure of net photosynthetic activity in plants, as well as many major factors that can influence carbon assimilation, such as chlorophyll content, stomatal conductance, and the efficiency of the light-dependent and light-independent reactions of photosynthesis (reviewed in Kerchev et al. 2012 and Goggin et al. 2017).

Carbon Assimilation

Many studies have reported altered carbon assimilation in different plant systems due to aphid feeding (reviewed in Kerchev et al. 2012). Significant decreases in carbon assimilation have been observed in several different compatible aphid-plant interactions, such as soybean aphid (*A. glycines*) on soybean (Macedo et al., 2003a), greenbug (*Schizophis grumimun*) on barley (Ryan et al., 1987; Cabrera et al., 1994), Russian wheat aphid (*D. noxia*) on wheat (Haile et al., 1999; Macedo et al., 2003b; Macedo et al., 2009), bird cherry-oat aphid (*Rhopalosiphum padi*) on wheat (Macedo et al., 2009), cotton aphid (*Aphis gossypii*) on cotton (Shannag et al., 1998), cotton aphid (*A. gossypii*) on chrysanthemum (Davies et al., 2004), *Essigella californica* on *Pinus radiata* (Eyles et al., 2011) and *Monellia caryella*, *Monelliopsis pecanis*, *Melanocallis caryaefolia* on pecan (Wood et al., 1985). Decreases in carbon assimilation are reported between 31% and 54%. However, it is difficult to generalize the impact of aphids on carbon assimilation since it depends on the aphid species, host plant species and variety, infestation level, the length of infestation and the stage of infestation at which carbon assimilation is measured. Two resistant wheat varieties infested with *R. padi* and *D. noxia* had shown that although both species reduced carbon assimilation, *D. noxia* had a greater influence compared to *R. padi* (Macedo et al., 2009).

Generally, the measurements were taken 1-10 days post-infestation. Due to the differences in experimental designs, it is difficult to say how quickly these decreases emerge after infestation and how persistent they are. While some studies have reported reductions in carbon assimilation by day 9 post infestation (Ryan et al., 1987; Cabrera et al., 1994; Haile et al., 1999; Macedo et al., 2003a), few studies have shown that there were no differences in carbon assimilation at day 9 (Shannag et al., 1998; Franzen et al., 2007). However, Shannag et al. (1998) reported significant reductions at day 18 and 27. This suggests that even though the reductions occurred later, they persisted for a long time. In contrast, Kucharik et al. (2016) have shown slightly higher carbon assimilation rates in control plants compared to soybean aphid infested plants at low aphid densities (less than 50 aphids per plant). This could be due to overcompensation at low aphid levels, since they did not report increases at high aphid levels. Generally, plant photosynthesis does not occur under its full capacity. Under an attack, plants may show limited increases in photosynthesis. This could aid in defense responses since photosynthesis – mainly light reactions – generates ROS.

The effect of aphids on carbon assimilation also depends on whether it is a susceptible, resistant or tolerant line. Some studies have shown that resistant/tolerant plants could increase photosynthesis to compensate for the infestations. Heng-Moss et al. (2006) reported enhanced photosynthetic rates in resistant buffalograss upon chinch bug feeding. Resistant genotypes of field-grown *Pinus radiata* trees showed significantly higher photosynthetic rates after aphid-induced defoliation (Eyles et al., 2011). In contrast, another study showed that although carbon assimilation was initially decreased in the infested tolerant line, and restored to the level of controls after 7 days; however, the carbon assimilation rates of the susceptible and the antibiotic lines were not restored (Haile et al., 1999). Ryan et al. (1987) reported no reductions in carbon

assimilation in greenbug resistant barley cultivars. These alterations in carbon assimilation could depend upon modifications in other processes and factors such as stomatal behavior, light-dependent reactions, light-independent reactions and chlorophyll content.

Stomatal behavior

Aphids can modify stomatal behavior, thus altering stomatal conductance, transpiration rates and intercellular CO_2. Stomata are small openings that are usually found in the leaf epidermis that facilitate gas exchange. Stomata can increase or decrease their aperture size as a response to environmental changes (Aasamaa and Sõber, 2011). Generally, plants with increased stomatal conductance and transpiration would show enhanced photosynthetic rates (Rosenthal et al., 1987; Munns, 2002). Moreover, intercellular CO_2 concentration (C_i) is an important parameter as it indicates the amount of CO_2 available for carbon assimilation (Farquhar et al., 1980). Reductions in stomatal conductance, transpiration and intercellular CO_2 have been reported in wheat in response to aphids (Ryan et al., 1987; Macedo et al., 2003a; Macedo et al., 2009). Aphids can induce stomatal closure by upregulating abscisic acid signaling, which would decrease CO_2 availability (Sun et al., 2015). This could in turn reduce stomatal conductance, transpiration and C_i. However, Franzen et al. (2007) reported no effects on stomatal conductance in *D. noxia* infested wheat. In some cases, aphids can increase stomatal conductance and transpiration (Shannag, 2007). Shannag et al. (1998) also reported increased transpiration, but the aphids negatively affected photosynthesis rates. Increase in transpiration would contribute to increased water loss in plants, although this will typically not limit the CO_2 availability for photosynthesis. The increase in transpiration could be due to an increase in stomatal aperture, which explains the enhanced stomatal conductance as well (Shannag, 2007). These increased

could be also be due to toxin that aphids inject during feeding (Shannag et al., 1998). It is not well understood how aphids influence carbon assimilation by modifying stomatal behavior.

Light-dependent Reactions of Photosynthesis

The light-dependent reactions occur in the thylakoid membrane and generate NADPH and ATP using light energy, which are energy storage molecules (Johnson, 2016). Several studies indicate that aphids can reduce the efficiency of electron transport (F_v/F_m) in photosystem II (PSII) (Burd and Elliott, 1996; Haile et al., 1999). F_v/F_m is widely used when reporting the photochemical efficiency of PSII, and is calculated using the equation $F_v = F_o-F_m$, where F_v = variable fluorescence, F_o = minimal fluorescence in dark-adapted state and F_m = maximal fluorescence in dark-adapted state (Baker, 2008). In contrast, a few studies have reported no apparent changes in F_v/F_m due to aphid feeding (Macedo et al., 2003a; Franzen et al., 2007). However, (Macedo et al., 2003a) reported increased F_o and F_m values. The enhanced non-variable fluorescence, particularly F_o, suggests that photo-inhibitory damage may have occurred in PSII. It appears that the decreases in carbon assimilation due to aphid infestations can be detected before any changes in the electron transport (Macedo et al., 2003a; Franzen et al., 2007). It is shown that downregulation of genes that are responsible for PSII leads to reductions in efficiency of PSII and can aid in defense responses (reviewed in Kangasjärvi et al., 2012). Such genotypes show hypersensitive response (HR)-associated resistance and a large oxidative bust, which could damage the PSII. This can be a reason for decreased PSII efficiency (Zou et al., 2005). It seems that the PSII efficiency may not strongly influence carbon assimilation.

Light-independent Reactions of Photosynthesis

The light-independent reaction, also known as the Calvin-Benson cycle occurs in the stroma and it converts carbon dioxide into sugars using NADPH and ATP generated from the light-dependent reaction. There are many enzymes involved in this carbon fixation process and the one that is involved in the first major step is called Ribulose-1,5-bisphosphate carboxylase/oxygenase (Rubisco) and it acts on the substrate Ribulose-1,5-bisphosphate (RuBP) (Johnson, 2016). The efficiency of Calvin cycle is estimated by measuring the efficiency of Rubisco enzyme (V_{cmax}) and the regeneration rate RuBP (J_{max}). The influence of aphids on carbon assimilation appears to be due in part to changes in the light-independent reactions of photosynthesis. In particular, aphids have been reported to reduce Rubisco efficiency and reduce RuBP regeneration (Franzen et al., 2007). Similarly, other studies have reported reductions in the Calvin cycle that were detected before observing impaired PSII efficiency (Ryan et al., 1987; Gutsche et al., 2009). In contrast, increased Rubisco efficiency and RUBP regeneration are reported in an aphid-resistant what cultivar compared to susceptible variety only after 3 days post-infestation (Franzen et al., 2007). Gutsche et al. (2009) speculate that the increases could be the source of increased carbon assimilation that has been observed in aphid-infested plants. It has been shown that the damage inflicted by biotic agents including pathogens and insects downregulate the expression of genes involved in photosynthesis such as genes coding for proteins in photosystem I (PSI) and photosystem II (PSII) reaction centers, and subunits of Rubisco (Bilgin et al., 2010). Calvin cycle is composed of a series of chemical reactions and there are many enzymes and intermediate substrates involved in the process. Further work is needed to identify which steps are mostly affected by aphids and what aspects of aphid feeding are responsible for these effects.

Chlorophyll Content

Several studies have reported decreased chlorophyll content due to aphid feeding (Ni and Quisenberry, 2006; Diaz-Montano et al., 2007; Golawska et al., 2010) and a few studies have shown that aphids have negatively impacted both carbon assimilation and chlorophyll content (Ryan et al., 1987; Cabrera et al., 1994). However, chlorophyll loss is not observed immediately after aphid infestation. The earliest time point that has been reported to observe chlorophyll loss is 6 days after infestation (Ryan et al., 1987). This effect could depend upon several other factors such as aphid species, crop variety and the infestation level. For example, two resistant soybean varieties showed significantly low chlorophyll loss compared to a susceptible variety (Diaz-Montano et al., 2007). It appears that chloroplasts may play a role in retaining the photosynthetic efficiency in resistant varieties (Botha et al., 2006). Russian wheat aphid (*D. noxia*) was reported to inject a phytotoxin during feeding that breaks down chloroplast membrane in susceptible lines and cause reductions in chlorophyll. However, in resistant varieties, limited chloroplast membrane breakdown was observed (Burd and Elliott, 1996). Some authors argue that chlorophyll content is not a very sensitive parameter that can be used to evaluate responses due to aphids since it does not rapidly respond and chlorophyll loss is a symptom rather than a cause for photosynthesis inhibition (Franzen et al., 2007; Gutsche et al., 2009).

Photosynthesis or defense?

The effects of aphids on photosynthesis can be a result of the direct damage inflicted by the aphid or they could occur due to adaptive responses by the plant. An example for such adaptive response is the induction of jasmonic acid dependent responses against insects causing a temporary downregulation of photosynthesis (Attaran et al., 2014). Downregulation of

photosynthesis related genes in response to abiotic stress has been reported in several studies (Reymond et al., 2004; Zou et al., 2005; Duke et al., 2017). Botha et al. (2006) showed that genes coding for chloroplast ATPase (cpATPase), which is an essential enzyme for photosynthesis significantly upregulated due to *D. noxia* feeding in resistant wheat plants compared to susceptible plants. It appears that cpATPase play an important role in maintaining the photosynthesis in resistant varieties and more generally, it seems that the ability to maintain photosynthesis even under infestation is component of the plant's resistant mechanism. A biological control agent *Pseudomonas chlororaphis* PA23 was shown to reduce the necrotrophic fungus *Sclerotinia sclerotiorum* infection in Canola and PA23 also increased the chlorophyll content prior to any fungus infection (Duke et al., 2017). The authors reported significant downregulation of *CHLOROPHYLLASE 1* (*CHL1*) in plants treated with PA23.*CHL1* is a gene that is involved in chlorophyll degradation pathway. In addition, Transmission Electron Microscopic images revealed an increase in the area of thylakoids in the chloroplasts of PA23 treated plants (Duke et al., 2017). These data suggests that the chloroplasts may have a role in defenses priming. Kariola et al. (2005) showed the silencing of *CHL1* in Arabidopsis increased H_2O_2 accumulation in response to a bacterial inoculation and activation of antioxidants. In addition, silenced *CHL1* enhanced salicylic acid dependant defenses and reduced jasmonic acid dependant defenses. It appears that *CHL1*, which is the first enzyme of the chlorophyll degradation pathway may moderate different defense pathways in plant (Kariola et al., 2005). These studies show that the reductions in photosynthesis during biotic stress could downregulate photosynthesis related genes, which could influence defense mechanisms by accumulating ROS and it may induce hypersensitive responses in leaves.

Plants typically divert resources that are allocated for growth processes to defense processes under stressed conditions. This is referred to as growth-defense tradeoff, which is evolved to optimize plant fitness in changing environments (reviewed in Meldau et al., 2012, Huot et al., 2014). Jasmonic acid (JA) and salicylic acid (SA) play key roles in allocating resources to growth and defense (reviewed in Nabity et al. 2009, Huot et al. 2014). It has been shown that the activation of JA signaling inhibit growth (Staswick et al., 1992). Attaran et al. (2014) showed reductions in growth and photosynthesis in Arabidopsis with exogenous applications of coronatine (COR), a structural mimic of a receptor-active form of JA. However, the COR treatment reduced photosynthesis after 24 hours, whereas growth inhibition occurred within 4 hours of treatment. They have observed strong inductions of defense related genes immediately after COR treatment. The results indicate that the resource allocation from growth to defense occurs quickly and the photosynthesis machinery could sustain its function without being affected immediately. This could contribute to induction of chloroplastic ROS accumulation, which could enhance the defense response.

Aphids and ROS

Reactive oxygen species

Reactive oxygen species (ROS) are highly reactive and oxygen-containing molecules that are generated during aerobic metabolism as byproducts. Examples of ROS species include molecules such as singlet oxygen ($^1O_2$), hydrogen peroxide (H_2O_2), superoxide radical ($^{\bullet}O_2^-$), and hydroxyl radical ($^{\bullet}OH$) (reviewed in Apel and Hirt, 2004; Sharma et al., 2012). These toxic ROS are scavenged by different antioxidative enzymes such as superoxide dismutase (SOD), catalase (CAT), glutathione reductase (GR), ascorbate peroxidase (APX), guaiacol peroxidase

(GPX) and monodehydroascorbate (MDHAR), and non-enzymatic antioxidants such as ascorbic acids (AsA), reduced glutathione (GSH) tocopherols and phenolics (Noctor and Foyer, 1998; Dinakar et al., 2009; Sharma et al., 2012). The equilibrium between ROS and its' scavengers can be disturbed by various biotic and abiotic stresses such as drought, salt, temperature, insects and pathogens. This can cause increases in ROS levels in cells (Apel and Hirt, 2004; Miller et al., 2010; Sharma et al., 2012). It has been shown that at high concentrations, ROS may cause deleterious effects on plant cells. When the ROS concentration is too high, it may lead to oxidative burst, which can damage the cells by causing lipid peroxidation, membrane electrolyte leakage, programmed cell death etc. (Jambunathan, 2010; Demidchik et al., 2014; Petrov et al., 2015; Yu et al., 2017). ROS can be also formed in response to stress by various oxidases and peroxidases such as NADPH oxidases. ROS can play a dual role by acting as signal transduction molecules. ROS generated during stress can signal and activate defense mechanisms in the cells (Millar et al., 2000).

In plants, ROS can be formed in various sub-cellular compartments including chloroplasts, mitochondria, endoplasmic reticulum and peroxisomes (Sharma et al., 2012; Tripathy and Oelmüller, 2012). In chloroplasts, the electron transport chains in PSI and PSII are identified as major sources of ROS due to unavoidable leakage of electrons on to O_2, and the process of photorespiration is another major source of ROS that is associated with photosynthesis (Sharma et al., 2012; Voss et al., 2013; Dietz et al., 2016). PSII is the source the molecular oxygen and it has extreme reducing and oxidizing potentials (Pospísil, 2009). In PSII antennae complex, triplet state chlorophyll (^{3}P680) can be generated due to insufficient energy transfer. This triplet state chlorophyll can then interact with triplet state oxygen ($^3O_2$) and produce singlet oxygen by donating an electron (Macpherson et al., 1993; Laloi et al., 2006;

Pospíšil, 2016). It is important to note that in both PSI and PSII antennae complexes, chlorophyll molecules are closely bound with carotenoids that act as quenchers of triplet chlorophyll or singlet oxygen (Edge and Truscott, 2018). However, in PSII reaction center, the carotenoids are not closely associated which makes the quenching of triplet chlorophyll not possible. Thus, the PSII reaction centers are constantly producing singlet oxygen, specifically under high light stress (Keren et al., 1995; Apel and Hirt, 2004). To protect the photosynthetic apparatus, plants dissipate the excess energy as heat or transfer the excess electrons to other sinks such as molecular oxygen (Laloi et al., 2006). Molecular oxygen can be reduced to superoxide in PSI. This reaction is called Mehler reaction (Mehler, 1951). Superoxide dismutase (SOD) can rapidly convert superoxide to hydrogen peroxide. Hydrogen peroxide can then react with superoxide when metal ions are present, and form highly reactive hydroxyl radical (Laloi et al., 2006). Hydrogen peroxide can also be produced during photorespiration. When the CO_2 availability is limited, Rubisco favors O_2 over CO_2 as a substrate. As a result of the oxygenation, glycolate is formed in the chloroplasts. Glycolate is then transported to peroxisomes, gets oxidized by glycolate oxidase and produces hydrogen peroxide (Tripathy and Oelmüller, 2012). The accumulation of excess ROS can lead to various effects such as photoinhibition, lipid peroxidation and activation of programmed cell death.

Effects of aphids on ROS

Several studies of plant transcript and protein profiles suggest that aphids can alter the accumulation of ROS and redox status of the host plant. The redox status depends on the relative balance between ROS and antioxidants. Although aphids cause minor wounding to leaf tissue compared to chewing insects, the injection of salivary compounds play a role in altering redox changes in plants (van Bel and Will, 2016). It is reported that aphid salivary compounds such as

glucose oxidases could potentially lead to production of H_2O_2 (Harmel et al., 2008). In addition, an increase in H_2O_2 and NADPH-dependant oxidases activity have been shown in resistant wheat plants in response to Russian what aphid feeding suggesting that NADPH-oxidases are involved in insect-induced ROS generation (Moloi and van der Westhuizen, 2006). Furthermore, it is possible that changing the plant's redox status can affect aphids. It has been shown that increase in ascorbic acid, which is an antioxidative compound, enhanced susceptibility of aphids. This could be partly due to decreases in ROS in the plant followed by alterations in the redox status (Kerchev et al., 2012). Also, it was shown an increase in the number of aphids on an Arabidopsis mutant that lacked *RBOHD* (*RESPIRATORY BURST OXIDASE HOMOLOG D*), which is a gene that is responsible for accumulation of H_2O_2 at the wound site (Miller et al., 2009). These results suggest that changes in ROS accumulation and changes in redox status could influence plant resistance or susceptibility to aphids. The ROS accumulation and photosynthesis can be influenced by plant's fatty acid desaturases (FADs).

Fatty acid desaturases and plant resistance to stress

One aspect of plant physiology that has recently been shown to impact host plant resistance against aphids is fatty acid metabolism; in particular, a recent study has shown that loss of function of ω-3-Fatty Acid Desaturase 7 (FAD7) confers resistance against aphids in tomato (*Solanum lycopersicum*, Solanaceae) and Arabidopsis (*Arabidopsis thaliana*, Brassicaceae) (Avila et al., 2012). Much further work is required to understand the biochemical and physiological basis of how FAD7 impacts aphid resistance. Since homologs of FAD7 are found throughout the vascular plants and even in algae (Nguyen et al., 2013), information on how this desaturase impacts aphid resistance will likely be relevant to many diverse crops.

Definition of Fatty Acids and Fatty Acid Desaturases

Each fatty acid consists of a hydrocarbon chain and a terminal carboxyl group, and they are essential components of the lipids that make up biological membranes or that are used for energy storage in organs such as seeds and pollen (Upchurch, 2008). Fatty acids differ based on the number of carbons in the hydrocarbon chain. Almost all plant membranes are made of 18-carbon fatty acids, and some plant membranes are composed of both 16-carbon and 18-carbon fatty acids (Millar et al., 2000). Fatty acids can also vary in the presence, number, and position of double bonds in the hydrocarbon chain. Fatty acids with one or more double bonds are called unsaturated fatty acids. About 70% of the leaf or root lipids are composed of trienoic (TA) and dienoic (DA) fatty acids, which have three or two double bonds, respectively (Douce and Joyard, 1990). Fatty acid desaturases (FADs) are enzymes that introduce double bonds into the acyl chains of fatty acids (Los and Murata, 1998). Omega-3 fatty acid desaturases (ω-3 FADs) are vital enzymes that desaturate the DAs to form TAs (Liu et al., 2013). In plants, ω-3 FADs can be found in the chloroplast or the endoplasmic reticulum (ER) (Zhang et al., 2011). FADs are also widely distributed among other taxa, except in some bacteria such as *Escherichia coli* (Los and Murata, 1998).

Fatty Acid Desaturases and Plant Stress

FADs are known to influence plant resistance to different abiotic stresses, including temperature extremes, drought, and salt stress, and can also influence vulnerability to some biotic stressors, including pathogens and insects (Table 1). For example, over-expression of the chloroplast localized ω-3 FADs, *FAD7* and *FAD8,* enhances survival of tobacco seedlings under cold stress (reviewed in Upchurch, 2008), whereas silencing *FAD7* and *FAD8* in tobacco

increases resistance to high temperatures (Iba, 2002). The influence of FADs on abiotic stress tolerance is due at least in part to their influence on the melting temperature and consequent fluidity of cellular membranes. Unsaturated fatty acids have lower melting temperatures than saturated fatty acids, and help maintain membrane fluidity (Andreu et al., 2007), which increases with the degree of unsaturation (Webb and Green, 1991). *FAD3*, which encodes an ER-localized ω-3 FAD, and *FAD8*, which encodes a chloroplast localized ω-3 FAD, have both been shown to influence membrane structure and fluidity of tobacco during biotic stresses (Upchurch, 2008). FADs can also influence biotic stress resistance. For example, loss of function or antisense suppression of genes encoding ω-3 FADs increase vulnerability to the bacterial pathogen *Pseudomonas syringae* (Yaeno et al., 2004) and the fungus gnat larva *Bradysia impatiens* in Arabidopsis (McConn et al., 1997; Stintzi et al., 2001), and to the caterpillar *Manduca sexta* (Li et al., 2003) and the whitefly *Bemisia tabaci* in tomato (Sánchez-Hernández et al., 2006). In contrast, decrease in the expression in antisense *FAD7* and *FAD8* lines increased the resistance to rice blast fungus *Magnaporthe grisea* in rice (Yara et al., 2007). These studies show that defects in some FADs could lead to increased resistance to some insects and pathogens, while there is an increased vulnerability to some other pathogens. The physiological basis for the influence of FADs on biotic stress is not fully understood, but is at least in part due to an influence of FADs on defense signaling.

FAD7 and aphid resistance

Loss of function of FATTY ACID DESATURASE7 (FAD7) regulates plant defenses against aphids in tomato (*S. lycopersicum*) and Arabidopsis (*A. thaliana*) (Avila et al., 2012). The *fad7-1* mutation in Arabidopsis is a single nucleotide substitution mutation that introduces a premature stop codon to the protein (Li et al., 2003) and thus it contains increased levels of 18:3

and 16:3 and deficient in 18:3 and 16:3 (Browse et al., 1986). The *suppressor of prosystemin-mediated response2* (*spr2*) mutation in tomato, which was generated through ethyl methanesulfonate (EMS) mutagenesis, results in the loss of function of FAD7 (Howe and Ryan, 1999; Li et al., 2003). The *spr2* mutation in tomato reduces survival and reproduction of potato aphids (*Macrosiphum euphorbiae*). Compared to WT plants, the aphid mortality rate was over 50 percent higher and the average aphid survival is about 3 days shorter on *spr2* mutants. The Arabidopsis *fad7-1* mutant, which is functionally analogous to the *spr2* mutation also increased resistance against green peach aphids (*M. persicae*) (Avila et al., 2012). This shows that loss of function of FAD7 enhances aphid resistance in more than one plant family. It was known that FAD7 was plastid specific (Wallis and Browse, 2002). Confocal analysis confirmed that FAD7 protein is localized in the thylakoid membrane of the chloroplast (Andreu et al., 2007). Therefore, *fad7* mutation dramatically modifies the fatty acid composition of chloroplast membranes (Li et al., 2003).

ROS and FADs

Several lines of evidence suggest that the loss of function of fatty acid desaturases increase ROS levels constitutively and in response to a variety of stresses. A study done with Luciferase reporter gene with a singlet oxygen responsive promoter has shown that *fad7* has constitutively higher reporter gene activity than wild-type (WT) plants. This indicates that *fad7* may have constitutively high levels of singlet oxygen (Alnasrawi, 2015). Lipid profiling of *spr2* (tomato) and *fad3fad7fad8* (Arabidopsis) has showed that these mutants have increased levels of fatty acid hydroperoxides, which are indicators of oxidative stress (unpublished data by M. Mueller and F. Goggin). These results suggest that these mutants may accumulate higher levels of ROS compared to its' respective WT plants. Moreover, it has been shown that *spr2* plants

have significantly higher ascorbic acid (antioxidant) levels than WT (Suza et al., 2010). It has been shown that the expression of *α-dioxygenae1* (*DOX1*) is upregulated in response to aphids,(Avila et al., 2013). In contrast, Yaeno et al. (2004) showed reduced accumulation of superoxide radicals and hydrogen peroxide in *fad7fad8* double mutant Arabidopsis in response to a pathogen *P. syringae*. This study also shows that linolenic acid (C18:3) activated NADPH oxidase, which is an enzyme that is responsible for ROS production. However, it is reported that linolenic acid can act as an antioxidant as well (Mène-Saffrané et al., 2009). These studies illustrate that changes in fatty acid composition in plants influence the accumulation of ROS, which can lead to enhanced defense responses.

The existing literature suggests that the fatty acid desaturation may affect primary metabolism in plants, and that could affect reactive oxygen species accumulation. To test whether the fatty acid desaturase 7 would affect primary metabolism and ROS, we studied photosynthesis and the changes in the overall redox status in plants with loss of function of FAD7. This will allow us to identify potential links between primary metabolism and plant defenses against aphids.

Research questions

The loss of function of Fatty Acid Desaturase7 (FAD7) enhances resistance against aphids. This research intends to contribute toward the long-term goal of identifying factors determining aphid resistance in FAD7 mutants. Therefore, we tested how primary metabolism and redox status differ in FAD7 mutants compared to WT plants. To investigate how fatty acid desaturation would affect photosynthesis, we compared the effects of loss of function of FAD7 on photosynthesis and growth of tomato in the absence of aphids using the *suppressor of*

prosystemin-mediated response2 (*spr2*) mutation, which has impaired *FAD7* function (Chapter II). Next, we studied the constitutive differences in primary metabolites between *spr2* and WT and also studied the effects of *spr2* on photosynthesis in response to potato aphids (*M. euphorbiae*) (Chapter III). Lastly, we looked at the changes in overall redox state in *fad7-1* mutation in Arabidopsis (Chapter IV). This study contributes to our understanding of how impaired *FAD7* affects plant's primary metabolism, specifically photosynthesis, and the overall redox status. Studying these aspects will give insight into how the plants divert energy to enhanced defenses against aphids.

Table 1: Influence of ω-3 FADs on resistance to abiotic and biotic stress.

FAD	**Plant Species**	**Modification**	**Impact on Stress Tolerance**	**Citation**
fad7	*S. lycopersicum*	Null mutation and antisense suppression	Enhanced resistance to *M. euphorbiae*	Avila et al., 2012
fad7-2 *fad7-1fad8-1*	*A. thaliana*	Null mutation	Enhanced resistance to *M. persicae*	
fad7fad8	*A. thaliana*	Null mutation	Increased vulnerability to *P. syringae*	Yaeno et al., 2004
fad7fad8	*Oryza sativa*	RNAi	Enhanced resistance against *M. grisea*	Yara et al., 2007
FAD3 and *FAD8*	*Nicotiana tabacum*	Overexpression	Enhanced drought tolerance, but *FAD8* reduced heat tolerance	Zhang et al., 2005
FAD7	*N. tabacum*	Overexpression	Increased cold tolerance	Kodama et al., 1995
fad7	*N. tabacum*	Overexpression	Increased cold tolerance	Kodama et al., 1994
fad7fad8	*A. thaliana*	Null mutation	Increased heat tolerance	Murakami et al., 2000
fad7	*A. thaliana*	Antisense	Reduced drought tolerance	Im et al., 2002
FAD3	*FAD3* of *Chorispora bungeana* in *N. tabacum*	Overexpression	Enhanced tolerance to cold, salt and drought stresses	Shi et al., 2018

Table 1 (Cont.)

FAD	Plant Species	Modification	Impact on Stress Tolerance	Citation
FAD7	*S. lycopersicum*	Antisense	Enhanced heat tolerance	Liu et al., 2006
fad7	*S. lycopersicum*	Overexpression	Enhanced cold tolerance	Liu et al., 2013
FAD3	*S. lycopersicum*	Overexpression	Enhanced cold tolerance	Yu et al., 2009
FAD3	*S. lycopersicum*	Overexpression	Enhanced salt tolerance	Wang et al., 2014

References

Aasamaa K, Sõber A (2011) Responses of stomatal conductance to simultaneous changes in two environmental factors. Tree Physiol **31**: 855–864

Alnasrawi AM (2015) Optimizing a luciferase-based tool for studying the effects of *fatty acid desaturase7* on singlet oxygen accumulation in *Arabidopsis thaliana*. Theses and Dissertations. 1319. http://scholarworks.uark.edu/etd/1319

Andreu V, Collados R, Testillano PS, Risueño M del C, Picorel R, Alfonso M (2007) In Situ molecular identification of the plastid ω3 *Fatty Acid Desaturase FAD7* from soybean: evidence of thylakoid membrane localization. Plant Physiol **145**: 1336–1344

Apel K, Hirt H (2004) Reactive oxygen species: Metabolism, oxidative stress, and signal transduction. Annu Rev Plant Biol **55**: 373–399

Attaran E, Major IT, Cruz JA, Rosa BA, Koo AJK, Chen J, Kramer DM, He SY, Howe GA (2014) Temporal dynamics of growth and photosynthesis suppression in response to jasmonate signaling. Plant Physiol **165**: 1302–1314

Avila CA, Arévalo-Soliz LM, Jia L, Navarre DA, Chen Z, Howe GA, Meng Q-W, Smith JE, Goggin FL (2012) Loss of function of FATTY ACID DESATURASE7 in tomato enhances basal aphid resistance in a salicylate-dependent manner. Plant Physiol **158**: 2028–2041

Avila CA, Arevalo-Soliz LM, Lorence A, Goggin FL (2013) Expression of α-*DIOXYGENASE 1* in tomato and Arabidopsis contributes to plant defenses against aphids. Mol Plant Microbe Interact **26**: 977–986

Baker NR (2008) Chlorophyll fluorescence: a probe of photosynthesis in vivo. Annu Rev Plant Biol **59**: 89–113

Bass C, Puinean AM, Zimmer CT, Denholm I, Field LM, Foster SP, Gutbrod O, Nauen R, Slater R, Williamson MS (2014) The evolution of insecticide resistance in the peach potato aphid, *Myzus persicae*. Insect Biochem Mol Biol **51**: 41–51

Beckendorf EA, Catangui MA, Riedell WE (2008) Soybean aphid feeding injury and soybean yield, yield components, and seed composition. Agron J **100**: 237–246

van Bel AJE, Will T (2016) Functional evaluation of proteins in watery and gel saliva of aphids. Front Plant Sci. doi: 10.3389/fpls.2016.01840

Bilgin DD, Zavala JA, Zhu J, Clough SJ, Ort DR, DeLucia EH (2010) Biotic stress globally downregulates photosynthesis genes. Plant Cell Environ **33**: 1597–1613

Boivin G, Hance T, Brodeur J (2012) Aphid parasitoids in biological control. Can J Plant Sci **92**: 1–12

Botha A-M, Lacock L, van Niekerk C, Matsioloko MT, du Preez FB, Loots S, Venter E, Kunert KJ, Cullis CA (2006) Is photosynthetic transcriptional regulation in *Triticum aestivum* L. cv. "TugelaDN" a contributing factor for tolerance to *Diuraphis noxia* (Homoptera: Aphididae)? Plant Cell Rep **25**: 41–54

Browse J, McCourt P, Somerville C (1986) A mutant of arabidopsis deficient in C18:3 and C16:3 leaf lipids. Plant Physiol **81**: 859–864

Burd JD, Elliott NC (1996) Changes in chlorophyll a fluorescence induction kinetics in cereals infested with Russian wheat aphid (Homopetra: Aphididea). J Econ Entomol **89**: 1332–1337

Cabrera HM, Argandoña VH, Corcuera LJ (1994) Metabolic changes in barley seedlings at different aphid infestation levels. Phytochemistry **35**: 317–319

Carvalho FP (2017) Pesticides, environment, and food safety. Food Energy Secur **6**: 48–60

Damalas CA, Eleftherohorinos IG (2011) Pesticide exposure, safety issues, and risk assessment indicators. Int J Environ Res Public Health **8**: 1402–1419

Davies FT, He C, Chau A, Heinz KM, Cartmill AD (2004) Fertility affects susceptibility of chrysanthemum to cotton aphids: influence on plant growth, photosynthesis, ethylene evolution, and herbivore abundance. J Am Soc Hortic Sci **129**: 344–353

De Vos M, Jander G (2009) *Myzus persicae* (green peach aphid) salivary components induce defence responses in *Arabidopsis thaliana*. Plant Cell Environ **32**: 1548–1560

Demidchik V, Straltsova D, Medvedev SS, Pozhvanov GA, Sokolik A, Yurin V (2014) Stress-induced electrolyte leakage: the role of K+-permeable channels and involvement in programmed cell death and metabolic adjustment. J Exp Bot **65**: 1259–1270

Dewar AM (2007) Chemical control. *In* HF van Emden, R Harrington, eds, Aphids Crop Pests. CABI, Wallingford, UK, pp 391–422

Diaz-Montano J, Reese JC, Schapaugh WT, Campbell LR (2007) Chlorophyll loss caused by soybean aphid (Hemiptera: Aphididae) feeding on soybean. J Econ Entomol **100**: 1657–1662

Dietz K-J, Turkan I, Krieger-Liszkay A (2016) Redox- and Reactive Oxygen Species-Dependent Signaling into and out of the Photosynthesizing Chloroplast. Plant Physiol **171**: 1541–1550

Dinakar C, Abhaypratap V, Yearla SR, Raghavendra AS, Padmasree K (2009) Importance of ROS and antioxidant system during the beneficial interactions of mitochondrial metabolism with photosynthetic carbon assimilation. Planta **231**: 461

Dooley EE (2009) The Beat. Environ Health Perspect **117**: A242–A243

Douce R, Joyard J (1990) Biochemistry and function of the plastid envelope. Annu Rev Cell Biol **6**: 173–216

Duke KA, Becker MG, Girard IJ, Millar JL, Dilantha Fernando WG, Belmonte MF, de Kievit TR (2017) The biocontrol agent *Pseudomonas chlororaphis* PA23 primes *Brassica napus* defenses through distinct gene networks. BMC Genomics **18**: 467

Edge R, Truscott TG (2018) Singlet oxygen and free radical reactions of retinoids and carotenoids - A review. Antioxid Basel **7**: 5

Emden HF van (2017) Host-plant resistance. *In* HF van Emden, R Harrington, eds, Aphids Crop Pests, 2nd ed. CABI, Wallingford, pp 515–532

Eyles A, Smith D, Pinkard EA, Smith I, Corkrey R, Elms S, Beadle C, Mohammed C (2011) Photosynthetic responses of field-grown *Pinus radiata* trees to artificial and aphid-induced defoliation. Tree Physiol **31**: 592–603

Farquhar GD, von Caemmerer S, Berry JA (1980) A biochemical model of photosynthetic CO_2 assimilation in leaves of C3 species. Planta **149**: 78–90

Foster SP, Devine G, Devonshire AL (2017) Insecticide resistance. *In* HF van Emden, R Harrington, eds, Aphids Crop Pests, 2nd ed. CABI, Wallingford, pp 426–447

Franzen LD, Gutsche AR, Heng-Moss TM, Higley LG, Sarath G, Burd JD (2007) Physiological and biochemical responses of resistant and susceptible wheat to injury by Russian wheat aphid. J Econ Entomol **100**: 1692–1703

Goggin FL (2007) Plant–aphid interactions: molecular and ecological perspectives. Curr Opin Plant Biol **10**: 399–408

Goggin FL, Quisenberry SS, Ni X (2017) Feeding injury. *In* HF van Emden, R Harrington, eds, Aphids Crop Pests, 2nd ed. CABI, Wallingford, UK, pp 303–322

Golawska S, Krzyzanowski R, Lukasik I (2010) Relationship between aphid infestation and chlorophyll content in Fabaceae species. Acta Biol Cracoviensia Ser Bot Kraków **52**: 76

Gutsche AR, Heng-Moss TM, Higley LG, Sarath G, Mornhinweg DW (2009) Physiological responses of resistant and susceptible barley, *Hordeum vulgare* to the Russian wheat aphid, *Diurpahis noxia* (Mordvilko). Arthropod-Plant Interact **3**: 233–240

Haile FJ, Higley LG, Ni X, Quisenberry SS (1999) Physiological and growth tolerance in wheat to Russian wheat aphid (Homoptera: Aphididae) injury. Environ Entomol **28**: 787–794

Harmel N, Létocart E, Cherqui A, Giordanengo P, Mazzucchelli G, Guillonneau F, De Pauw E, Haubruge E, Francis F (2008) Identification of aphid salivary proteins: a proteomic investigation of *Myzus persicae*. Insect Mol Biol **17**: 165–174

Heng-Moss T, Macedo T, Franzen L, Baxendale F, Higley L, Sarath G (2006) Physiological responses of resistant and susceptible buffalograsses to *Blissus occiduus* (Hemiptera: Blissidae) feeding. J Econ Entomol **99**: 222–228

Hill CB, Li Y, Hartman GL (2006) Single dominant gene for resistance to the soybean aphid in the soybean cultivar Dowling. Crop Sci.

Hill CB, Shiao D, Fox CM, Hartman GL (2017) Characterization and genetics of multiple soybean aphid biotype resistance in five soybean plant introductions. Theor Appl Genet **130**: 1335–1348

Hodgson EW, McCornack BP, Tilmon K, Knodel JJ (2012) Management recommendations for soybean aphid (Hemiptera: Aphididae) in the United States. J Integr Pest Manag **3**: E1–E10

Howe GA, Ryan CA (1999) Suppressors of systemin signaling identify genes in the tomato wound response pathway. Genetics **153**: 1411–1421

Huot B, Yao J, Montgomery BL, He SY (2014) Growth–defense tradeoffs in plants: A balancing act to optimize fitness. Mol Plant **7**: 1267–1287

Iba K (2002) Acclimative response to temperature stress in higher plants: approaches of gene engineering for temperature tolerance. Annu Rev Plant Biol **53**: 225–245

Im YJ, Han O, Chung GC, Cho BH (2002) Antisense expression of an Arabidopsis omega-3 fatty acid desaturase gene reduces salt/drought tolerance in transgenic tobacco plants. Mol Cells **13**: 264–271

Jambunathan N (2010) Determination and detection of reactive oxygen species (ROS), lipid peroxidation, and electrolyte leakage in plants. Methods Mol Biol **639**: 292–298

Johnson MP (2016) Photosynthesis. Essays Biochem **60**: 255–273

Kaakeh W, Pfeiffer DG, Marini RP (1992) Combined effects of spirea aphid (Homoptera: Aphididae) and nitrogen fertilization on net photosynthesis, total chlorophyll content, and greenness of apple leaves. J Econ Entomol **85**: 939–946

Kangasjärvi S, Neukermans J, Li S, Aro E-M, Noctor G (2012) Photosynthesis, photorespiration, and light signalling in defence responses. J Exp Bot **63**: 1619–1636

Kariola T, Brader G, Li J, Palva ET (2005) Chlorophyllase 1, a damage control enzyme, affects the balance between defense pathways in plants. Plant Cell **17**: 282–294

Kerchev PI, Fenton B, Foyer CH, Hancock RD (2012) Plant responses to insect herbivory: interactions between photosynthesis, reactive oxygen species and hormonal signalling pathways. Plant Cell Environ **35**: 441–453

Keren N, Gong H, Ohad I (1995) Oscillations of reaction center II-D1 protein degradation in vivo induced by repetitive light flashes. Correlation between the level of RCII-QB- and protein degradation in low light. J Biol Chem **270**: 806–814

Khan SA, Murugan M, Starkey S, Manley A, Smith CM (2009) Inheritance and categories of resistance in wheat to Russian wheat aphid (Hemiptera: Aphididae) biotype 1 and biotype 2. J Econ Entomol **102**: 1654–1662

Koch RL, Hodgson EW, Knodel JJ, Varenhorst AJ, Potter BD (2018) Management of insecticide-resistant soybean aphids in the upper midwest of the United States. J Integr Pest Manag. doi: 10.1093/jipm/pmy014

Kodama H, Hamada T, Horiguchi G, Nishimura M, Iba K (1994) Genetic enhancement of cold tolerance by expression of a gene for chloroplast ω-3 fatty acid desaturase in transgenic tobacco. Plant Physiol **105**: 601–605

Kodama H, Horiguchi G, Nishiuchi T, Nishimura M, Iba K (1995) Fatty acid desaturation during chilling acclimation is one of the factors involved in conferring low-temperature tolerance to young tobacco leaves. Plant Physiol **107**: 1177–1185

Kucharik CJ, Mork AC, Meehan TD, Serbin SP, Singh A, Townsend PA, Stack Whitney K, Gratton C (2016) Evidence for compensatory photosynthetic and yield response of soybeans to aphid herbivory. J Econ Entomol **109**: 1177–1187

Laloi C, Przybyla D, Apel K (2006) A genetic approach towards elucidating the biological activity of different reactive oxygen species in *Arabidopsis thaliana*. J Exp Bot **57**: 1719–1724

Li C, Liu G, Xu C, Lee GI, Bauer P, Ling H-Q, Ganal MW, Howe GA (2003) The tomato *suppressor of prosystemin-mediated responses2* gene encodes a fatty acid desaturase required for the biosynthesis of jasmonic acid and the production of a systemic wound signal for defense gene expression. Plant Cell **15**: 1646–1661

Li Q, Xie Q-G, Smith-Becker J, Navarre DA, Kaloshian I (2006) *Mi-1*-mediated aphid resistance involves salicylic acid and mitogen-activated protein kinase signaling cascades. Mol Plant-Microbe Interact **19**: 655–664

Liu XY, Teng YB, Li B, Meng QW (2013) Enhancement of low-temperature tolerance in transgenic tomato plants overexpressing *Lefad7* through regulation of trienoic fatty acids. Photosynthetica **51**: 238–244

Liu X-Y, Yang J-H, Li B, Yang X-M, Meng Q-W (2006) Antisense-mediated depletion of tomato chloroplast omega-3 fatty acid desaturase enhances thermal tolerance. J Integr Plant Biol **48**: 1096–1107

Los DA, Murata N (1998) Structure and expression of fatty acid desaturases. Biochim Biophys Acta **1394**: 3–15

Louis J, Singh V, Shah J (2012) *Arabidopsis thaliana* - Aphid interaction. Arab Book Am Soc Plant Biol. doi: 10.1199/tab.0159

Macedo TB, Bastos CS, Higley LG, Ostlie KR, Madhavan S (2003a) Photosynthetic responses of soybean to soybean aphid (Homoptera: Aphididae) injury. J Econ Entomol **96**: 188–193

Macedo TB, Higley LG, Ni X, Quisenberry SS (2003b) Light activation of Russian wheat aphid-elicited physiological responses in susceptible wheat. J Econ Entomol **96**: 194–201

Macedo TB, Peterson RKD, Weaver DK, Ni X (2009) Impact of *Diuraphis noxia* and *Rhopalosiphum padi* (Hemiptera: Aphididae) on primary physiology of four near-isogenic wheat lines. J Econ Entomol **102**: 412–421

Macpherson AN, Telfer A, Barber J, Truscott TG (1993) Direct detection of singlet oxygen from isolated Photosystem II reaction centres. Biochim Biophys Acta - Bioenerg **1143**: 301–309

McConn M, Creelman RA, Bell E, Mullet JE, Browse J (1997) Jasmonate is essential for insect defense in Arabidopsis. Proc Natl Acad Sci **94**: 5473–5477

Mehler AH (1951) Studies on reactions of illuminated chloroplasts: I. Mechanism of the reduction of oxygen and other hill reagents. Arch Biochem Biophys **33**: 65–77

Meldau S, Erb M, Baldwin IT (2012) Defence on demand: mechanisms behind optimal defence patterns. Ann Bot **110**: 1503–1514

Mène-Saffrané L, Dubugnon L, Chételat A, Stolz S, Gouhier-Darimont C, Farmer EE (2009) Nonenzymatic oxidation of trienoic fatty acids contributes to reactive oxygen species management in Arabidopsis. J Biol Chem **284**: 1702–1708

Mewis I, Appel HM, Hom A, Raina R, Schultz JC (2005) Major signaling pathways modulate Arabidopsis glucosinolate accumulation and response to both phloem-feeding and chewing insects. Plant Physiol **138**: 1149–1162

Millar AA, Smith MA, Kunst L (2000) All fatty acids are not equal: discrimination in plant membrane lipids. Trends Plant Sci **5**: 95–101

Miller G, Schlauch K, Tam R, Cortes D, Torres MA, Shulaev V, Dangl JL, Mittler R (2009) The plant NADPH oxidase RBOHD mediates rapid systemic signaling in response to diverse stimuli. Sci Signal **2**: ra45

Miller G, Suzuki N, Ciftci-Yilmaz S, Mittler R (2010) Reactive oxygen species homeostasis and signalling during drought and salinity stresses. Plant Cell Environ **33**: 453–467

Moloi MJ, van der Westhuizen AJ (2006) The reactive oxygen species are involved in resistance responses of wheat to the Russian wheat aphid. J Plant Physiol **163**: 1118–1125

Morrison WP, Peairs FB (1998) Response model concept and economic impact. *In* SS Quisenberry, FB Peairs, eds, A Response Model for an Introduced Pest – The Russian Wheat Aphid. Thomas Say Publications in Entomology, Entomological Society of America, Lanham, USA, pp 1–11

Munns R (2002) Comparative physiology of salt and water stress. Plant Cell Environ **25**: 239–250

Murakami Y, Tsuyama M, Kobayashi Y, Kodama H, Iba K (2000) Trienoic fatty acids and plant tolerance of high temperature. Science **287**: 476–479

Nabity PD, Zavala JA, DeLucia EH (2009) Indirect suppression of photosynthesis on individual leaves by arthropod herbivory. Ann Bot **103**: 655–663

Ng JCK, Perry KL (2004) Transmission of plant viruses by aphid vectors. Mol Plant Pathol **5**: 505–511

Nguyen HM, Cuiné S, Beyly-Adriano A, Légeret B, Billon E, Auroy P, Beisson F, Peltier G, Li-Beisson Y (2013) The green microalga *Chlamydomonas reinhardtii* has a single ω-3 fatty acid desaturase that localizes to the chloroplast and impacts both plastidic and extraplastidic membrane lipids. Plant Physiol **163**: 914–928

Ni X, Quisenberry SS (2006) *Diuraphis noxia* and *Rhopalosiphum padi* (Hemiptera: Aphididae) interactions and their injury on resistant and susceptible cereal seedlings. J Econ Entomol **99**: 551–558

Noctor G, Foyer CH (1998) Ascorbate and glutathione: keeping active oxygen under control. Annu Rev Plant Physiol Plant Mol Biol **49**: 249–279

Pallipparambil GR, Reese JC, Avila CA, Louis JM, Goggin FL (2010) *Mi*-mediated aphid resistance in tomato: tissue localization and impact on the feeding behavior of two potato aphid clones with differing levels of virulence. Entomol Exp Appl **135**: 295–307

Parrella MP (2008) Biological control in protected culture: Will it continue to expand? Phytoparasitica **36**: 3–6

Petrov V, Hille J, Mueller-Roeber B, Gechev TS (2015) ROS-mediated abiotic stress-induced programmed cell death in plants. Front Plant Sci. doi: 10.3389/fpls.2015.00069

Pimentel D, Burgess M (2014) Environmental and economic costs of the application of pesticides primarily in the United States. *In* D Pimentel, R Peshin, eds, Integr. Pest Manag. Pestic. Probl. Vol3. Springer Netherlands, Dordrecht, pp 47–71

Pospísil P (2009) Production of reactive oxygen species by photosystem II. Biochim Biophys Acta **1787**: 1151–1160

Pospíšil P (2016) Production of reactive oxygen species by photosystem II as a response to light and temperature stress. Front Plant Sci **7**: 1950

Powell W, Pell JK (2007) Biological control. *In* HF van Emden, R Harrington, eds, Aphids Crop Pests. CABI, Wallingford, UK, pp 469–513

Reymond P, Bodenhausen N, Van Poecke RMP, Krishnamurthy V, Dicke M, Farmer EE (2004) A conserved transcript pattern in response to a specialist and a generalist herbivore. Plant Cell **16**: 3132–3147

Rosenthal WD, Arkin GF, Shouse PJ, Jordan WR (1987) Water deficit effects on transpiration and leaf growth. Agron J **79**: 1019–1026

Rossi M, Goggin FL, Milligan SB, Kaloshian I, Ullman DE, Williamson VM (1998) The nematode resistance gene *Mi* of tomato confers resistance against the potato aphid. Proc Natl Acad Sci **95**: 9750–9754

Rutledge CE, O'Neil RJ, Fox TB, Landis DA (2004) Soybean aphid predators and their use in integrated pest management. Ann Entomol Soc Am **97**: 240–248

Ryan JD, Johnson RC, Eikenbary RD, Dorschner KW (1987) Drought/greenbug interactions: photosynthesis of greenbug resistant and susceptible wheat. Crop Sci **27**: 283–288

Sánchez-Hernández C, López MG, Délano-Frier JP (2006) Reduced levels of volatile emissions in jasmonate-deficient *spr2* tomato mutants favour oviposition by insect herbivores. Plant Cell Environ **29**: 546–557

Shannag HK (2007) Effect of black bean aphid, *Aphis fabae*, on transpiration, stomatal conductance and crude protein content of faba bean. Ann Appl Biol **151**: 183–188

Shannag HK, Thorvilson H, El-Shatnawi MK (1998) Changes in photosynthetic and transpiration rates of cotton leaves infested with the cotton aphid, *Aphis gossypii*: Unrestricted infestation. Ann Appl Biol **132**: 13–18

Sharma P, Jha AB, Dubey RS, Pessarakli M (2012) Reactive oxygen species, oxidative damage, and antioxidative defense mechanism in plants under stressful conditions. J Bot. doi: 10.1155/2012/217037

Shi Y, Yue X, An L (2018) Integrated regulation triggered by a cryophyte ω-3 desaturase gene confers multiple-stress tolerance in tobacco. J Exp Bot **69**: 2131–2148

Song F, M Swinton S, Difonzo C, O'Neal M, Ragsdale D (2006) Profitability analysis of soybean aphid control treatments in three north-central states.

Staswick PE, Su W, Howell SH (1992) Methyl jasmonate inhibition of root growth and induction of a leaf protein are decreased in an *Arabidopsis thaliana* mutant. Proc Natl Acad Sci **89**: 6837–6840

Stintzi A, Weber H, Reymond P, Browse J, Farmer EE (2001) Plant defense in the absence of jasmonic acid: The role of cyclopentenones. Proc Natl Acad Sci **98**: 12837–12842

Sun Y, Guo H, Yuan L, Wei J, Zhang W, Ge F (2015) Plant stomatal closure improves aphid feeding under elevated CO_2. Glob Change Biol **21**: 2739–2748

Suza WP, Avila CA, Carruthers K, Kulkarni S, Goggin FL, Lorence A (2010) Exploring the impact of wounding and jasmonates on ascorbate metabolism. Plant Physiol Biochem **48**: 337–350

Tatchell GM, Collier RH, Hough GL (2017) IPM case studies: leafy salad crops. *In* HF van Emden, R Harrington, eds, Aphids Crop Pests, 2nd ed. CABI, Wallingford, UK, pp 569–577

Tripathy BC, Oelmüller R (2012) Reactive oxygen species generation and signaling in plants. Plant Signal Behav **7**: 1621–1633

Upchurch RG (2008) Fatty acid unsaturation, mobilization, and regulation in the response of plants to stress. Biotechnol Lett **30**: 967–977

Voss I, Sunil B, Scheibe R, Raghavendra AS (2013) Emerging concept for the role of photorespiration as an important part of abiotic stress response. Plant Biol **15**: 713–722

Wallis JG, Browse J (2002) Mutants of Arabidopsis reveal many roles for membrane lipids. Prog Lipid Res **41**: 254–278

Wang H-S, Yu C, Tang X-F, Zhu Z-J, Ma N-N, Meng Q-W (2014) A tomato endoplasmic reticulum (ER)-type omega-3 fatty acid desaturase (LeFAD3) functions in early seedling tolerance to salinity stress. Plant Cell Rep **33**: 131–142

Webb MS, Green BR (1991) Biochemical and biophysical properties of thylakoid acyl lipids. Biochim Biophys Acta - Bioenerg **1060**: 133–158

White C, Eigenbrode SD (2000) Effects of surface wax variation in *Pisum sativum* on herbivorous and entomophagous insects in the field. Environ Entomol **29**: 773–780

Wood BW, Tedders WL, Thompson JM (1985) Feeding influence of 3 pecan aphid species on carbon exchange and phloem integrity of seedling pecan foliage. J Am Soc Hortic Sci **110**: 393–396

Yaeno T, Matsuda O, Iba K (2004) Role of chloroplast trienoic fatty acids in plant disease defense responses. Plant J Cell Mol Biol **40**: 931–941

Yara A, Yaeno T, Hasegawa M, Seto H, Montillet J-L, Kusumi K, Seo S, Iba K (2007) Disease resistance against *Magnaporthe grisea* is enhanced in transgenic rice with suppression of ω-3 fatty acid desaturases. Plant Cell Physiol **48**: 1263–1274

Yu C, Wang H-S, Yang S, Tang X-F, Duan M, Meng Q-W (2009) Overexpression of endoplasmic reticulum omega-3 fatty acid desaturase gene improves chilling tolerance in tomato. Plant Physiol Biochem PPB **47**: 1102–1112

Yu S-X, Feng Q-N, Xie H-T, Li S, Zhang Y (2017) Reactive oxygen species mediate tapetal programmed cell death in tobacco and tomato. BMC Plant Biol **17**: 76

Zhang M, Barg R, Yin M, Gueta-Dahan Y, Leikin-Frenkel A, Salts Y, Shabtai S, Ben-Hayyim G (2005) Modulated fatty acid desaturation via overexpression of two distinct omega-3 desaturases differentially alters tolerance to various abiotic stresses in transgenic tobacco cells and plants. Plant J Cell Mol Biol **44**: 361–371

Zhang YM, Wang CC, Hu HH, Yang L (2011) Cloning and expression of three fatty acid desaturase genes from cold-sensitive lima bean (*Phaseolus lunatus* L.). Biotechnol Lett **33**: 395–401

Zou J, Rodriguez-Zas S, Aldea M, Li M, Zhu J, Gonzalez DO, Vodkin LO, DeLucia E, Clough SJ (2005) Expression profiling soybean response to *Pseudomonas syringae* reveals new defense-related genes and rapid HR-specific downregulation of photosynthesis. Mol Plant-Microbe Interact MPMI **18**: 1161–1174

Chapter II

Enhanced photosynthetic efficiency in tomato with loss of function of FATTY ACID DESATURASE 7

Abstract

Loss of function of Fatty Acid Desaturase 7 (FAD7) in tomato alters the fatty acid profiles of chloroplast membranes and enhances resistance against potato aphids. We hypothesize that FAD7 also influences photosynthesis as a result of its effects on the chloroplast membrane. Here, we compared chlorophyll content, gas exchange, and chlorophyll fluorescence in isogenic tomato genotypes with wild-type (WT) (cv. Castlemart) and impaired *FAD7* function (the *spr2* mutant) under two light intensities (220 µmol/m^2/sec and 440 µmol/m^2/sec). At 220 µmol m^{-2} s^{-1}, the *spr2* mutants had significantly lower chlorophyll content compared to WT plants, but there was no significant difference in chlorophyll content at higher light intensities. Surprisingly, carbon assimilation (A) was significantly higher in *spr2* than in WT plants at both light levels. The maximum quantum efficiency (F_v/F_m) of photosystem II (PSII) and PSII operating efficiency (ΦPSII) were higher in *spr2* than in wild-type plants, and this appeared to be due to the fact that *spr2* had lower values for minimal chlorophyll fluorescence (F_o) and non-photochemical quenching (NPQ) than WT controls. CO_2 response curves also indicated higher *in vivo* Rubisco activity in *spr2* under saturating light intensity (1200 µmol/m^2/sec). These data demonstrate that FAD7 influences photosynthetic activity, which may in part explain its influence on resistance to biotic and abiotic stresses.

Introduction

Fatty acids are essential components of cell membranes (Li et al., 2003). Almost all plant membranes are made of 18-carbon fatty acids and some also have 16-carbon fatty acids. Both 18 and 16-carbon fatty acids contain up to three double bonds (Millar et al., 2000). Fatty acid desaturases (FADs) are enzymes that introduce double bonds into the acyl chains of fatty acids and influence plants' levels of resistance to a variety of stresses (Li et al., 2003). FADs are widely distributed, except in some bacteria such as *Escherichia coli* (Los and Murata, 1998). Most FADs are membrane proteins that are localized in the plastids or the endoplasmic reticulum. Fatty Acid Desaturase7 (FAD7) is a chloroplast localized enzyme that converts linoleic acid (C18:2) to linolenic acid (C18:3) (Li et al., 2003). It's chloroplast specificity was proven by a RNA gel blot analysis comparing leaves and roots (Li et al., 2003) and also by confocal image analysis (Andreu et al., 2007).

The *suppressor of prosystemin-mediated response2* (*spr2*) mutant in tomato, *Solanum lycopersicum*, which was generated through ethyl methanesulfonate (EMS) mutagenesis, results in the loss of function of Fatty Acid Desaturase7 (FAD7) (Howe and Ryan, 1999; Li et al., 2003). The *spr2* contains a point mutation that introduces a premature stop codon to the protein (Li et al., 2003), thus it contains increased levels of 18:2 and 16:2 and decreased levels of 18:3 and 16:3 fatty acids (Browse et al., 1986; Li et al., 2003; Hiremath et al., 2017).

The *spr2* mutant in tomato reduces survival and reproduction of potato aphids (*Macrosiphum euphorbiae*). Compared to wild-type (WT) tomato plants, the aphid mortality rate was over 50 percent higher and the average aphid survival is about 3 days shorter on *spr2* mutants. The Arabidopsis *fad7* mutant, which is functionally analogous to the *spr2* mutant also

increased resistance against green peach aphids (*Myzus persicae*) (Avila et al., 2012) showing that loss of function of FAD7 enhances aphid resistance in more than one plant family.

The *spr2* mutant has compromised jasmonic acid (JA) signaling compared to WT plants (Li et al., 2003). During defense responses, JA induction is known to inhibit growth and photosynthesis (Staswick et al., 1992; Havko et al., 2016). A study that used exogenous coronatine (COR), a structural mimic of a receptor-active form of JA, on Arabidopsis has shown reductions in photosynthesis and growth within 24 hours and strong inductions of defense genes immediately (Attaran et al., 2014). Nabity et al. (2009) have shown immediate reductions in carbon assimilation and electron transport in response to herbivore damage in WT *Nicotiana attenuata* plants compared to antisense LOX3 plants with suppressed JA signaling. These studies show that after stresses such as wounding or insect attack, JA mutants have higher photosynthetic rates than WT plants. To understand how *spr2* plants may contribute to enhanced aphid resistance, we investigated whether the growth and photosynthesis would enhance when the JA levels are constitutively suppressed in the absence of stress. One study has reported that, in the absence of cadmium treatment, photosynthetic parameters in *spr2* were similar to those of WT tomato plants (Zhao et al., 2016). However, these measurements were taken at very low light intensity (150 μmol/m^2/sec); therefore, we cannot make conclusions on how the suppressed JA levels in *spr2* would affect growth and photosynthesis under optimal conditions.

The objective of this study was to determine whether the *spr2* mutants affect photosynthetic activity and growth in tomato under moderate temperature and low to moderate light levels. Therefore, we compared total chlorophyll content, the net carbon assimilation rate (A, a measure of photosynthetic activity), the maximum quantum efficiency of photosystem II (F_v/F_m, a measure of plants' capacity for photosynthetic electron transport), PSII operating

efficiency (ΦPSII, the fraction of light energy captured by PSII that is used in photochemistry), non-photochemical quenching (NPQ, fraction of light energy that is lost as heat) and the efficiency of Rubisco (the first major enzyme involved in light-independent reactions of photosynthesis) in *spr2* mutants and WT plants.

Materials and Methods

Plant materials and growth conditions

Wild-type (WT) tomato (*Solanum lycopersicum* cv. Castlemart) and a *FAD7*-impaired mutant – *suppressor of prosystemin-mediated response2* (*spr2*) – were grown in LC1 Sunshine Professional Growing Mix (Sungro Horticulture, Agawam, MA) amended with slow-release fertilizer (Osmocote Plus; 15-9-12) (Scotts-MiracleGro Company, Marysville, OH) in a Conviron growth chamber (Temp: 23 °C, RH: ~60%, light intensity: 220 µmol/m^2/sec, and 16-h/8-h light/dark photoperiod). Plants were watered with a nutrient solution containing 1000 ppm $CaNO_3$ (Hydro Agri North America, Tampa, FL), 500 ppm $MgSO_4$ (Giles Chemical, Waynesville, NC) and 500 ppm 4-18-38 Gromore fertilizer (Grow More, Gardena, CA). Forty-eight hours before measurements were taken, half of the plants were exposed to 440 µmol/m^2/sec and the remaining plants were kept at 220 µmol/m^2/sec. Two light levels were used since our preliminary observations have shown that the *spr2* plants were greener when they were grown under a higher light intensity. Plant height and the number of leaves of 4-week old WT and *spr2* plants were recorded prior to the light exposure.

Chlorophyll content measurements

Chlorophyll content of 4-week old *spr2* and WT plants was measured using a SPAD-502 meter (Minolta) on the 5th leaf below the apical meristem to determine if the total chlorophyll

content of the two genotypes differed under two light intensities. Fifth leaf was selected since it was a fully expanded medium-aged leaf and the damage that can be caused by the measuring instruments is minimal on a medium-aged leaf compared to very young leaf.

Gas exchange and fluorescence measurements

Gas exchange and fluorescence measurements were performed simultaneously using a LI-6400XT open portable photosynthesis system with a leaf chamber fluorometer, an LED-based fluorescence attachment (LCF 6400-40) (LI-COR, Lincoln, NE, USA) on the 5^{th} leaf of 4-week old *spr2* and WT plants under the two light intensities. First, all the plants were dark-adapted overnight and minimal fluorescence (F_o) and maximum fluorescence (F_m) measurements were taken while the plants were in the dark. After the dark-adapted measurements were taken, lights were turned on in the growth chamber and the plants were allowed to adapt to the respective light intensity for 30-45 minutes. Then, light-adapted fluorescence measurements and gas exchange measurements were recorded simultaneously. During the measurements, the conditions in the LCF chamber was maintained at 400 ppm reference CO_2 concentration, 55-65% relative humidity and 300 µmol/m^2/sec airflow. The following parameters were analyzed using the gas exchange and fluorescence data: carbon assimilation (A), minimal fluorescence in dark-adapted leaves (F_o), maximum quantum efficiency of photosystem II (F_v/F_m), PSII operating efficiency (ΦPSII), and non-photochemical quenching (NPQ). NPQ was calculated according to Tietz et al. (2017). Formulas and variable definitions are as follows:

$$\frac{F_v}{F_m} = \frac{F_m - F_o}{F_m}$$

$$\Phi PSII = \frac{F_m' - F_s}{F_m'}$$

$$NPQ_{(T)} = \frac{4.88}{\left(\frac{F_m'}{F_o'}\right) - 1} - 1$$

F_o = minimal fluorescence in dark-adapted leaves

F_m = maximal fluorescence in dark-adapted leaves

F_o' = minimal fluorescence in light-adapted leaves

F_m' = maximal fluorescence in light-adapted leaves

F_s = steady-state fluorescence

All light-adapted gas exchange and fluorescence measurements were performed between 8:00 am and 12:00 pm each day in order to avoid diurnal fluctuations in photosynthetic parameters. Eight plants (two plants per treatment group) were measured per day in order to allow ample time for gas exchange rates to be stabilized. Therefore, the experiment was replicated in time, over the course of eight days. Planting dates for the experiment were staggered to ensure that all replicates were the same age at the time of measurement (4 weeks after planting). The data were analyzed by two-way ANOVA and the days each plant was measured (measurement days) were treated as random blocks. If significant differences were found, mean separations were done by a Tukey's HSD. The statistical analyses were conducted with JMP® Pro 13 (SAS Institute Inc.).

CO_2 response curves

In a separate experiment, WT and *spr2* plants were grown at 440 µmol/m^2/sec and CO_2 response (A/Ci) curves were generated using a different set of plants to determine plant responses to varying intercellular CO_2 concentrations. Leaves (5^{th} leaf from apical meristem) were exposed to different levels of CO_2, and the net photosynthetic rate at each CO_2 level was measured under saturating light intensity (1200 µmol/m^2/sec), which was determined by a light

response curve. Before recording measurements, the designated leaf was placed inside the LCF chamber head, and the CO_2 assimilation rate was allowed to stabilize at 1200 µmol/m^2/sec light intensity, 400 ppm (ambient) CO_2 concentration and 55-65% relative humidity. Once the photosynthesis rates stabilized (assessed by observing real-time graphs), the A-Ci curve was generated using the auto-program feature of the LI-6400XT. It was programmed to change the CO_2 concentration through the following sequence of levels: 300, 200, 100, 50, 400, 400, 600, 800, 1000 ppm. At each CO_2 concentration, the carbon assimilation readings were automatically recorded immediately after stabilization, which was generally within 2 minutes. Two 400 ppm points were logged in order to allow the leaf to recover after being exposed to low CO_2 concentrations. The maximum carboxylation rate of Rubisco/*in vivo* apparent Rubisco activity (V_{cmax}) and the maximum rate of electron transport used in the regeneration of ribulose-1,5-bisphosphate (RuBP) (J_{max}) of 4-week old *spr2* and WT plants were estimated using the A/Ci curve fitting utility provided by Sharkey et al. (2007) by fitting the Farquhar, von Caemmerer, Berry (FvCB) model (Farquhar et al., 1980). All the CO_2 response curves were generated between 8:00 am and 12:00 pm. A total of seven plants per genotype were measured over 4 days (1 plant per genotype on the day 1, and 2 plants per genotype on day 2, 3 and 4). To make sure the plants were at the same age at the time of measurement, the planting dates were staggered. The data were analyzed by one-way ANOVA and the days each plant was measured were treated as random blocks. The statistical analyses were conducted with JMP® Pro 13 (SAS Institute Inc.).

Results

WT and spr2 plants are phenotypically different

WT plants were taller compared to *spr2* plants by 4% (t = 3.90; df = 1, 62; $P = 0.0003$). In addition, *spr2* plants have significantly greater number of leaves (19%) compared to WT plants (t = -9.53; df = 1, 62; $P<0.0001$) (Figure 1).

Chlorophyll content is higher in WT than in spr2 under low light intensity

The WT line had significantly greater total chlorophyll content compared to *spr2* plants under 220 µmol/m^2/sec light exposure (Genotype: $F = 40.63$, df = 1, 7, $P = 0.0004$; Light intensity: $F = 29.16$, df = 1, 14, $P<0.0001$; Genotype x Light intensity: $F = 7.70$, df = 1, 14, $P = 0.0149$) (Figure 2). When the plants were subjected to a short-term exposure to a higher light intensity, chlorophyll content of the *spr2* increased by 11%. There was no significant difference in chlorophyll content between the genotypes under 440 µmol/m^2/sec light exposure.

spr2 has a higher carbon assimilation rate compared to WT

Under both light intensities, *spr2* had 12-15% higher carbon assimilation than WT plants (Genotype: $F = 18.11$, df = 1, 7, $P = 0.0038$; Light intensity: $F = 247.93$, df = 1, 14, $P<0.0001$; Genotype x Light intensity: $F = 1.96$, df = 1, 14, $P = 0.1834$) (Figure 3).

The spr2 mutant exhibits better efficiency of light-dependent reactions compared to WT

Minimum chlorophyll fluorescence in dark-adapted leaves (F_o) was significantly greater in WT by 15% compared to *spr2* under both light intensities (Figure 4A). However, the light intensity did not influence F_o (Genotype: $F = 50.34$, df = 1, 7, $P = 0.0002$; Light intensity: $F = 4.10$, df = 1, 14, $P = 0.0624$; Genotype x Light intensity: $F = 0.94$, df = 1, 14, $P = 0.3491$).

Maximum chlorophyll fluorescence in dark-adapted leaves (F_m) did not show significant differences among the genotypes under either of the light intensities (at 220 µmol/m^2/sec: WT = 753.67 ± 26.84, *spr2* = 742.39 ± 37.07; at 440 µmol/m^2/sec: WT = 715.23 ± 87.05, *spr2* = 719.55 ± 27.79) (mean ± SD). The maximum quantum efficiency of PSII in dark-adapted leaves (F_v/F_m) was also significantly greater in *spr2* under both light intensities (Genotype: F = 63.60, df = 1, 7, P<0.0001; Light intensity: F = 0.61, df = 1, 14, P = 0.4488; Genotype x Light intensity: F = 0.01, df = 1, 14, P = 0.9188) (Figure 4B). At 440 µmol/m^2/sec light exposure, WT had significantly lower F_v/F_m values compared to *spr2*. Similar to F_o, the increasing light levels did not affect F_v/F_m values. PSII operating efficiency (ΦPSII) was significantly higher in *spr2* compared to WT under both light intensities and it decreased as the light level increases (Genotype: F = 28.10, df = 1, 7, P = 0.0011; Light intensity: F = 66.22, df = 1, 14, P<0.0001, Genotype x Light intensity: F = 0.64, df = 1, 14, P = 0.4359) (Figure 4C). Non-photochemical quenching (NPQ), which estimates the fraction of light lost to heat was significantly higher in WT by 53% at 220 µmol/m^2/sec and 37% at 440 µmol/m^2/sec than *spr2* (Genotype: F = 74.39, df = 1, 7, P<0.0001; Light intensity: F = 21.65, df = 1, 14, P = 0.0004; Genotype x Light intensity: F = 0.00002, df = 1, 14, P = 0.9965) (Figure 4D).

The spr2 mutant has more efficient light-independent reactions compared to WT

The CO_2 response curves generated are shown in Figure 5. Rubisco-mediated carboxylation rate (V_{cmax}) was significantly higher in *spr2* plants than WT plants by 28% (One-way ANOVA: F = 12.44; df = 1, 2.9; P = 0.042). Similarly, the maximum rate of electron transport used in the regeneration of RuBP (J_{max}) of *spr2* plants was significantly higher than that of WT plants by 24% (One-way ANOVA: F = 52.54; df = 1, 2.9; P = 0.009) (Table 1).

Discussion

Here we demonstrate that a tomato mutant with impaired *FAD7* function (*spr2*) has significantly greater carbon assimilation rates than the corresponding wild-type plants. Although carbon assimilation increased with increasing light intensity, as expected from previous reports (Harley et al., 1985), light intensity – at least at the levels tested here – did not influence the differences in carbon assimilation observed between *spr2* and WT plants. Differences in carbon assimilation were not due to differences in chlorophyll content. In fact, at low light, *spr2* had significantly lower chlorophyll levels than WT plants, despite higher assimilation rates. Instead, increased photosynthetic efficiency in *spr2* was associated with enhancements in both light-dependent and light-independent reactions of photosynthesis.

The operating efficiency of PSII (ΦPSII), where the light-dependent reactions of photosynthesis are initiated, was significantly greater in *spr2* than in WT plants. This indicates that a higher fraction of light-energy captured by PSII was directed toward the photochemical quenching in *spr2* compared to WT. Consistent with this, *spr2* plants also had lower NPQ values than WT, indicating that less light energy was dissipated as heat in *spr2* mutant. It was reported that under high temperature levels, PSII reaction centers could dislodge from the thylakoid membranes due to increased fluidity (Janka et al., 2013). Although, we do not know whether the WT has increased fluidity at the temperature they were grown in this study, it is possible that the membrane fluidity in WT could alter the location of reaction center, which leads to reduced efficiency of PSII.

Another measure of the light-dependent reactions, the maximum quantum yield of photosystem II (F_v/F_m) was significantly greater in *spr2* plants compared to WT plants. The ratio

F_v/F_m is calculated based on measurements of maximal chlorophyll fluorescence (F_m) in response to saturating light and minimal chlorophyll fluorescence (F_o) in the absence of light levels adequate for photosynthesis ($F_v/F_m = (F_m - F_o)/F_m$) (Baker, 2008). The enhanced F_v/F_m in *spr2* was due to significant reductions in F_o, a parameter that is sometimes used as an indicator of photodamage (Krause and Weis, 1991; Rodrigues et al., 2008). These data suggest that *spr2* may have greater photosynthetic efficiency because the *spr2* mutants accumulate less photodamage than wild-type plants. The increased NPQ in WT can be explained by this as well, since NPQ can be increased as a result of photodamage in the PSII, which leads to oxidative damage and increases in F_o (Baker, 2008). The primary site of photodamage is the D1 protein in PSII (Mattoo et al., 1999). Sun et al. (2010) showed that the increased membrane unsaturation can increase the rate of D1 protein degradation during salt stress. Degradation of the D1 protein is a repair mechanism that is essential to maintain the photosynthetic efficiency (Andersson and Aro, 2001). This suggests that WT may have a high rate of D1 protein degradation. Since it is an essential repair mechanism, the WT plants may put more energy towards D1 protein degradation rather than on photosynthesis. These results suggest that the light-dependent reactions of photosynthesis are more efficient in *spr2* mutants, since it had significantly higher F_v/F_m and ΦPSII, and significantly lower NPQ than WT.

Consistently, V_{cmax} and J_{max} were significantly greater in *spr2* than in WT. This supports the previous claims; decreased photosynthetic capacity is followed by reductions in V_{cmax} and J_{max}. These results indicate that photosynthesis in WT plants could be limited by both Rubisco enzyme and RuBP regeneration (Sharkey et al., 2007; Sharkey, 2016). The reductions in V_{cmax} are associated with inactivation or loss of Rubisco (Zhou et al., 2004). Reductions in the amount of Rubisco protein in response to JA in rice (Rakwal and Komatsu, 2000) and in barley (Popova

and Vaklinova, 1988) have been reported. Supporting this claim, gene expression studies have shown that genes encoding small and large subunits of Rubisco are downregulated by JA (Reinbothe et al., 1994). However, another study has shown that gene expression of the Rubisco small subunit was decreased in antisense LOX3 plants, which have suppressed JA signaling compared to controls in *N. attenuata* in response to herbivore damage (Halitschke and Baldwin, 2003). These results are not consistent with one another. The results observed in this study is consistent with Reinbothe et al. (1994) since the *spr2* mutants have compromised JA signaling and greater Rubisco activity compared to WT.

In addition to photosynthesis, the growth of *spr2* plants differed from WT plants in terms of height and number of leaves. The *spr2* plants were shorter, but had more leaves compared to WT indicating that they are compact and have shorter internodal length than WT. However, stunted growth has been reported in *N. attenuata* plants with enhanced levels of JA (Heinrich et al., 2013). The authors indicate that JA could suppress internode elongation by influencing synthesis of gibberellins, which are known to promote stem and leaf growth. Moreover, they measured the plant height over time and it appears that 29 days after germination, the height did not differ. The difference between the heights increases as the plants got older. Although their (Heinrich et al., 2013) results showed the opposite pattern of our results, it could be useful to measure the plant height over time to see how it changes.

Despite having lower chlorophyll levels and shorter internodal length, *spr2* plants enhanced photosynthesis compared to WT plants under the light levels we tested. Further work is needed to understand how this enhanced photosynthesis in *spr2* mutants would affect the primary metabolites and whether the changes in metabolite profiles would contribute to aphid resistance.

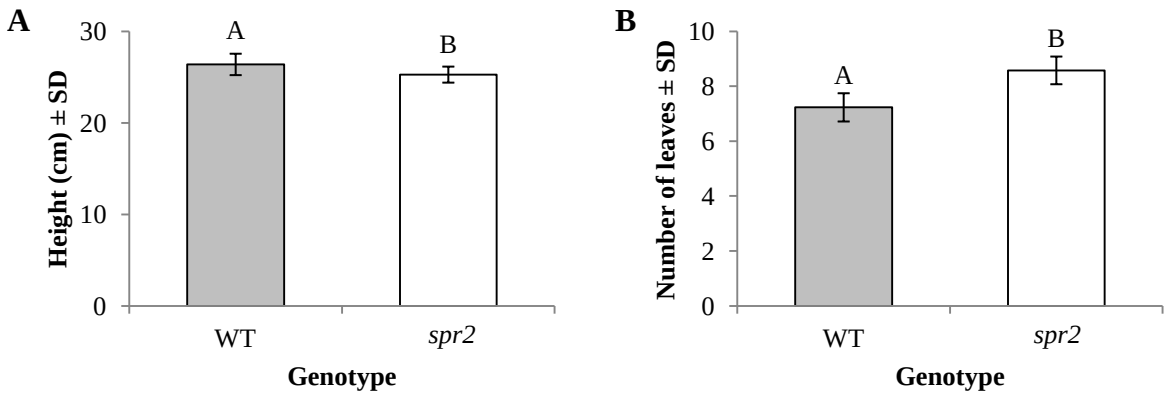

Figure 1. Height (A) and the number of leaves (B) of 4-week old WT and *FAD7*-impaired (*spr2*) tomato plants. Data were analyzed by Student's t-test. Error bars represent SD and the bars labeled with different letters differ significantly at $\alpha = 0.05$, n=32.

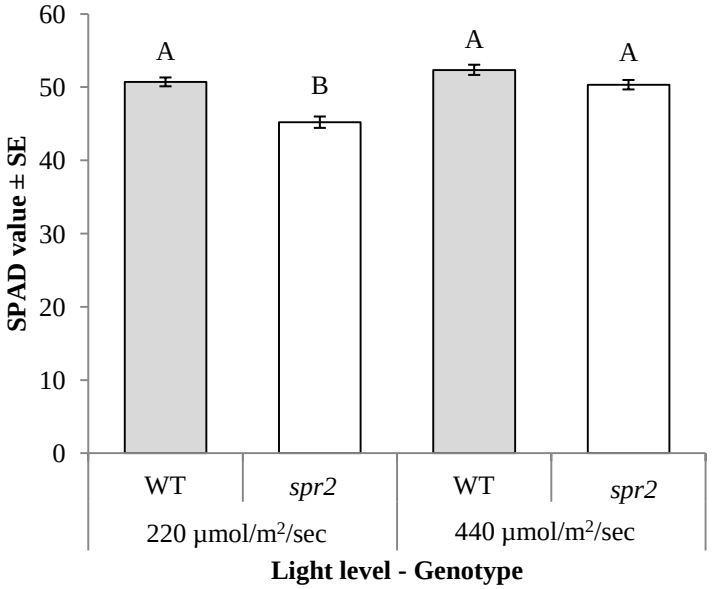

Figure 2. Chlorophyll content of 4-week old WT and *FAD7*-impaired (*spr2*) tomato plants. SPAD readings of the 5th leaf from apical meristem were analyzed by two-way ANOVA, and mean separations were performed using Tukey-Kramer HSD. Error bars represent SEM and the bars labeled with different letters differ significantly at $\alpha = 0.05$, n = 16.

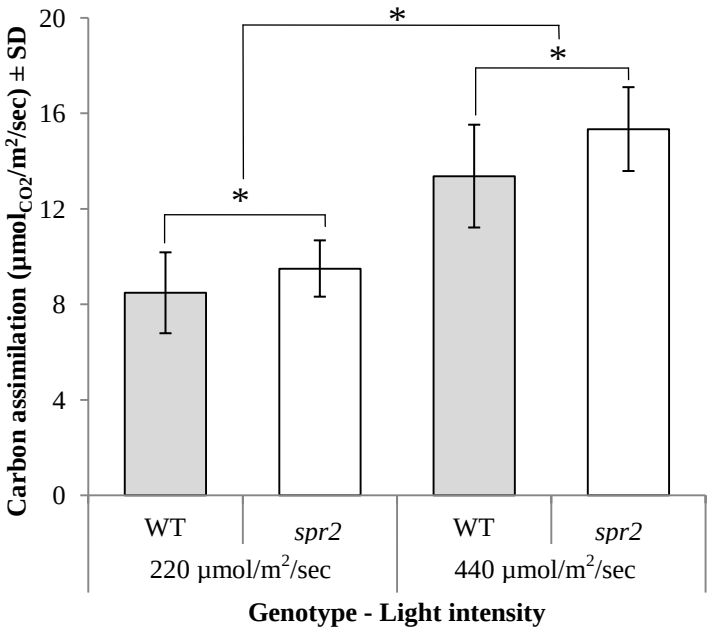

Figure 3. Carbon Assimilation of 4-week old WT and *FAD7*-impaired (*spr2*) tomato plants measured on the 5th leaf from apical meristem. Data were analyzed by two-way ANOVA. Error bars represent SD. Marked pairwise comparisons denote significant differences according to paired t-tests at $\alpha = 0.05$, n=16.

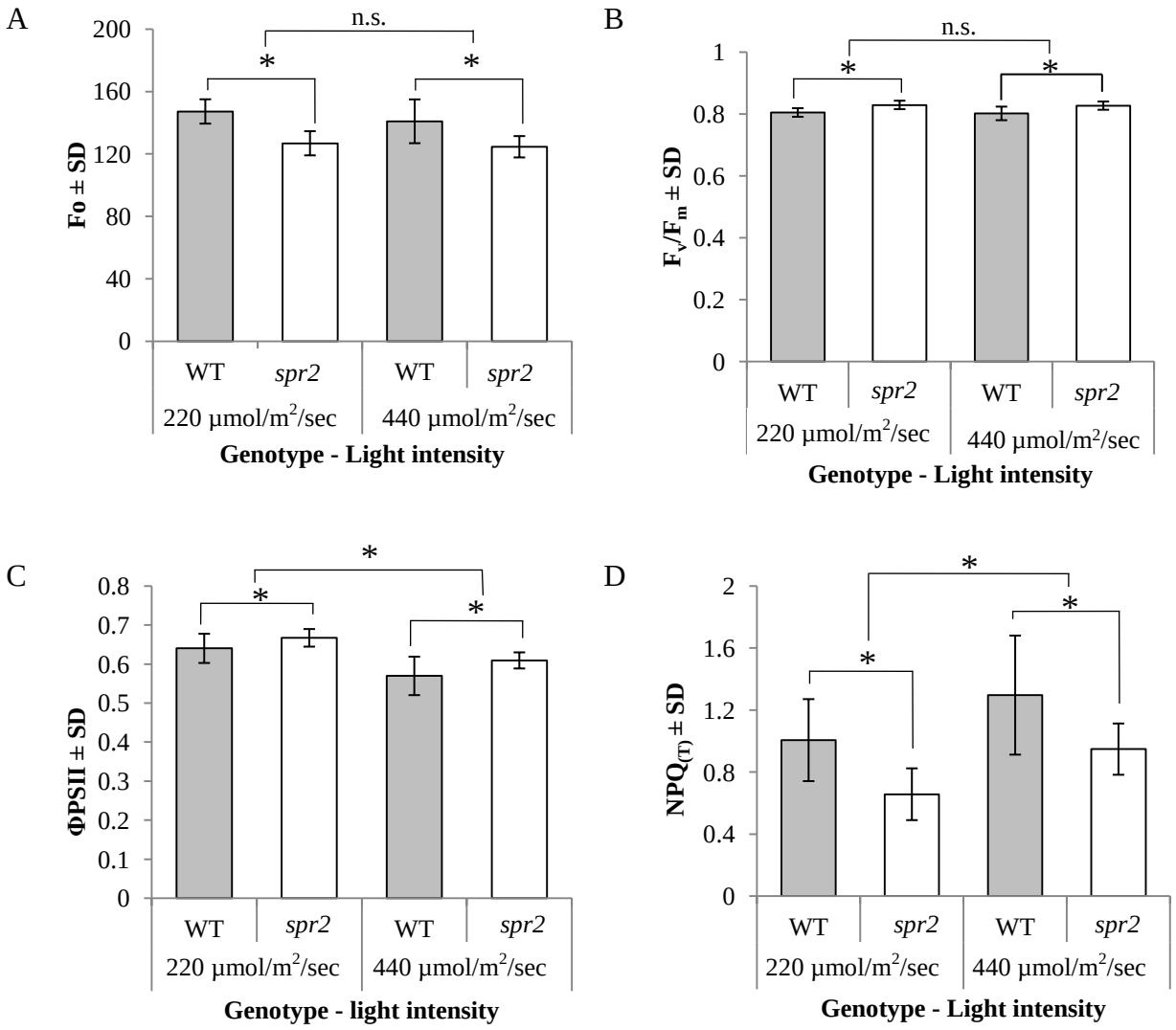

Figure 4. The efficiency of the light-dependent reactions of photosynthesis of 4-week old WT and *FAD7*-impaired (*spr2*) tomato plants. Minimal fluorescence of dark-adapted leaves (F_o, in A), maximum quantum efficiency of photosystem II (PSII) when dark-adapted (F_v/F_m, in B), PSII operating efficiency (ΦPSII, in C) and non-photochemical quenching ($NPQ_{(T)}$, in D) were compared in the 5th leaf of WT and *FAD7*-impaired plants (*spr2*). Data were analyzed by two-way ANOVA. Error bars represent SD. Marked pairwise comparisons denote significant differences according to paired t-tests at $\alpha = 0.05$, n = 16, n.s. = not significant.

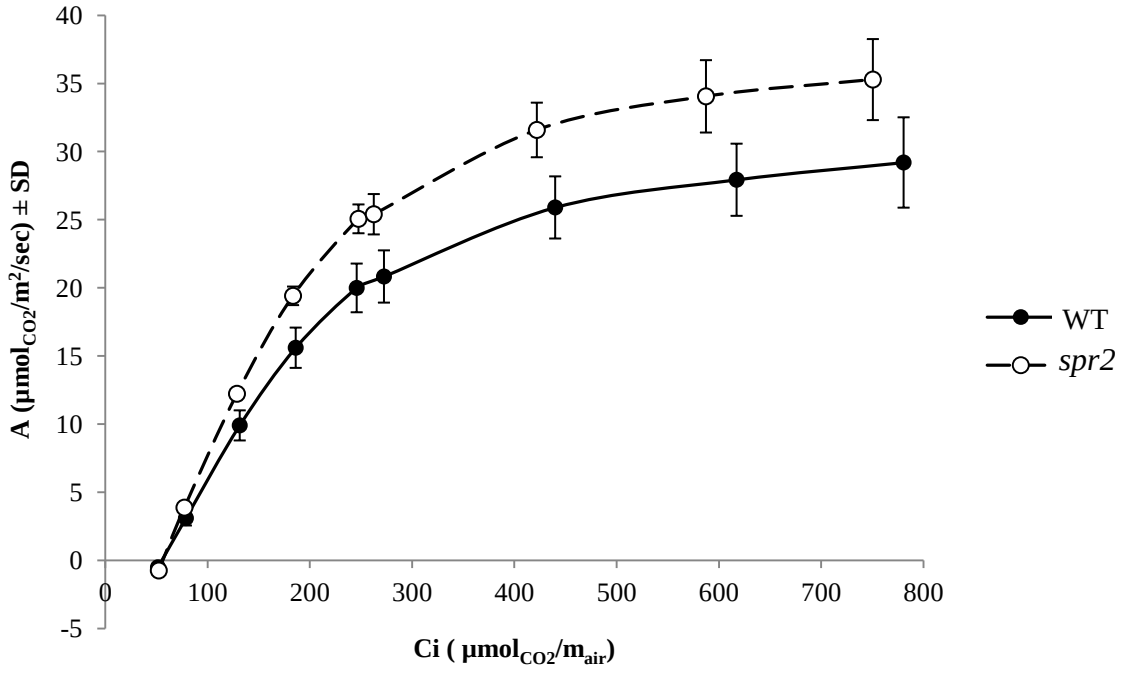

Figure 5. CO_2 response (A/Ci) curves of 4-week old WT and *FAD7*-impaired (*spr2*) tomato plants. From these data, maximum carboxylation rate of Rubisco (V_{cmax}) and maximum rate of electron transport used in the regeneration of RuBP (J_{max}) were calculated using the utility provided by Sharkey et al. (2007). The calculated values are shown in Table 1. Error bars represent SD.

Table 1. Maximum carboxylation rate of Rubisco (V_{cmax}) and maximum rate of electron transport used in the regeneration of RuBP (J_{max}) of 4-week old WT and *FAD7*-impaired (*spr2*) tomato plants. V_{cmax} and J_{max} were calculated using CO_2 response curves with ± SD, n=7.

	WT	***spr2***	**p-value**
V_{cmax} (µmol/m^2/sec)	110.57 ± 21.4	141.57 ± 26.5	0.033
J_{max} (µmol/m^2/sec)	153.00 ± 20.1	190.29 ± 23.9	0.008

References

Andersson B, Aro E-M (2001) Photodamage and D1 protein turnover in Photosystem II. *In* E-M Aro, B Andersson, eds, Regul. Photosynth. Springer Netherlands, Dordrecht, pp 377–393

Andreu V, Collados R, Testillano PS, Risueño M del C, Picorel R, Alfonso M (2007) In situ molecular identification of the plastid ω3 Fatty Acid Desaturase FAD7 from soybean: evidence of thylakoid membrane localization. Plant Physiol **145**: 1336–1344

Attaran E, Major IT, Cruz JA, Rosa BA, Koo AJK, Chen J, Kramer DM, He SY, Howe GA (2014) Temporal dynamics of growth and photosynthesis suppression in response to jasmonate signaling. Plant Physiol **165**: 1302–1314

Avila CA, Arévalo-Soliz LM, Jia L, Navarre DA, Chen Z, Howe GA, Meng Q-W, Smith JE, Goggin FL (2012) Loss of function of FATTY ACID DESATURASE7 in tomato enhances basal aphid resistance in a salicylate-dependent manner. Plant Physiol **158**: 2028–2041

Baker NR (2008) Chlorophyll fluorescence: a probe of photosynthesis in vivo. Annu Rev Plant Biol **59**: 89–113

Browse J, McCourt P, Somerville C (1986) A mutant of arabidopsis deficient in C18:3 and C16:3 leaf lipids. Plant Physiol **81**: 859–864

Farquhar GD, von Caemmerer S, Berry JA (1980) A biochemical model of photosynthetic CO_2 assimilation in leaves of C3 species. Planta **149**: 78–90

Halitschke R, Baldwin IT (2003) Antisense LOX expression increases herbivore performance by decreasing defense responses and inhibiting growth-related transcriptional reorganization in *Nicotiana attenuata*. Plant J Cell Mol Biol **36**: 794–807

Harley PC, Weber JA, Gates DM (1985) Interactive effects of light, leaf temperature, CO_2 and O_2 on photosynthesis in soybean. Planta **165**: 249–263

Havko N, Major I, Jewell J, Attaran E, Browse J, Howe G, Havko NE, Major IT, Jewell JB, Attaran E, et al (2016) Control of carbon assimilation and partitioning by jasmonate: An accounting of growth–defense tradeoffs. Plants **5**: 7

Heinrich M, Hettenhausen C, Lange T, Wünsche H, Fang J, Baldwin IT, Wu J (2013) High levels of jasmonic acid antagonize the biosynthesis of gibberellins and inhibit the growth of *Nicotiana attenuata* stems. Plant J **73**: 591–606

Hiremath SS, Sajeevan RS, Nataraja KN, Chaturvedi AK, Chinnusamy V, Pal M (2017) Silencing of fatty acid desaturase (FAD7) gene enhances membrane stability and photosynthetic efficiency under heat stress in tobacco (*Nicotiana benthamiana*). Indian J Exp Biol **55**: 532–541

Howe GA, Ryan CA (1999) Suppressors of systemin signaling identify genes in the tomato wound response pathway. Genetics **153**: 1411–1421

Janka E, Körner O, Rosenqvist E, Ottosen C-O (2013) High temperature stress monitoring and detection using chlorophyll a fluorescence and infrared thermography in chrysanthemum (*Dendranthema grandiflora*). Plant Physiol Biochem **67**: 87–94

Krause G, Weis E (1991) Chlorophyll fluorescence and photosynthesis: The basics. Annu Rev Plant Physiol Plant Mol Biol **42**: 313–349

Li C, Liu G, Xu C, Lee GI, Bauer P, Ling H-Q, Ganal MW, Howe GA (2003) The tomato *suppressor of prosystemin-mediated responses2* gene encodes a fatty acid desaturase required for the biosynthesis of jasmonic acid and the production of a systemic wound signal for defense gene expression. Plant Cell **15**: 1646–1661

Los DA, Murata N (1998) Structure and expression of fatty acid desaturases. Biochim Biophys Acta **1394**: 3–15

Mattoo AK, Giardi M-T, Raskind A, Edelman M (1999) Dynamic metabolism of photosystem II reaction center proteins and pigments. Physiol Plant **107**: 454–461

Millar AA, Smith MA, Kunst L (2000) All fatty acids are not equal: discrimination in plant membrane lipids. Trends Plant Sci **5**: 95–101

Nabity PD, Zavala JA, DeLucia EH (2009) Indirect suppression of photosynthesis on individual leaves by arthropod herbivory. Ann Bot **103**: 655–663

Popova LP, Vaklinova SG (1988) Effect of jasmonic acid on the synthesis of Ribulose-1,5-bisphosphate carboxylase-oxygenase in barley leaves. J Plant Physiol **133**: 210–215

Rakwal R, Komatsu S (2000) Role of jasmonate in the rice (*Oryza sativa* L.) self-defense mechanism using proteome analysis. Electrophoresis **21**: 2492–2500

Reinbothe S, Mollenhauer B, Reinbothe C (1994) JIPs and RIPs: the regulation of plant gene expression by jasmonates in response to environmental cues and pathogens. Plant Cell **6**: 1197–1209

Rodrigues LJ, Grottoli AG, Lesser MP (2008) Long-term changes in the chlorophyll fluorescence of bleached and recovering corals from Hawaii. J Exp Biol **211**: 2502–2509

Sharkey TD (2016) What gas exchange data can tell us about photosynthesis. Plant Cell Environ **39**: 1161–1163

Sharkey TD, Bernacchi CJ, Farquhar GD, Singsaas EL (2007) Fitting photosynthetic carbon dioxide response curves for C3 leaves. Plant Cell Environ **30**: 1035–1040

Staswick PE, Su W, Howell SH (1992) Methyl jasmonate inhibition of root growth and induction of a leaf protein are decreased in an *Arabidopsis thaliana* mutant. Proc Natl Acad Sci U S A **89**: 6837–6840

Sun YL, Li F, Su N, Sun XL, Zhao SJ, Meng QW (2010) The increase in unsaturation of fatty acids of phosphatidylglycerol in thylakoid membrane enhanced salt tolerance in tomato. Photosynthetica **48**: 400–408

Tietz S, Hall CC, Cruz JA, Kramer DM (2017) NPQ(T): a chlorophyll fluorescence parameter for rapid estimation and imaging of non-photochemical quenching of excitons in photosystem-II-associated antenna complexes. Plant Cell Environ **40**: 1243–1255

Zhao S, Ma Q, Xu X, Li G, Hao L (2016) Tomato jasmonic acid-deficient mutant *spr2* seedling response to cadmium stress. J Plant Growth Regul **35**: 603–610

Zhou YH, Yu JQ, Huang LF, Nogués S (2004) The relationship between CO_2 assimilation, photosynthetic electron transport and water–water cycle in chill-exposed cucumber leaves under low light and subsequent recovery. Plant Cell Environ **27**: 1503–1514

Chapter III

Effects of *suppressor of prosystemin-mediated response2* on primary metabolism and photosynthetic responses to aphids

Abstract

The *spr2* mutant of tomato, which carries a null mutation in *Fatty Acid Desaturase 7*, was previously shown to have higher photosynthetic activity than the corresponding wild-type (WT) cultivar, cv. Castlemart, when plants were grown under optimal conditions. In this study, chlorophyll fluorescence was measured in *spr2* and WT plants with and without infestation by the potato aphid, *Macrosiphum euphorbiae*, to determine if *spr2* also enhances photosynthetic activity under herbivore pressure. In both aphid-infested plants and in uninoculated controls, the maximum quantum efficiency of photosystem II (PSII) (F_v/F_m) was significantly higher in *spr2* than in WT plants at both experimental time points (one and six days after infestation). Furthermore, in both treatment groups at both time points, non-photochemical quenching ($NPQ_{(T)}$) was significantly lower in *spr2* compared to WT plants, suggesting that less light energy is lost to heat in *spr2* than in WT. These results indicate that *spr2* enhances photosynthetic activity in both the presence and absence of aphids. Aphid infestation did not significantly affect F_v/F_m in either genotype, indicating that the aphid densities used here did not have deleterious effects on photosynthesis. In fact, one day after infestation, infested plants had significantly higher PSII operating efficiency (ΦPSII) (5% in WT and 20% in *spr2*) and significantly lower $NPQ_{(T)}$ (20% in WT and 58% in *spr2*) than uninfested plants. The decrease in $NPQ_{(T)}$ persisted at day 6 after inoculation, although there were no significant differences in ΦPSII among treatment groups at this later time point. These findings suggest that aphid infestation triggered a short-term compensatory increase in photochemical quenching. Because

the greatest and most persistent differences in photosynthetic activity were attributable to the constitutive effects of the *spr2* mutant rather than to the effects of aphid infestation, subsequent metabolomics analyses focused on comparisons of uninfested *spr2* and WT plants to identify metabolites associated with enhanced photosynthetic activity. Although no significant differences were detected in sugar contents, starch accumulation, or intermediates of the Calvin cycle, the TCA cycle, or glycolysis, the abundance of glutamate was significantly higher in *spr2* compared to WT plants. It has been shown that glutamate enhances the expression of defense related genes and can act as a signaling compound. These results suggest that *spr2* is capable of maintaining photosynthetic efficiency under aphid pressure and increased glutamate levels may contribute to aphid resistance in *spr2* plants.

Introduction

Fatty acid desaturases (FADs) introduce double bonds into the acyl chains of fatty acids and are known to influence plants' levels of resistance to a variety of stresses (Li et al., 2003; Upchurch, 2008). Fatty Acid Desaturase 7 (FAD7) adds a double bond to C16:2 and C18:2 to synthesize C16:3 and C18:3. Loss of function of FAD7 is shown to increase plant defenses against aphids in tomato (*Solanum lycopersicum*), Arabidopsis (*Arabidopsis thaliana*) (Avila et al., 2012) and against *Magnaporthe grisea* in rice (*Oryza sativa*) (Yara et al., 2007).

The *suppressor of prosystemin-mediated response2* (*spr2*) mutant in tomato, which was generated through ethyl methanesulfonate (EMS) mutagenesis, eliminates the function of FAD7 (Howe and Ryan, 1999; Li et al., 2003). The mutation in *spr2* is a single nucleotide substitution that introduces a premature stop codon to the protein (Li et al., 2003), which results in a loss of enzymatic activity, increased levels of 18:2 and 16:2, and decreased levels of 18:3 and 16:3

(Browse et al., 1986; Li et al., 2003; Hiremath et al., 2017). The *spr2* mutant of tomato reduces survival and reproduction of potato aphids (*Macrosiphum euphorbiae*) (Avila et al., 2012). We have previously studied whether changes in chloroplastic fatty acid composition would affect plant's photosynthesis using *spr2* mutant of tomato. Our results have shown significantly greater carbon assimilation, efficiency of light-dependent and light-independent reactions of photosynthesis between *spr2* and its wild-type (WT) (Chapter II).

When studying the light-dependent reactions of photosynthesis, the efficiency of electron transport (F_v/F_m) in photosystem II (PSII) is a commonly used parameter, which is calculated using the equation $F_v = F_o\text{-}F_m$, where F_v = variable fluorescence, F_o = minimal fluorescence in dark-adapted state and F_m = maximal fluorescence in dark-adapted state (Baker, 2008). Some studies have reported that aphids can reduce F_v/F_m (Burd and Elliott, 1996; Haile et al., 1999), while others detected no changes in this parameter (Macedo et al., 2003; Franzen et al., 2007).

Since we have observed differences in photosynthesis between *spr2* and WT in the absence of stresses, we also looked at whether the abundance of several important metabolites associated with primary metabolism varies between these genotypes. We compared the abundance of sugars, starch, and intermediates of glycolysis, Tricarboxylic acid (TCA) cycle and Calvin cycle (Figure 1). The ATP and NADPH synthesized by the light-dependent reactions are used by the light-independent reactions (Calvin cycle) and generate glucose. Some of this glucose is converted to sucrose and starch (storage) and the rest is then converted to pyruvate through a series of reactions by glycolysis. Pyruvate is converted to acetyl-CoA and this step generates CO_2, which gets used in the Calvin cycle, and the acetyl CoA enters the TCA cycle. One of the intermediates of TCA cycle, α-ketoglutarate, generates glutamate, which is one of the first products of nitrogen assimilation in plants. The NADH synthesized by the TCA cycle is

used in oxidative phosphorylation, which generates O_2 to be used in the light-dependent reactions.

In a previous study (Chapter II), we observed that tomato plants with the *spr2* mutants have enhanced photosynthetic efficiency compared to WT controls. The goals of this study were to determine whether the *spr2* also enhances photosynthesis under aphid pressure and to identify metabolites associated with enhanced photosynthetic activity in uninfested *spr2* and WT plants. This study will contribute to our understanding of how the *spr2* plants may spend the energy gained from enhanced photosynthesis.

Materials and methods

Plant materials and growth conditions

The plant material used in this study – wild-type (WT) tomato (*Solanum lycopersicum* cv. Castlemart) and *FAD7*-impaired *suppressor of prosystemin-mediated response2* (*spr2*) mutant of tomato – were grown in LC1 Sunshine Professional Growing Mix (Sun Gro Horticulture, Agawam, MA) and a slow release fertilizer (Osmocote Plus; 15-9-12) (Scotts-MiracleGro Company, Marysville, OH) was added to the soil mix. The WT and *spr2* plants were grown in the greenhouse (Temp: 23 - 25 °C, RH: ~ 60%, light intensity: 500 - 900 µmol/m^2/sec, and 16-h/8-h light/dark photoperiod). Plants were watered with a nutrient solution containing 1000 ppm 15.5-0-0 $CaNO_3$ (Hydro Agri North America, Tampa, FL), 500 ppm $MgSO_4$ (Giles Chemical, Waynesville, NC) and 500 ppm 4-18-38 Grow More fertilizer (Grow More, Gardena, CA). Then the plants were transferred into two Conviron growth chambers (Controlled Environments, Inc., Winnipeg, Canada) (Temp: 23 °C, RH: ~ 60%, light intensity: 400 µmol/m^2/sec, and 16-h/8-h light/dark photoperiod), where one chamber was assigned for aphid infestation and the other

chamber was assigned for the control treatment. Temperature, light intensity and humidity were maintained at the same level in both growth chambers.

Aphids

Potato aphids (*Macrosiphum euphorbiae*) were reared on tomato (*S. lycopersicum* cv. BHN 871) grown at 20 ºC and 16-h/8-h light/dark photoperiod. Three leaves (3^{rd}, 4^{th} and 5^{th} leaves from the apical meristem) of 4-week old plants were infested with 30 aphids (10 aphids per leaf). All the plants from one chamber were infested with aphids, while the plants in the other growth chamber remained as control plants with no aphids. No cages were used when infesting plants with aphids, since the cages would interfere with clamping the fluorescence meter on the leaves. Fluorescence measurements were taken at 1 and 6 days after the infestation. Numbers of adult and juvenile aphids on all the three leaves were counted on day 5.

Fluorescence measurements

A handheld fluorescence meter, MultispeQ (v1.0) (PhotosynQ LLC, East Lansing, MI), was used to estimate the efficiency of light-dependent reactions of photosynthesis using a series of fluorescence parameters. The built-in protocol of MutlispeQ, "Leaf Photosynthesis MultispeQ V1.0" was used and the fluorescence parameters were measured on 3^{rd} leaves of the plants. The dark-adapted parameters (minimal fluorescence in dark-adapted state (F_o), maximal fluorescence in dark-adapted state (F_m), and the quantum efficiency of photosystem II (PSII) (F_v/F_m)) were measured on the plants that were dark-adapted overnight. The light-adapted parameters (PSII operating efficiency (ΦPSII), and non-photochemical quenching ($NPQ_{(T)}$) were measured between 8:00 am and 12:00 pm to avoid diurnal fluctuations.

Tissue collection for metabolite analyses

To determine whether the primary metabolites differ between *spr2* and WT, the sugar profiles and the intermediates of glycolysis, TCA cycle and Calvin cycle were extracted from leaf tissue. As a first step in looking into nitrogen assimilation in plants, we determined the abundance of glutamate, since it is one of the first products of nitrogen assimilation in plants. Only the uninfested WT and *spr2* plants were used for metabolite analysis, due to high sample processing costs and because the largest and most persistent differences in photosynthesis were associated with constitutive genotypic differences. At the end of the assay (day 6), two leaflets from the 3rd leaves of two plants of the same genotype were pooled for metabolite analyses. For each genotype, there were 6 pooled replicates. The leaflets were quickly detached, placed in Whirl-Pak® sampling bags and immediately flash frozen in liquid nitrogen. Pooled samples were ground in liquid nitrogen and stored at -80 °C for further processing.

Analysis of glycolysis, TCA cycle and Calvin cycle intermediates

Glycolysis and TCA cycle analyses were conducted at the Proteomics and Metabolomics Facility at the Center for Biotechnology at University of Nebraska-Lincoln using Liquid Chromatography – Tandem Mass Spectrometry, using a protocol modified from Yuan et al. (2012). Metabolites were extracted from the ground leaf tissue using 600 µL chilled H_2O: chloroform: methanol (3:5:12 v/v) spiked with PIPES (piperazine-N,N′-bis(2-ethanesulfonic acid) as internal standard. The tissue samples were disrupted using the TissueLyserII (Qiagen, Gaithersburg, MD). After centrifugation at 16,000 g for 15 minutes, the supernatants were collected, and extraction of pellet was repeated one more time. The supernatants were pooled and 300 µL chloroform and 450 µL of chilled water were added. The tubes were vortexed and

centrifuged at 16, 000 g for 15 minutes. The upper layer was transferred to a new tube and dried down using a speed-vac until the all the liquid is evaporated. The pellets were re-dissolved in 100 µL of 80% acetonitrile.

For LC separation, SeQuant ZIC-pHILIC column (5 µm polymeric, 150 X 2.1 mm) was used flowing at 0.25 mL/min. The gradient of the mobile phases A (20 mM ammonium acetate, pH 9.8, 5% ACN) and B (100% acetonitrile) were as follows: 85% B for 1 min, to 58% B in 1.5 min, held at 58% B for 6.5 min, then back to 85% B in 0.5 min. The LC system was interfaced with a Sciex QTRAP 6500+ mass spectrometer equipped with a TurboIonSpray (TIS) electrospray ion source. Analyst software (v. 1.6.3) was used to control sample acquisition and data analysis. The QTRAP 6500+ mass spectrometer was tuned and calibrated according to the manufacturer's recommendations. All the metabolites were detected using MRM transitions that were previously optimized using standards. The instrument was set-up to acquire in positive/negative mode switching. For quantification, an external standard curve was prepared using a series of standard samples containing different concentrations of metabolites and fixed concentration of the internal standard.

Analysis of sugars

Sugar analysis was conducted by Dr. David Braun (University of Missouri, Columbia) using HPLC according to the protocol by Leach and Braun (2016). Soluble sugars and starch were extracted from ground leaf tissue using an extraction buffer containing methanol, chloroform and water (12:5:3) followed by incubation at 50 °C for 30 minutes and centrifugation at 14000 rpm for 5 minutes. For soluble sugar extraction, the supernatant was transferred to a new tube and the extraction was repeated two more times. Supernatants were pooled and 0.6

volumes of water were added to the sample, centrifuged at 4650 g for 5 minutes and the upper aqueous phase was separated. The pellet that remained after three extractions was saved for starch quantification. The pellet was dissolved in dimethyl sulfoxide and incubated in boiling water bath for 5 minutes. Then the solution was diluted 1:20 in sodium acetate and added α-amylase. After incubation in boiling water for 15 minutes and cooling in 50 °C for 3 minutes, amyloglucosidase was added. Then the sample was incubated again at 50 °C for 1 hour and centrifuged at 14000 rpm for 5 minutes to retrieve the supernatant. The soluble sugar extracts were processed according to support protocol 2 in (Leach and Braun (2016) to remove strongly charged or large molecules. The samples were analyzed with HPLC and compared to standards.

Statistical analysis

All the statistical analyses were conducted with JMP® Pro 13 (SAS Institute Inc.). The mean differences in fluorescence parameters were analyzed by two-way ANOVA to analyze the effects of plant genotype and aphid damage. No significant interactions were found and therefore, only the main effects were analyzed using Student's t-test. The data from metabolite analyses were analyzed by Student's t-tests for each metabolite since these analyses involved comparisons of only the two genotypes.

Results

Aphid numbers

The total number of adult and juvenile potato aphids (*M. euphorbiae*) on WT plants was 78% greater than that of on *spr2* plants five days after the infestation ($t = 5.50$, $df = 17$, $P < 0.0001$) (Figure 2).

Light-dependent reactions

Minimum chlorophyll fluorescence in dark-adapted leaves (F_o) was significantly higher in WT by ~11% on both day 1 and day 6 compared to *spr2* (Fig 2A and 2E). However, aphid infestation did not influence F_o on either day 1 (Genotype: $F = 26.24$, df = 1, 35, $P < 0.0001$; Aphids: F = 2.75, df = 1, 35, $P = 0.12$; Genotype x Aphids: $F = 1.00$, df = 1, 35, $P = 0.32$) or day 6 (Genotype: $F = 34.93$, df = 1, 35, $P < 0.0001$; Aphids: F = 2.09, df = 1, 35, $P = 0.16$; Genotype x Aphids: $F = 1.45$, df = 1, 35, $P = 0.24$).

Maximum chlorophyll fluorescence in dark-adapted leaves (F_m) did not show significant differences among the genotypes or in response to aphids on either of the days (Day 1: WT-control: 20,827.4 ± 900.9, WT-aphids: 20,299.4 ± 881.2, *spr2*-control: 20,620.5 ± 810.8, *spr2*-aphids: 20,153.6 ± 770.1; Day 6: WT-control: 20,273.8 ± 609.6, WT-aphids: 19,940.8 ± 450.2, *spr2*-control: 19,873.4 ± 1,1185.5, *spr2*-aphids: 20,470.7 ± 763.7) (mean ± SD). As a result of differences in F_o, the maximum quantum efficiency of PSII in dark-adapted leaves F_v/F_m, where $F_v = F_m - F_o$ was greater in *spr2* than WT by 3% on both day 1 ($F = 30.14$, df = 1, 35, $P<0.0001$; Aphids: $F = 0.40$, df = 1, 35, $P = 0.53$; Genotype x Aphids: $F = 1.70$, df = 1, 35, $P = 0.20$) and day 6 (Genotype: $F = 41.45$, df = 1, 35, $P<0.0001$; Aphids: $F = 1.37$, df = 1, 35, $P = 0.25$; Genotype x Aphids: $F = 0.02$, df = 1, 35, $P = 0.89$). Aphid infestation did not affect F_v/F_m values (Figures 3B and 3F).

One day after infestation, the fraction of light energy used in photochemistry, measured by PSII operating efficiency (ΦPSII), was significantly greater in *spr2* compared to WT and it was increased by aphids by 5% in WT and by 20% in *spr2* (Genotype: $F = 13.32$, df = 1, 35, $P = 0.0008$; Aphids: $F = 9.00$, df = 1, 35, $P = 0.005$; Genotype x Aphids: $F = 3.42$, df = 1, 35, $P =$

0.07) (Figure 3C). No significant genotypic and aphid effects were seen on day 6 (Genotype: F = 0.004, df = 1, 35, P = 0.95; Aphids: F = 0.0001, df = 1, 35, P = 0.99; Genotype x Aphids: F = 0.01, df = 1, 35, P = 0.92) (Figure 3G). NPQ significantly declined in response to aphids by 20% in WT and by 58% in *spr2* on day 1 (Genotype: F = 28.99, df = 1, 35, P<0.0001; Aphids: F = 16.35, df = 1, 35, P = 0.0003; Genotype x Aphids: F = 1.32, df = 1, 35, P = 0.26), and by 36% in WT and 12% in *spr2* on day 6 (Two-way ANOVA: Genotype: F = 12.99, df = 1, 35, P<0.001; Aphids: F = 8.84, df = 1, 35, P = 0.005; Genotype x Aphids: F = 2.30, df = 1, 35, P = 0.14).

Metabolite analysis

No significant differences were detected in total sucrose, total fructose, total glucose and total starch between WT and *spr2* (Figure 4). Also, significant differences were not detected between *spr2* and WT were observed in the Calvin cycle intermediates (Figure 5B) or the TCA cycle or glycolysis (Figure 6B). Calvin cycle intermediates tested in this study were: 2-phosphoglycerate/3-phosphoglycerate (2PGA/3PGA), Dihydroxyacetone phosphate/Glyceraldehyde-3-phosphate (DHAP/G3P), Fructose-1,6-bisphosphate (FBP), Glucose-6-phosphate/Fructose-6-phosphate/Glucose-1-phosphate (G6P/F6P/G1P), Erythrose-4-phosphate (E4P), Sedoheptulose-7-phosphate (S7P), Ribose-5-phosphate/Ribulose-5-phosphate (R5P/Ru5P) (Figure 5B). The intermediates of glycolysis and TCA cycle tested were: G6P/F6P/G1P, FBP, DHAP/G3P, 2PGA/3PGA, Phosphoenolpyruvate (PEP), α-ketoglutarate (KGLU), Succinate (SUC), Fumarate (FUM), Malate (MAL) (Figure 6B). However, glutamate concentration was significantly greater in *spr2* compared to WT (Figure 7). The statistics are shown in Table 1.

Discussion

In this study, we observed that potato aphids (*M. euphorbiae*) did not cause significant changes in the efficiency of PSII, where the light-dependent reactions of photosynthesis initiate. The genotypic differences between the mutant with impaired *FAD7* function (*spr2*) and its WT were similar to what was reported in chapter II. The efficiency of PSII was significantly higher in *spr2* compared to WT on day 1 and 6 after aphid infestation and no aphid effect was observed. Similarly, the minimum chlorophyll fluorescence (F_o) was significantly higher in WT than in *spr2* and an aphid effect was not observed. These results show that aphids did not affect F_o and F_v/F_m values at the aphid densities tested here. Similar results have been shown in response to soybean aphids on soybean by Macedo et al. (2003) and Russian wheat aphid on wheat by Franzen et al. (2007).

In addition, ΦPSII and $NPQ_{(T)}$ followed similar genotypic trends as were found in our previous study (Chapter II) and significant aphid effects were observed on both parameters on day 1. The results indicate a higher fraction of light energy is directed towards photochemistry in the aphid-infested tomato plants. This could be due to a compensatory photosynthetic response. Although no prior studies have reported an increase in ΦPSII in response to aphids, a few studies have shown increased carbon assimilation following aphid infestation (Heng-Moss et al., 2006; Eyles et al., 2011; Kucharik et al., 2016). These results suggest that the *spr2* plants may be able to allocate energy for recovery from aphid feeding.

The constitutive levels of metabolite profiles suggest that there are no differences in sugar and starch accumulation, and intermediates of Calvin cycle and aerobic respiration between *spr2* and WT. However, there is a possibility that the differences may not be reflected in

metabolite accumulation because metabolites may simply be diverted to differences in growth and development of the plants. Also, it is noteworthy that the analysis method was not able to differentiate some metabolites due to having the same molecular weight, and therefore, they were co-eluted. Another possibility is that we missed the critical metabolites, or we did not have enough replications to account for the differences. In addition, we noted that there is a large within-treatment variation in metabolite abundance.

Sugars can act as plant signaling molecules (Wind et al., 2010; Morkunas and Ratajczak, 2014). Glucose signaling is involved in regulation of photosynthesis (Bolouri-Moghaddam et al., 2010) and sucrose impacts biosynthesis of anthocyanins, a plant secondary metabolite that is shown to mediate plant defenses against microbes (Solfanelli et al., 2006). However, we did not detect differences in sugars tested here (glucose, fructose and sucrose) between *spr2* and WT. Apart from glucose and sucrose, trehalose is another sugar that has been shown to enhance resistance against the green peach aphid (*Myzus persicae*) in Arabidopsis and tomato (Singh et al., 2011; Singh and Shah, 2012). These authors have shown that a gene that encodes a trehalose synthesizing enzyme, *TPS11* (*TREHALOSE PHOSPHATE SYNTHASE11*) reduced green peach aphid infestation. In addition, *TPS11* promoted starch accumulation and upregulated the expression of *PAD4* (*PHYTOALEXIN-DEFICIENT4*), which is known to regulate resistance against green peach aphids (Pegadaraju et al., 2007). Although we did not observe a significant increase of starch in *spr2* plants, analyzing trehalose may provide more insight into how the sugar metabolism and aphid defenses are related in *spr2* plants.

Similarly, no differences were detected in the intermediates of glycolysis, TCA cycle and Calvin cycle. This is surprising since we have shown that increased photosynthetic efficiency in *spr2* was associated with enhancements in both light-dependent and light-independent reactions

of photosynthesis (Chapter II). However, it is important to note that there are certain intermediate compounds that we were not able to measure in this study, especially, ribulose-1,5-bisphosphate (RuBP). We have shown in Chapter II that the maximum rate of electron transport used in the regeneration of RuBP (J_{max}) is significantly higher in *spr2* compared to WT.

However, we report that glutamate – a plant derived amino acid – is significantly higher in *spr2* compared to WT. Wendler et al. (1990) reported that glufosinate inhibits photosynthesis by irreversibly inhibiting glutamine synthetase under photorespiratory conditions. Glutamine synthetase catalyzes the ligation of glutamate and ammonia to form glutamine (Miflin and Habash, 2002). Inhibiting glutamine synthetase causes a lack of amino donors, which inhibits transamination of glyoxylate to glycine in photorespiration, and glyoxylate accumulation inhibits Rubisco (Wild and Wendler, 1993). This supports our previous findings since we observed both enhanced Rubisco efficiency (Chapter II) and enhanced glutamate synthesis in *spr2* plants. In addition, high levels of glutamate have been found in phloem sap with reduced nutritional quality (Douglas, 1993). Also, increased glutamate levels were found in melon aphid (*Aphis gossypii*) resistant melon plants (Chen et al., 1997). Kan et al. (2017) have reported exogenous application of glutamate have induced the expression of several defense response related gens in rice such as *CIGR2*, which encodes a transcriptional activator involved in hypersensitive response; *bHLH35*, a JA responsive gene involved in disease resistance; and *OsHI-LOX* an herbivore-induced gene involved in defense response. Also, Toyota et al. (2018) have recently showed that glutamate can trigger long-distance signaling in plants. These studies suggest that glutamate may be involved in plant defense responses against aphids. It is worthwhile to investigate how glutamate is affected in aphid infested *spr2* plants compared to WT plants.

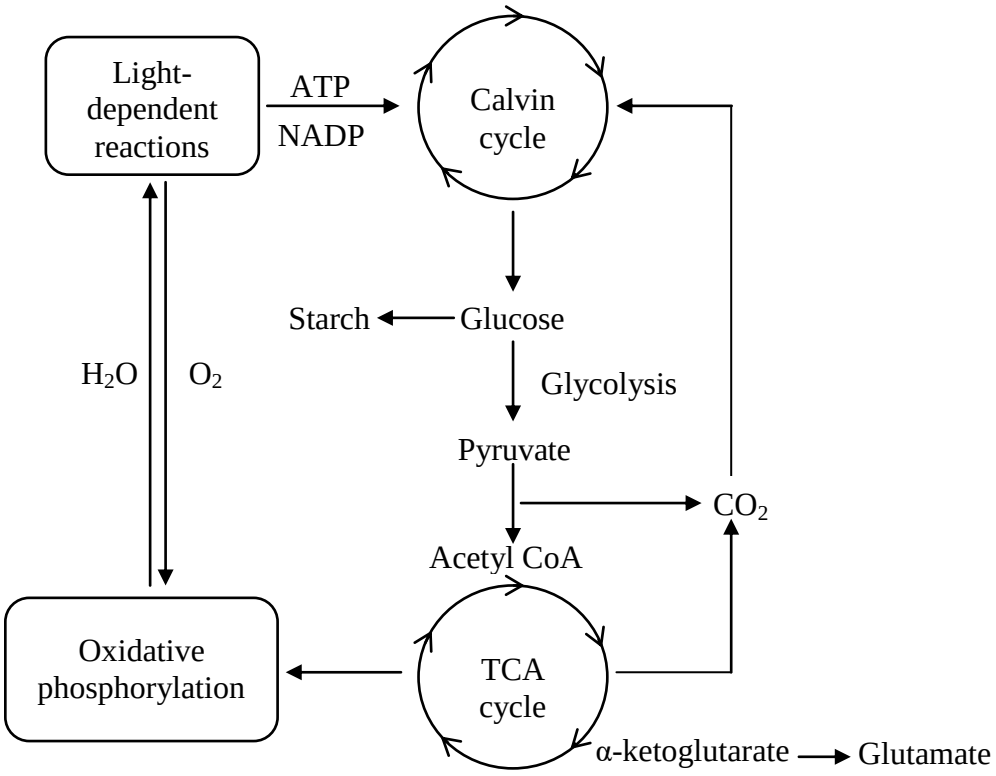

Figure 1. Schematic representation of the link between light-dependent reaction and light-independent reaction (Calvin cycle), glycolysis, Tricarboxylic acid (TCA) cycle, and glutamate synthesis.

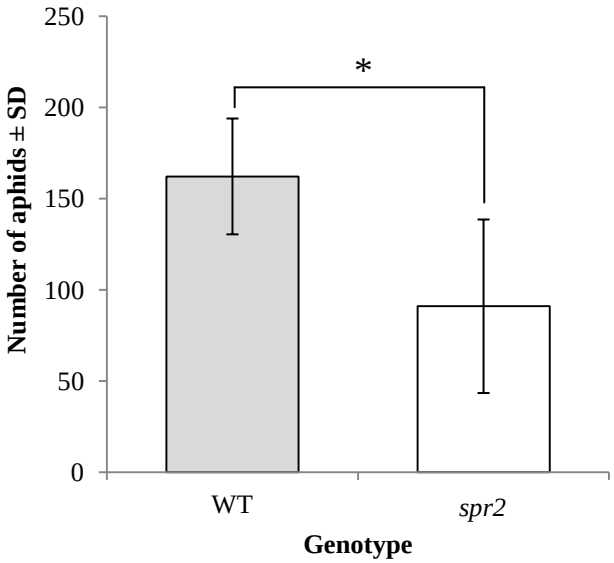

Figure 2. Total number of adult and juvenile aphids on 5-week old WT and *FAD7*-impaired (*spr2*) tomato plants at five days after the infestation. Data were analyzed by Student's t-test. Error bars represent SD and the asterisk indicates a statistically significant difference compared to WT at $\alpha = 0.05$; n=10 for WT and 9 for *spr2*.

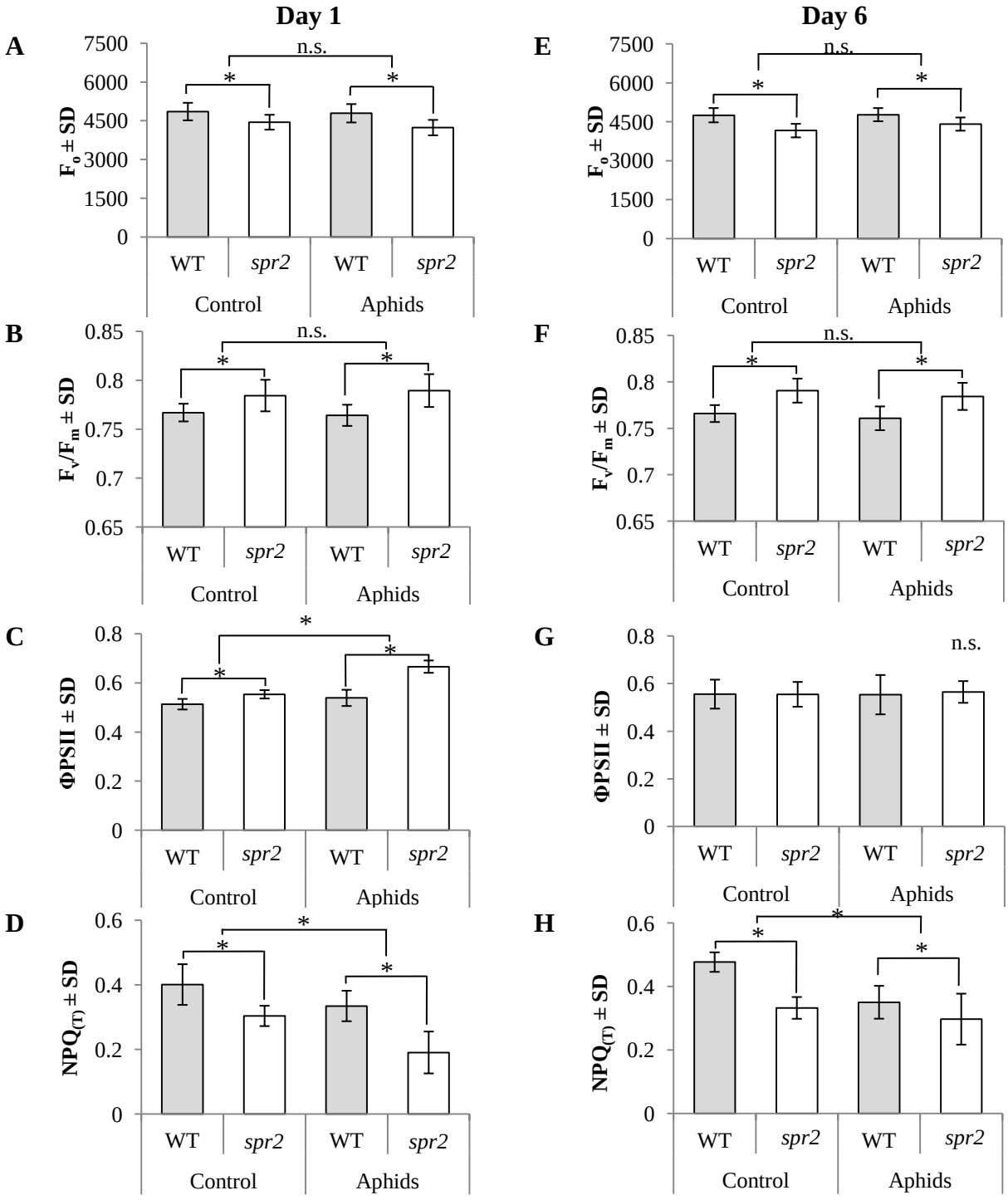

Figure 3. The efficiency of the light-dependent reactions of photosynthesis. Minimal fluorescence of dark-adapted tomato leaves (F_o, in A and E), maximum quantum efficiency of PSII when dark-adapted (F_v/F_m, in B and F), PSII operating efficiency (ΦPSII, in C and G) and non-photochemical quenching ($NPQ_{(T)}$, in D and H) were compared in the 5th leaf of WT and *FAD7*-impaired plants (*spr2*) in response to potato aphids at 1 and 6 days post-infestation. Data were analyzed by two-way ANOVA. Error bars represent SD and the bars labeled with asterisks differ significantly at $\alpha = 0.05$; n=10 for WT and 9 for *spr2*; n.s. = not significant.

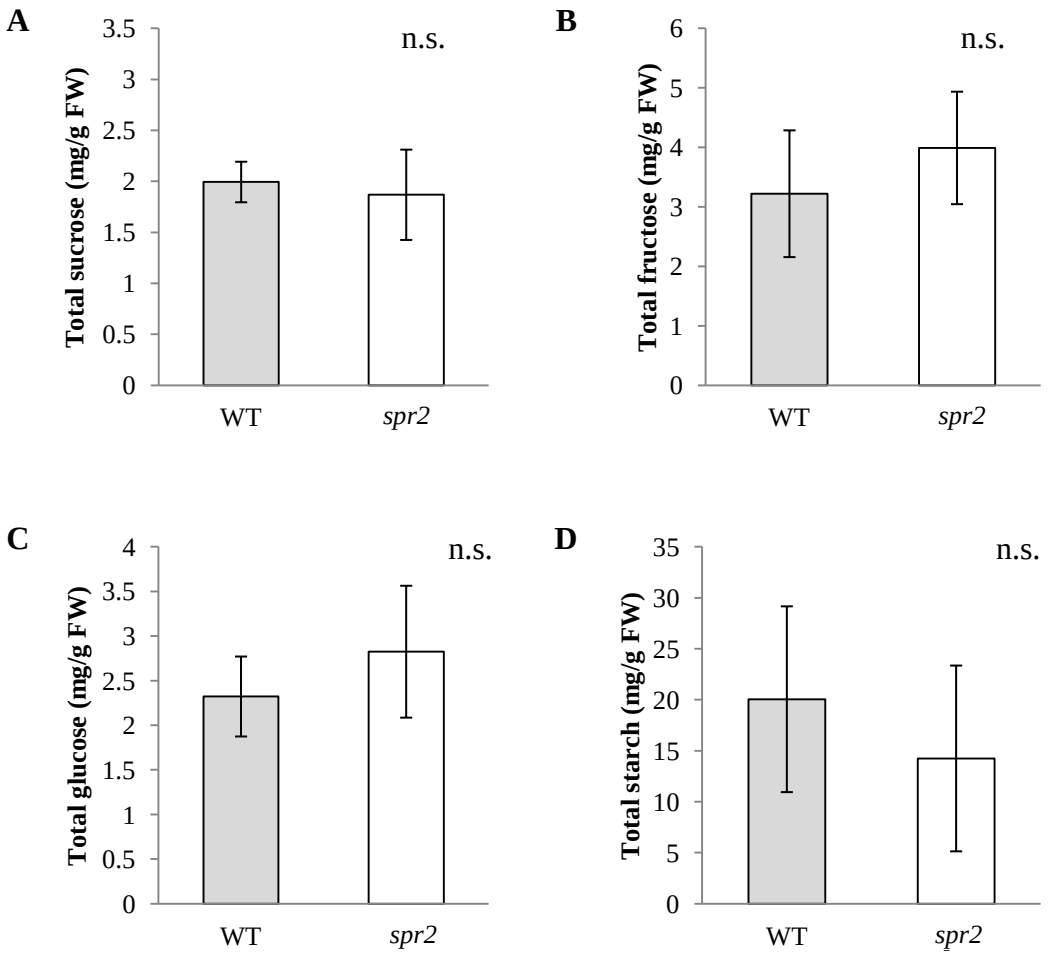

Figure 4. Soluble sugars and starch concentrations. Sucrose (A), fructose (B), glucose (C) and starch (D) were compared in the 3rd leaf of 5-week old WT and *spr2* tomato plants. Data were analyzed by Student's t-test. Error bars represent SD and none of the variables showed statistically significant differences at $\alpha = 0.05$; n = 6 for WT and 5 for *spr2* (each sample was pooled from 2 plants); n.s. = not significant.

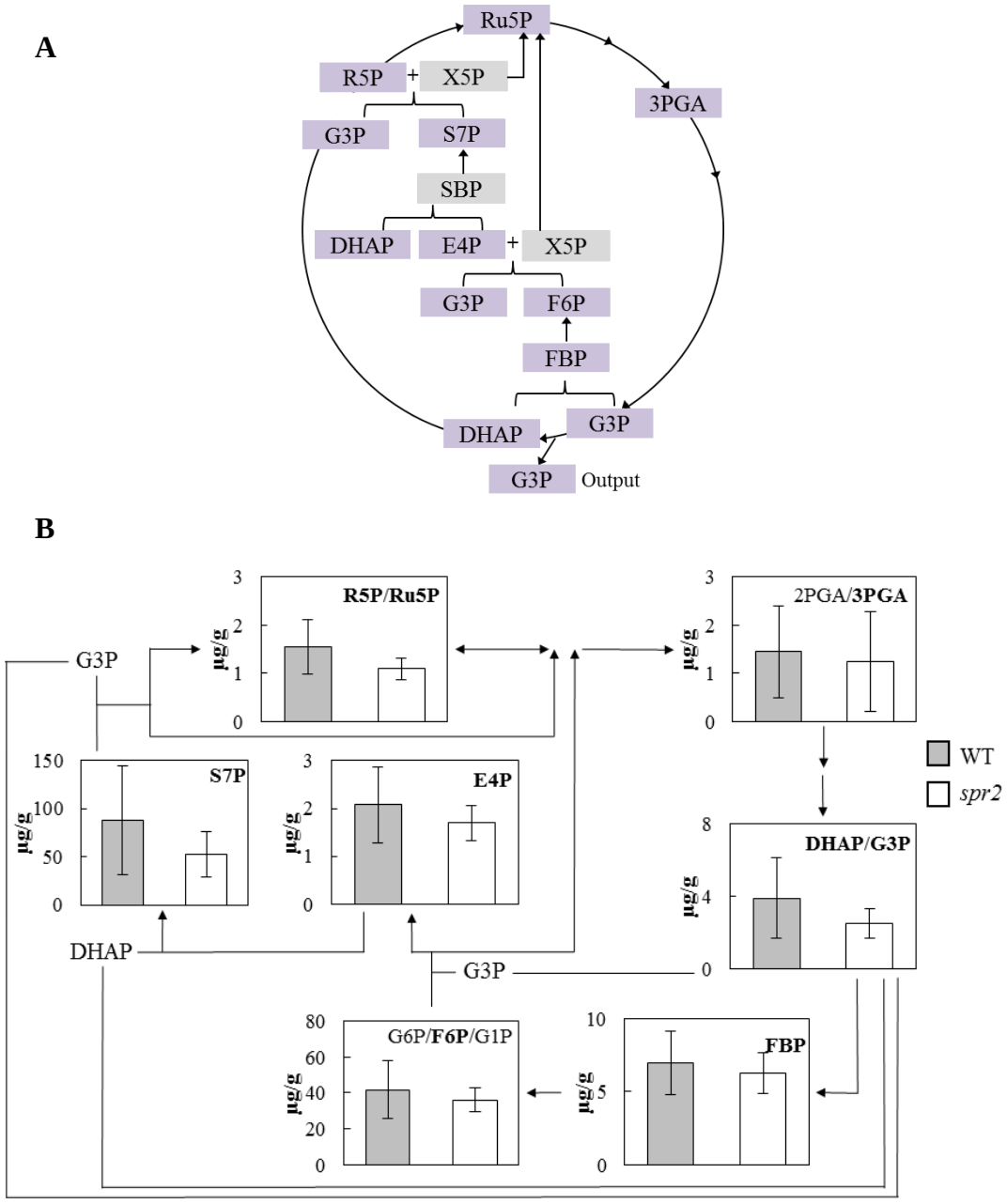

Figure 5. Metabolites of the Calvin cycle. **A.** Schematic representation of the Calvin cycle (purple = intermediates measured in this study, grey = intermediates not measured in this study). **B.** Calvin cycle intermediates of 5-week old WT and *spr2* tomato plants. Data were analyzed by Student's t-test. Error bars represent SD and none of the variables showed statistically significant differences at $\alpha = 0.05$, n=6 (each sample was pooled from 2 plants). The directions of enzymatic reactions are represented by arrowheads; reversible reactions are indicated by double sided arrows. Abbreviations: 2PGA, 2-phosphoglycerate; 3PGA, 3-phosphoglycerate; DHAP, Dihydroxyacetone phosphate; G3P, Glyceraldehyde-3-phosphate; FBP, Fructose-1,6-bisphosphate; G6P, Glucose-6-phosphate; F6P, Fructose-6-phosphate; G1P, Glucose-1-phosphate; E4P, Erythrose-4-phosphate; S7P, Sedoheptulose-7-phosphate; R5P, Ribose-5-phosphate; Ru5P, Ribulose-5-phosphate.

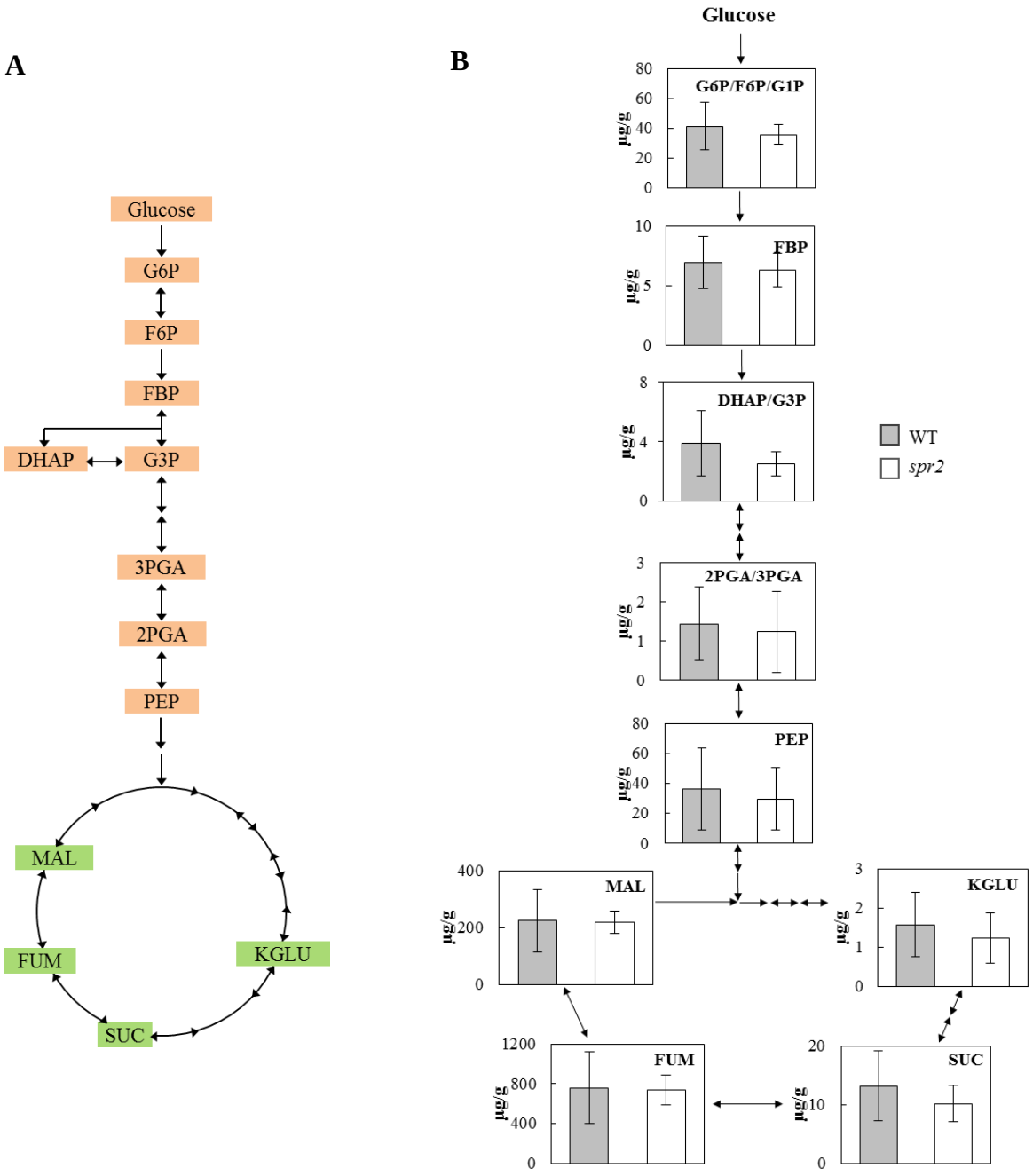

Figure 6. Metabolites of glycolysis and TCA cycle. **A.** Schematic representation of glycolysis and citric acid cycle. **B.** Glycolysis and citric acid cycle intermediates of 5-week old WT and *spr2* tomato plants. Data were analyzed by Student's t-test. Error bars represent SD and none of the variables showed statistically significant differences at $\alpha = 0.05$, n=6 (each sample was pooled from 2 plants). The directions of enzymatic reactions are represented by arrowheads; reversible reactions are indicated by double sided arrows. Abbreviations: G6P, Glucose-6-phosphate; F6P, Fructose-6-phosphate; G1P, Glucose-1-phosphate; FBP, Fructose-1,6-bisphosphate; DHAP, Dihydroxyacetone phosphate; G3P, Glyceraldehyde-3-phosphate; 2PGA, 2-phosphoglycerate; 3PGA, 3-phosphoglycerate; PEP, Phosphoenolpyruvate; KGLU, α-ketoglutarate; SUC, Succinate; FUM, Fumarate; MAL, Malate.

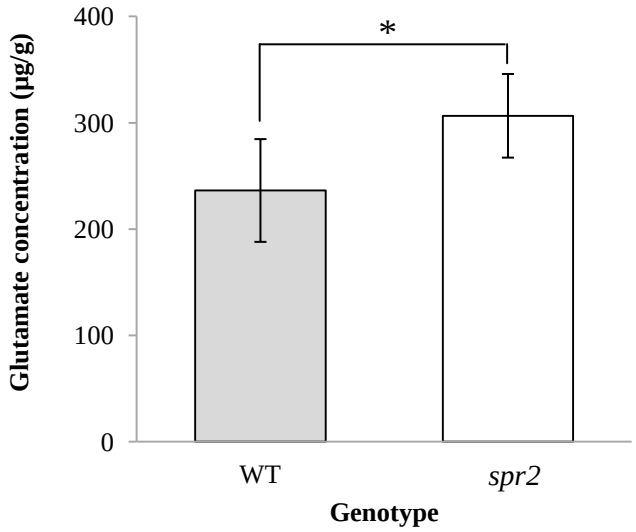

Figure 7. Glutamate concentration of 5-week old WT and *FAD7*-impaired (*spr2*) tomato plants. Data were analyzed by Student's t-test. Error bars represent SD and the asterisk indicates a statistically significant difference compared to WT at $\alpha = 0.05$; n=6 (each sample was pooled from two plants).

Table 1. Test statistics for all metabolites including sugars and intermediates of Calvin cycle, glycolysis, tri-carboxylic acid (TCA) cycle and glutamate.

Metabolite	t - value	df	*P* – value
Sucrose	0.58	9	0.58
Fructose	-1.20	9	0.26
Glucose	-1.30	9	0.23
Starch	0.99	9	0.35
2-phosphoglycerate/3-phosphoglycerate (2PGA/3PGA)	0.32	10	0.75
Dihydroxyacetone phosphate/Glyceraldehyde-3-phosphate (DHAP/G3P)	1.41	10	0.19
Fructose-1,6-bisphosphate (FBP)	0.64	10	0.53
Glucose-6-phosphate/Fructose-6-phosphate/Glucose-1-phosphate (G6P/F6P/G1P)	0.45	10	0.45
Erythrose-4-phosphate (E4P)	1.05	10	0.32
Sedoheptulose-7-phosphate (S7P)	1.45	10	0.18
Ribose-5-phosphate/Ribulose-5-phosphate (R5P/Ru5P)	1.86	10	0.09
Phosphoenolpyruvate (PEP)	0.45	10	0.66
α-ketoglutarate (KGLU)	0.79	10	0.45
Succinate (SUC)	1.11	10	0.29
Fumarate (FUM)	0.16	10	0.88
Malate (MAL)	0.14	10	0.88
Glutamate	-2.76	10	0.02

References

Avila CA, Arévalo-Soliz LM, Jia L, Navarre DA, Chen Z, Howe GA, Meng Q-W, Smith JE, Goggin FL (2012) Loss of function of FATTY ACID DESATURASE7 in tomato enhances basal aphid resistance in a salicylate-dependent manner. Plant Physiol **158**: 2028–2041

Baker NR (2008) Chlorophyll fluorescence: a probe of photosynthesis in vivo. Annu Rev Plant Biol **59**: 89–113

Bolouri-Moghaddam MR, Le Roy K, Xiang L, Rolland F, Van den Ende W (2010) Sugar signalling and antioxidant network connections in plant cells. FEBS J **277**: 2022–2037

Browse J, McCourt P, Somerville C (1986) A mutant of arabidopsis deficient in C18:3 and C16:3 leaf lipids. Plant Physiol **81**: 859–864

Burd JD, Elliott NC (1996) Changes in chlorophyll a fluorescence induction kinetics in cereals infested with Russian wheat aphid (Homopetra: Aphididea). J Econ Entomol **89**: 1332–1337

Chen JQ, Rahbé Y, Delobel B, Sauvion N, Guillaud J, Febvay G (1997) Melon resistance to the aphid *Aphis gossypii*: behavioural analysis and chemical correlations with nitrogenous compounds. Entomol Exp Appl **85**: 33–44

Douglas AE (1993) The nutritional quality of phloem sap utilized by natural aphid populations. Ecol Entomol **18**: 31–38

Eyles A, Smith D, Pinkard EA, Smith I, Corkrey R, Elms S, Beadle C, Mohammed C (2011) Photosynthetic responses of field-grown *Pinus radiata* trees to artificial and aphid-induced defoliation. Tree Physiol **31**: 592–603

Franzen LD, Gutsche AR, Heng-Moss TM, Higley LG, Sarath G, Burd JD (2007) Physiological and biochemical responses of resistant and susceptible wheat to injury by Russian wheat aphid. J Econ Entomol **100**: 1692–1703

Haile FJ, Higley LG, Ni X, Quisenberry SS (1999) Physiological and growth tolerance in wheat to Russian wheat aphid (Homoptera: Aphididae) injury. Environ Entomol **28**: 787–794

Heng-Moss T, Macedo T, Franzen L, Baxendale F, Higley L, Sarath G (2006) Physiological responses of resistant and susceptible buffalograsses to *Blissus occiduus* (Hemiptera: Blissidae) feeding. J Econ Entomol **99**: 222–228

Hiremath SS, Sajeevan RS, Nataraja KN, Chaturvedi AK, Chinnusamy V, Pal M (2017) Silencing of fatty acid desaturase (*FAD7*) gene enhances membrane stability and photosynthetic efficiency under heat stress in tobacco (*Nicotiana benthamiana*). Indian J Exp Biol **55**: 532–541

Howe GA, Ryan CA (1999) Suppressors of systemin signaling identify genes in the tomato wound response pathway. Genetics **153**: 1411–1421

Kan C-C, Chung T-Y, Wu H-Y, Juo Y-A, Hsieh M-H (2017) Exogenous glutamate rapidly induces the expression of genes involved in metabolism and defense responses in rice roots. BMC Genomics. doi: 10.1186/s12864-017-3588-7

Kucharik CJ, Mork AC, Meehan TD, Serbin SP, Singh A, Townsend PA, Stack Whitney K, Gratton C (2016) Evidence for compensatory photosynthetic and yield response of soybeans to aphid herbivory. J Econ Entomol **109**: 1177–1187

Leach KA, Braun DM (2016) Soluble sugar and starch extraction and quantification from maize (*Zea mays*) leaves. Curr Protoc Plant Biol **1**: 139–161

Li C, Liu G, Xu C, Lee GI, Bauer P, Ling H-Q, Ganal MW, Howe GA (2003) The tomato *suppressor of prosystemin-mediated responses2* gene encodes a fatty acid desaturase required for the biosynthesis of jasmonic acid and the production of a systemic wound signal for defense gene expression. Plant Cell **15**: 1646–1661

Macedo TB, Bastos CS, Higley LG, Ostlie KR, Madhavan S (2003) Photosynthetic responses of soybean to soybean aphid (Homoptera: Aphididae) injury. J Econ Entomol **96**: 188–193

Miflin BJ, Habash DZ (2002) The role of glutamine synthetase and glutamate dehydrogenase in nitrogen assimilation and possibilities for improvement in the nitrogen utilization of crops. J Exp Bot **53**: 979–987

Morkunas I, Ratajczak L (2014) The role of sugar signaling in plant defense responses against fungal pathogens. Acta Physiol Plant **36**: 1607–1619

Pegadaraju V, Louis J, Singh V, Reese JC, Bautor J, Feys BJ, Cook G, Parker JE, Shah J (2007) Phloem-based resistance to green peach aphid is controlled by Arabidopsis *PHYTOALEXIN DEFICIENT4* without its signaling partner *ENHANCED DISEASE SUSCEPTIBILITY1*. Plant J **52**: 332–341

Singh V, Louis J, Ayre BG, Reese JC, Pegadaraju V, Shah J (2011) *TREHALOSE PHOSPHATE SYNTHASE11*-dependent trehalose metabolism promotes *Arabidopsis thaliana* defense against the phloem-feeding insect *Myzus persicae*. Plant J **67**: 94–104

Singh V, Shah J (2012) Tomato responds to green peach aphid infestation with the activation of trehalose metabolism and starch accumulation. Plant Signal Behav **7**: 605–607

Solfanelli C, Poggi A, Loreti E, Alpi A, Perata P (2006) Sucrose-specific induction of the anthocyanin biosynthetic pathway in arabidopsis. Plant Physiol **140**: 637–646

Toyota M, Spencer D, Sawai-Toyota S, Jiaqi W, Zhang T, Koo AJ, Howe GA, Gilroy S (2018) Glutamate triggers long-distance, calcium-based plant defense signaling. Science **361**: 1112–1115

Upchurch RG (2008) Fatty acid unsaturation, mobilization, and regulation in the response of plants to stress. Biotechnol Lett **30**: 967–977

Wendler C, Barniske M, Wild A (1990) Effect of phosphinothricin (glufosinate) on photosynthesis and photorespiration of C3 and C4 plants. Photosynth Res **24**: 55–61

Wild A, Wendler C (1993) Inhibitory action of glufosinate on photosynthesis. Z N aturforsch **48**: 369–373

Wind J, Smeekens S, Hanson J (2010) Sucrose: metabolite and signaling molecule. Phytochemistry **71**: 1610–1614

Yara A, Yaeno T, Hasegawa M, Seto H, Montillet J-L, Kusumi K, Seo S, Iba K (2007) Disease resistance against *Magnaporthe grisea* is enhanced in transgenic rice with suppression of ω-3 fatty acid desaturases. Plant Cell Physiol **48**: 1263–1274

Yuan M, Breitkopf SB, Yang X, Asara JM (2012) A positive/negative ion-switching, targeted mass spectrometry-based metabolomics platform for bodily fluids, cells, and fresh and fixed tissue. Nat Protoc **7**: 872–881

Chapter IV

Development of transgenic lines containing *roGFP2* reporter gene to study the overall redox status of Arabidopsis plants with impaired *FAD7-1* function

Abstract

In plants, biotic and abiotic stresses can cause a shift in plant's redox status and the accumulation of reactive oxygen species (ROS) is one of the reasons for it. When the redox status is changed, plants can signal and modify regulatory processes, which could lead to defense responses. Several evidence points out that impaired fatty acid desaturases constitutively enhance ROS levels as well as in response to a variety of stresses. In this study, a reduction-oxidation sensitive green fluorescent (*roGFP2*) reporter gene was used to compare the overall redox status in wild-type *Arabidopsis thaliana* plants (Col-0) and a mutant line with impaired fatty acid desaturation (*fad7-1*). The goals of this study were to develop transgenic *fad7-1* line that contains *roGFP2* reporter gene, confirm the fluorescence, optimize the measurement technique and compare the overall redox status in *fad7-1* and Col-0 plants. The *roGFP2* reporter gene was successfully introduced into *fad7-1* background, and ratiometric analyses were conducted to compare the redox status by placing leaf discs in 24-well plates and measuring the fluorescence emission at 400 and 490 nm. Also, the wound response of the leaf discs were studied and no strong redox changes in response to wounding were observed. An oxidizing agent, H_2O_2, was used to confirm the reporter gene activity in the two genetic backgrounds. Immediate reductions in the ratios of 490/400 nm in both backgrounds were observed, confirming that H_2O_2 had oxidized the leaf discs. It was also established that the type of multi-well plate is important, and the black plates were more suitable than clear plates. However, the statistical interpretation of the redox ratios and total fluorescence levels obtained by the two types of plates were different;

therefore, it was not possible to conclude that *fad7-1* plants were constitutively oxidized compared to Col-0 plants.

Introduction

Reactive oxygen species (ROS) are highly reactive, oxygen containing molecules and they can play a dual role in plant stress responses by acting as signaling compounds or by causing deleterious effects on plant cells (Miller et al., 2010). In plants, ROS are generated in various sub-cellular compartments as a result of photosynthesis and other aerobic metabolism (Sharma et al., 2012; Tripathy and Oelmüller, 2012). Chloroplasts are major sources of ROS in plants, since they generate singlet oxygen ($^1O_2$) in photosystem II, and superoxide radical ($^{\bullet}O_2^-$), hydroxyl radical ($^{\bullet}OH$) and hydrogen peroxide (H_2O_2) in photosystem I (Keren et al., 1995; Apel and Hirt, 2004; Laloi et al., 2006). Cells have mechanisms to scavenge these toxic ROS by different antioxidative enzymes such as superoxide dismutase (SOD), catalase (CAT), glutathione reductase (GR), ascorbate peroxidase (APX), and non-enzymatic antioxidants such as ascorbic acids (AsA), tocopherols and phenolics (Noctor and Foyer, 1998; Dinakar et al., 2009; Sharma et al., 2012). Generally, an equilibrium is maintained between ROS and its scavengers to avoid harmful effects on the cells. Various biotic and abiotic stresses can disturb this equilibrium, and can damage the cells by causing an oxidative burst (Jambunathan, 2010; Demidchik et al., 2014; Petrov et al., 2015; Yu et al., 2017).

Several lines of evidence suggest that the impaired fatty acid desaturases constitutively enhance ROS levels as well as in response to a variety of stresses. Using a luciferase reporter gene with a singlet oxygen responsive promoter, Alnasrawi (2015) has shown that *fatty acid desaturase 7-1* (*fad7-1*) may have constitutively high levels of singlet oxygen. Lipid profiling of

spr2 mutation in tomato with impaired *fad7-1* function, and *fad3fad7fad8* triple mutant in Arabidopsis have shown that these mutants have increased levels of fatty acid hydroperoxides, which are indicators of oxidative stress, demonstrating that plants with impaired fatty acid desaturase function may accumulate high levels of ROS (unpublished data by M. Mueller and F. Goggin). In addition, it has been shown that the expression of *α-dioxygenae1* (*DOX1*) is upregulated in response to aphids (Avila et al., 2013). These studies illustrate that changes in fatty acid composition in plants influence the accumulation of ROS, which can lead to enhanced defense responses. The enhanced defense responses could in turn increase plant's resistance against stresses.

In order to maintain optimal efficiency of cellular activities, it is important that the overall reduction-oxidation (redox) processes are under control. The redox status depends on the relative balance between ROS and antioxidants. Under stress conditions, the redox status can change. The change in redox state can generate and transmit information in order to induce various regulatory responses (Scheibe and Dietz, 2012). For example, it has been shown that changes in redox status elicit retrograde signaling between the chloroplast and the nucleus (Dietz et al., 2016), which can influence the expression of defense-related genes (León et al., 2013).

It is challenging to study the ROS production because of their high reactivity and short life span. The methods that were used in the past to study the temporal nature of redox status required extraction of tissue and they were labor intensive (Hanson et al., 2004). The development of redox-sensitive reporter genes has introduced the ability to monitor the redox status *in vivo*. An example for such sensors is reduction–oxidation sensitive yellow fluorescent protein (rxYFP) and green fluorescent protein (roGFP) (Hanson et al., 2004). roGFP can be used in ratiometric assays due to having two excitation peaks at 400 and 490 nm (Dooley et al., 2004).

roGFP is created by substituting surface exposed elements with two cysteines on the GFP protein which allows the disulfide bridges to be formed between the two cysteines (Hanson et al., 2004). When oxidized, the two cysteines on the GFP protein form a disulfide bridge and increases fluorescence intensity at 400 nm, and the disulfide bridge breaks when reduced and increases fluorescence intensity at 490 nm (Bhaskar et al., 2014). Therefore, the ratio of 400/490 nm can be used to accurately measure the overall redox status.

There are different versions of roGFP. roGFP2 has an additional mutation, S65T, compared to roGFP1. This mutation causes a shift in excitation wavelengths. roGFP2 is a sensor for redox potential of glutathione. Glutathione participates in maintaining cellular redox equilibrium. The changes in the redox status is expressed in reduced glutathione (GSH) to oxidized glutathione-disulfide (GSSG) ratio (Dooley et al., 2004; Hanson et al., 2004). In the seeds we received, the *roGFP2* transgenes are under the ubiquitin promoter (Aller et al., 2013) and the roGFP2 is fused with the Glutaredoxin1 (GRX1) mediator. The GRX1 mediates the glutathione redox buffer changes by reversibly transferring electrons between GSH and roGFP2 (Meyer et al., 2007). This *roGFP2* reporter gene can be targeted to different organelles in the cells such as plastids, peroxisomes and cytoplasm to measure the redox status (Hanson et al., 2004). In this study, the overall redox status using the *roGFP2* reporter gene was used to understand how *fad7* may influence ROS.

FAD7 is a chloroplast-localized protein (Wallis and Browse, 2002; Andreu et al., 2007) and the *fad7* mutation dramatically modifies the fatty acid composition of chloroplast membranes (Li et al., 2003). The *roGFP2* reporter gene used in this study is localized in the plastids and that allowed us to study the overall redox status in chloroplasts. The plastid-*roGFP2* is referred to as *roGFP2* hereafter in this paper. The goals of this study were to generate

transgenic *fad7-1* lines containing *roGFP2* reporter gene, confirming the fluorescence in the transgenic lines, testing methods to optimize the use of multi-well plates and compare the baseline differences in overall redox status between *fad7-1 – roGFP2* and WT (Col-0 – *roGFP2*) to see if alterations in fatty acid desaturation affect the redox status. The hypothesis is that *fad7-1* plants are constitutively oxidized compared to the wild-type plants. Highly oxidized environments are a result of accumulation of ROS and reductions of reducing molecules (Ye et al., 2015). Studying the overall redox status should provide a better understanding of ROS accumulation in *fad7-1* and Col-0 plants.

Methods and materials

Plant materials and growth conditions

All the Arabidopsis seeds were surface sterilized in a sterile hood prior to plating. The seeds were rinsed with 70% ethanol for 5 minutes and the ethanol was eliminated followed by centrifugation. Then the seeds were rinsed with freshly prepared 50% bleach and 0.05% Tween 20 for 10 minutes. The seeds were then washed with autoclaved distilled water for 6 - 7 times until the bleach smell disappeared. The sterilized seeds were plated in petri dishes with 1X Murashige and Skoog (MS) media with 0.8% agar, 3% sucrose and adjusted pH of 5.5 - 5.9. The petri dishes with seeds were vernalized at 4 °C for 3 days and transferred to a growth chamber (Temp: 23 °C, RH: ~60%, light intensity: 200 µmol/m^2/sec, and 11-h/13-h light/dark photoperiod). After 2 weeks, the Arabidopsis seedlings were transplanted in a mix of peat moss, vermiculite, perlite (4:3:2 ratio) supplemented with slow release fertilizer (Osmocote Plus; 15-9-12) (Scotts-MiracleGro Company, Marysville, OH) and placed back in the growth chamber.

Plants were watered 2-3 times a week and fertilized once a week by adding MiracleGro to the water per manufacture's recommendations.

We used *A. thaliana* plants with *roGFP2* reporter gene to measure the overall redox status of *fad7-1* mutants. However, the *roGFP2* reporter gene was in Col-0 background (seeds provided by Dr. Andreas Meyer). Therefore, we introduced the *roGFP2* reporter gene into *fad7-1* to compare the overall redox status in *fad7-1* and wild-type (Col-0) plants. The generation of *fad7-1* plants with *roGFP2* reporter gene was done in the laboratory by crossing Col-0-*roGFP2* (paternal) with *fad7-1* plants that carry the mutation *glabra-1* (*gl1*) (maternal). The recessive *gl1* mutation lacks the trichome differentiation protein GL1 and the presence of one allele will cause the expression of GL1 (Marks and Feldmann, 1989). Therefore, the presence of trichomes was used as a phenotypic screening measure to identify the F1 plants containing the *roGFP2* reporter gene in *fad7-1* background. Seeds collected from F1 generation were replanted and allowed to self-pollinate in order to generate F2 and subsequent generations.

DNA extraction

One-step DNA extraction protocol developed by Kasajima et al. (2004) was used to extract DNA. The extraction buffer was prepared by diluting the Edward's solution (200 mM Tris-HCl (pH 7.5), 25 mM EDTA, 250 mM NaCl, and 0.5% SDS) (Edwards et al., 1991) with TE buffer (10 mM Tris (pH 8.0) and 1mM EDTA) by 10 folds. Three autoclaved glass beads (3 mm) were added to microcentrifuge tubes along with 3-5 mg of Arabidopsis leaf tissue and 200 µL of the extraction buffer. The leaf tissues were homogenized using Geno/Grinder® 2010 (SPEX SamplePrep, Metuchen, NJ) at 1750 rpm for 30 seconds and then stored at -20 °C.

Screening for fad7-1-roGFP2 plants

Initially, the F2 *fad7-1-roGFP2* plants were screened for fluorescence using Cytation3 Cell Imaging Multi-mode Reader (BioTek® Instruments, Inc., Winooski, VT). The plants that showed fluorescence were then screened for homozygous *fad7-1* using PCR. A total volume of 25 µL PCR reaction was prepared by adding 25 mM $MgCl_2$ (2.5 µL), 5x GoTaq Flexi buffer (5 µL), 10 µM forward and reverse primers (1 µL each), 10 mM dNTPs (0.5 µL), Taq polymerase (0.2 µL), nuclease free water (12.8 µL) and extracted DNA from leaf tissue (2 µL). Fifty plants were PCR screened for the presence of *FAD7-1* and *fad7-1* alleles using the forward primer for *AtFAD7* 5'-TTTCAGTGGGCTCGAAGTCC-3', the forward primer for *Atfad7-1* 5'-TTTCAGTGGGCTCGAAGACT-3' and the shared reverse primer 5'-ATCTGCGGGAAAAGATGATG-3'. Touch down (TD) PCR (Korbie and Mattick, 2008) was used to increase the specificity of the amplification using the following conditions for the *FAD7-1*: initial denaturation at 95 °C for 5 min; phase I = 95 °C for 45 s, 67 °C to 58 °C for 45 s, and 72 °C for 45 s (reducing 1 °C per cycle); phase II = 95 °C for 45 s, 57 °C for 45 s, and 72 °C for 45 s (20 cycles); and final extension = 72 °C for 5 min. For the *fad7-1* phase I, the temperature was reduced from 65 °C to 56 °C (1 °C per cycle) and in phase II, the 20 cycles were run at annealing temperature of 55 °C. PCR products were viewed on 1% agarose gels containing GelRed® stain (Biotium, Inc., Fremont, CA). PCR was repeated again with the plants that were positive for homozygous *fad7-1* alleles to verify that they were truly homozygous *fad7-1*. Once this was confirmed, the F3 seeds were collected.

F3 Arabidopsis plants were also tested for fluorescence using Cytation3 Cell Imaging Multi-mode Reader. Since the fluorescence was not uniform in F3 plants, PCR was done to confirm whether they carry the *roGFP2* reporter gene. DNA were extracted from six F3 *fad7-1* –

roGFP2 lineages and they were screened using PCR for the presence of *roGFP2* using the forward primer 5'-GGATCCCATGGTGAGCAAGGGCGAG-3' and the reverse primer 5'-GTCGACTTACTTGTACAGCTCGTCC-3' (Meyer et al., 2007). A total volume of 25 µL PCR reaction was prepared by adding 25 mM $MgCl_2$ (2.5 µL), 5x GoTaq Flexi buffer (5 µL), 10 µM forward and reverse primers (0.5 µL each), 10 mM dNTPs (0.5 µL), Taq polymerase (0.2 µL), nuclease free water (13.8 µL) and extracted DNA from leaf tissue (2 µL). PCR program for the *roGFP2* reporter gene is as follows: initial denaturation = 95 °C for 5 min; annealing = 95 °C for 45 s, 55 °C for 45 s, and 72 °C for 45 s; and final extension for 72 °C for 5 min. PCR products were visualized on 1% agarose gels containing GelRed® stain (Biotium, Inc., Fremont, CA). The percent fluorescence and the percent germination rates of the 6 lineages were also calculated. Once the plants with strong fluorescence and better germination rates were identified, the F4 seeds were collected. These seeds were used in subsequent experiments.

Experiment 1 – Assessing wound response and measuring redox status of fad7-1 – roGFP2 plants

F4 Arabidopsis seeds were planted according to the protocol mentioned above. The leaf position was standardized by marking the top leaf with a string when the Arabidopsis rosette had 7 leaves. The marked leaf was harvested about 3 weeks after transplanting. One leaf disc per leaf was cut using a 10 mm (diameter) cork borer. Wounding can cause an oxidative response (Savatin et al., 2014). Hence, the tissue collection by cutting a leaf disc using a cork borer can cause an oxidative response independent of any treatments applied. For that reason, previous protocols have let the collected tissue sit overnight to recover from wounding; however, that can cause the tissue to dry out and it shortens the time period over which the experiment can run. In this study, the extensiveness of wound response was determined to see whether it would skew

the results if the analysis used wounded leaf without overnight incubation. The oxidative response to wounding that occurs during tissue collection was measured in two ways. One was by taking fluorescence intensity measurements of the leaf disc, and the other was using imaging to look for effects that were limited to the edges where the wounding occurred.

The cut leaf disc was immediately added to the designated well of the clear 24-well plate (Techno Plastic Products AG, Trasadingen, Switzerland). Prior to placing the leaf disc, 200 µL of autoclaved water was added to each well to avoid desiccation of the leaf discs. Two 24-well plates were used in this experiment. Once all the leaf discs were placed, the plates were covered with lids and the fluorescence intensities of each plate were measured at 400 and 490 nm immediately. Additional measurements were taken at 30, 60 and 120 minutes after the leaf discs were cut.

Seven extra leaf discs were placed on microscope slides with cover slips and imaged using 500/542 nm and 390/542 nm filter cubes at 0, 30, 60 and 120 minutes after the leaf discs were cut to visualize if there are any wounding effects along the edges of the leaf discs. The images were processed using ImageJ software (nih.gov) by dividing the image from 500/542 nm filter by the image from 390/542 nm filter.

Experiment 2 – Measuring redox status in fad7-1 x roGFP2 using black multi-well plates and confirmation of reporter gene activity

Black 24-well plates with clear bottoms (Eppendorf AG, Hamburg, Germany) were used in this experiment instead of clear plates. Leaf discs preparation was carried out as previously described in experiment 1 using new F4 plants and the leaf discs were added to the designated well with 200 µL of autoclaved water. Three 24-well plates were used for the experiment. Once

all the leaf discs were placed, the plates were covered with lids and set aside for 60 minutes to recover from wounding. After 60 minutes, the fluorescence intensities of each plate were measured at 400 and 490 nm. Then, to study the responsiveness of the *roGFP2* reporter gene in both backgrounds, the autoclaved water was pipetted out of one plate, 150 µL of 100 mM H_2O_2 was added and fluorescence intensities at 400 and 490 nm were measured. Since H_2O_2 is an oxidizing agent, the calculated ratio of 490/400 nm is expected to decrease (Meyer et al., 2007). Fluorescence intensities were measured at 400 and 490 nm at every 10 minutes for the first 30 minutes, then every 15 minutes for a total of two hours.

Statistical analysis

Both experiment 1 and 2 were set up as Randomized Complete Block (RCB) designs. The mean differences in the ratio of 490/400 nm and total fluorescence (400 + 490 nm) of *roGFP2* in *fad7-1* and Col-0 were analyzed by one-way ANOVA and plates were considered as random blocks. All the data from experiment 1 were log transformed to meet the requirements to achieve normal distribution of the dependent variable. Repeated measures analysis of experiment 1 data was used to see if there was a wounding effect over time. All the statistical analyses were conducted with RStudio v.1.0.136 (RStudio, Inc.,).

Results

Introduction of the roGFP2 reporter gene into fad7-1 background

To obtain *fad7-1 – roGFP2* Arabidopsis plants, the *roGFP2* reporter gene that was in a Col-0 background was crossed with *fad7-1*/*gl1* Arabidopsis plants. F1 plants containing the *roGFP2* reporter gene in *fad7-1* background was identified by the presence of trichomes. All the

F1 plants (100%) had trichomes, which confirmed that they were products of cross-pollination (Figure 1).

Screening for fad7-roGFP2 plants

Eighty-five Arabidopsis plants from the F2 generation were screened for fluorescence using the GFP filter in the Cytation3 imager and 48 out of 85 F2 plants expressed fluorescence (56%). The plants that expressed fluorescence were then screened using PCR to select for homozygous *fad7-1* mutants. Initial PCR screening had identified that 11 plants were homozygous for the *FAD7-1* allele, 14 plants were homozygous for the *fad7-1* allele, and 23 plants were heterozygotes (Figure 2). However, re-testing of the *fad7-1* homozygotes had revealed that two of them are heterozygotes (Figure 3). Possibly, contamination may have caused the detection of false negatives. In addition, the crude DNA extraction may affect the efficacy, since it may not remove some PCR inhibitors. It was confirmed that 11 plants were homozygous for the *FAD7-1* allele (23%), 12 plants were homozygous for the *fad7-1* allele (25%), and 25 plants were heterozygous (52%). Seeds were collected from the F2 plants that expressed fluorescence and were homozygous for the *fad7-1* allele. Fluorescence was tested again using GFP filters in F3 plants to confirm that they have uniform fluorescence. However, most of the lineages did not show uniform fluorescence suggesting that all the F2 plants probably did not have two copies of the roGFP2 transgene. Six lineages were screened using roGFP2 primers (Figure 4). Based on the percent fluorescence and the germination rates, lineage 17 was selected for the subsequent experiments (Table 1).

Experiment 1 – Wound response and edge effects of leaf discs

The calculated ratio of 490/400 nm ($t = -1.525$, $df = 119$, $P = 0.13$) and total fluorescence ($t = -1.48$, $df = 119$, $P = 0.14$) did not significantly differ over time (Figure 5).

There was a slight edge effect that was detectable by imaging the leaf discs; but it did not influence the fluorescence measurements even at 0 minutes. This edge effect seemed to be decline quickly (Figure 6). However, as a precaution, the leaf discs were incubated for 1 hour prior to taking fluorescence measurements in subsequent experiments.

Experiment 1 – Measuring overall redox status and total fluorescence in fad7-1 and Col-0 in clear plates

The transgenic *fad7-1* containing *roGFP2* had a significantly higher ratio of 490/400 nm compared to Col-0 – *roGFP2* line at 0 min ($F = 4.33$, $df = 1, 38$, $P = 0.0442$), 30 min ($F = 11.22$, $df = 1, 38$, $P = 0.0018$), 60 min ($F = 10.46$, $df = 1, 38$, $P = 0.0026$) and 120 min ($F = 9.47$, $df = 1, 38$, $P = 0.0039$) (Figure 5A) indicating that *fad7-1* plants are constitutively reduced more than Col-0 plants. Similarly, the total fluorescence was also significantly higher in *fad7-1* than in Col-0 at 0 min ($F = 9.41$, $df = 1, 38$, $P = 0.004$), 30 min ($F = 15.48$, $df = 1, 38$, $P = 0.0003$), 60 min ($F = 15.16$, $df = 1, 38$, $P = 0.0003$) and 120 min ($F = 12.87$, $df = 1, 38$, $P = 0.0009$) (Figure 5B), which show that the *roGFP2* transgene was expressed more strongly in *fad7-1* than in Col-0. However, the total fluorescence values were low according to the technical assistance services at Biotek; therefore, possible ways of addressing these low values were investigated. It was discovered that using black plates instead of clear plates produce better readings. Therefore, subsequent experiments were designed to compare the redox status of *fad7-1* and Col-0 using black plates.

Experiment 2 – measurements of overall redox status and total fluorescence of Col-0 and fad7-1 using black plates

The baseline differences of overall redox status between Col-0 and *fad7-1* Arabidopsis plants were examined using *roGFP2* reporter gene constructs. Based on the results from the experiment 1, the tissue recovery time was reduced to 60 minutes and black plates were used instead of clear plates to improve the fluorescence values. The ratio of 490/400 nm and the total fluorescence (400 + 490 nm) was used to compare the baseline differences of leaf discs at 60 minutes after the tissue collection. There were 29 replicates for Col-0 – *roGFP2* and 27 replicates for *fad7-1 – roGFP2*. No significant difference was observed in the ratio of 490/400 nm between *fad7-1* and Col-0 (one-way ANOVA: $F = 1.92$, df = 1, 2.02, $P = 0.30$) (Figure 7A). Moreover, significant differences were not observed in total fluorescence between *fad7-1* and Col-0 (one-way ANOVA: $F = 2.04$, df = 1, 2.02, $P = 0.34$) (Figure 7B).

Experiment 2 – Reporter gene activity in response to H_2O_2 using black plates

The results showed that the 490/400 nm ratios of both Col-0 – *roGFP2* and *fad7-1 – roGFP2* dropped immediately after adding H_2O_2 (Figure 8A). Significant differences in ratio of 490/400 nm between Col-0 – *roGFP2* and *fad7-1 – roGFP2* were seen at all time points except on 60 min and 180 min. However, a significant difference in total fluorescence between Col-0 – *roGFP2* and *fad7-1 – roGFP2* was only seen at 61 min, which was immediately after adding H_2O_2 (Figure 8B). The test statistics are shown in Table 2 for both the ratio of 490/400 nm and total fluorescence.

Discussion

Generation of transgenic line and optimization of fluorescence measurement technique

To study the overall redox status in *fad7-1* plants, a transgenic *fad7-1* line that carried the *roGFP2* reporter gene was generated. This was done by crossing Arabidopsis plants (Col-0) that have *roGFP2* reporter gene with *fad7-1* Arabidopsis plants. The crossing method was used to ensure that the *roGFP2* transgene was inserted on the same location and the same number of copies of the transgene was present in both Col-0 and *fad7-1* backgrounds. A transgenic *fad7-1* – *roGFP2* line was developed after screening 3 generations for the presence of homozygous *fad7-1* allele and roGFP2 allele, and considering the uniformity of fluorescence and good seed germination rates.

As the first step of optimizing the fluorescent measurements, fluorescent readings were taken to determine if wounding affect the fluorescence. Several studies reported that wounding can increase ROS accumulation leading to a shift in plant's redox status (reviewed in Suzuki and Mittler, 2012). Leaf discs were monitored for changes over time to see whether there was a shift in redox status as the leaf discs recover. There were no differences in ratio of 490/400 nm and total fluorescence over time. In addition, the images were captured to see if there were any edge effects on the leaf discs as a result of cutting. A slight edge effect was seen soon after the leaf discs were cut, although the edge effect did not influence the fluorescence measurements. No strong wound responses were observed; therefore, the second set of experiments was initiated earlier. A shorter wait time after the tissue collection reduced aging and dehydration of the leaf discs.

However, the fluorescence intensities measured in this experiment were low, so investigated possible ways of improving the fluorescence values. In experiment 2, black plates were used for fluorescence intensity measurements and the black plates gave better values than clear plates. When using clear plates, a cross-talk between the samples can occur. This cross-talk would be lower in 24-well plates compared to 96-well plates; however, it would be better to use black plates for fluorescence measurements. Black plates absorb the scattered light and only emit wavelengths that are coming from the sample. White plates are also available on the market; however, this is not ideal for fluorescence measurements since the white plate itself can reflect fluorescence. The fluorescence intensity values from black plates were 4-fold higher than for clear plates. Due to the quality of the fluorescence readings, it was decided to use black 24-well plates in subsequent experiments.

To confirm the activity of the *roGFP2* in Col-0 and *fad7-1* backgrounds, the fluorescence intensities were measured at 400 and 490 nm to study the reporter gene's responsiveness to H_2O_2. In both backgrounds, *roGFP2* showed a fast response, which was consistent with previously published data by Meyer et al. (2007). Both *fad7-1* and Col-0 showed a rapid decrease in 490/400 nm ratio immediately after adding H_2O_2 and the plants slowly recovered to their initial redox status over time. This confirms that the crossing was done successfully and the *roGFP2* reporter gene in the *fad7-1* background responded to H_2O_2. The total fluorescence in both backgrounds reduced immediately after H_2O_2 was added. However, it recovered faster and no significant differences were seen after 70 minutes.

A transgenic *fad7-1* line of Arabidopsis with *roGFP2* was successfully generated by crossing the Col-0 – *roGFP2* Arabidopsis plants with *fad7-1/gl1* Arabidopsis plants. A significant wound response was not observed. Thus, the leaf disc incubation time was

significantly reduced. Black plates were found to be more suitable than clear plates for measuring fluorescence measurements in *fad7-1 – roGFP2* and Col-0 – *roGFP2*.

Baseline differences of redox status in fad7-1 – roGFP2 and Col-0 – roGFP2

Clear plates used in experiment 1 produced significantly greater 490/400 nm ratios in *fad7-1 – roGFP2* compared to Col-0 – *roGFP2*. This indicates that *fad7-1* plants were constitutively more reduced than Col-0 plants (Meyer et al., 2007). In addition, the total fluorescence measured in this experiment was also higher in *fad7-1* compared to Col-0. This suggests that the *roGFP2* reporter gene was strongly expressed in *fad7-1* plants. In the second experiment using black plates, no significant differences were observed in the ratio of 490/400 nm and the total fluorescence between *fad7-1 – roGFP2* and Col-0 – *roGFP2*. These results from the experiment 2 suggest that the overall redox status and the level of expression of the reporter gene do not differ between *fad7-1* and Col-0 in the absence of stress.

Since the statistical interpretation of the two experiments was inconclusive, there was no comparison made of the overall redox status between *fad7-1* and Col-0 plants with high confidence. The results could be different due to the type of plate used. As explained above, there could be fluorescence signal cross-talk between the samples in clear plates. Further experiments need to be conducted using black multi-well plates with more replicates. The redox status also depends on the amounts of both ROS and antioxidants that are present. Therefore, it is worthwhile to study the abundance of individual ROS and antioxidants in FAD7 mutants.

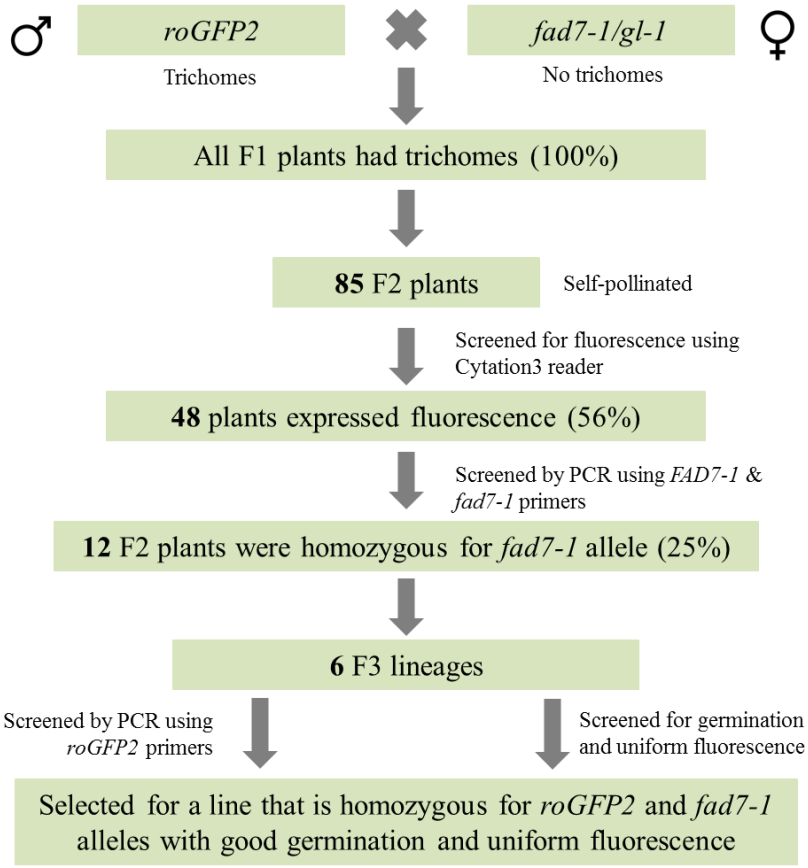

Figure 1: Selection of *fad7-1* x *roGFP2* line of Arabidopsis plants.

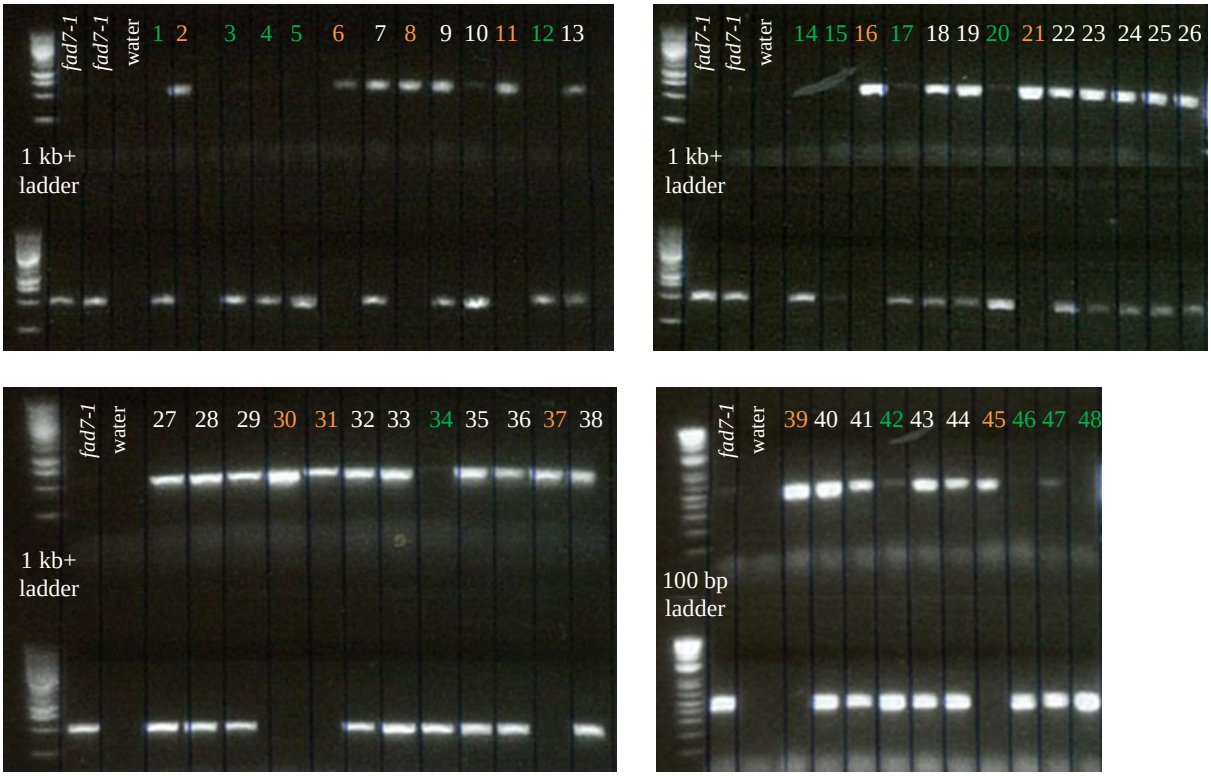

Figure 2: F2 Arabidopsis plants that expressed fluorescence were screened for the presence of the *FAD7* (top) and/or *fad7* (bottom) alleles. First round of PCR screening identified 11 plants homozygous for the *FAD7* allele (orange), 14 plants homozygous for the *fad7* allele (green), and 23 heterozygotes (white).

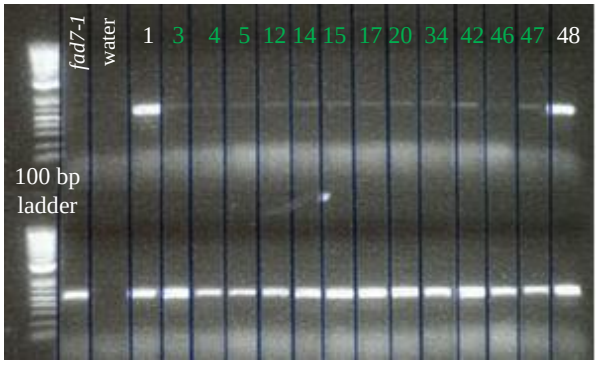

Figure 3: F2 Arabidopsis plants that were positive for *roGFP2* and homozygous for *fad7-1* were reanalyzed using PCR to verify that each was truly homozygous for PCR (Top: *FAD7* primers, bottom: *fad7* primers). Two of the plants that were homozygous according to the first PCR were found to be heterozygous. This confirmed that twelve plants were homozygous for *fad7-1*.

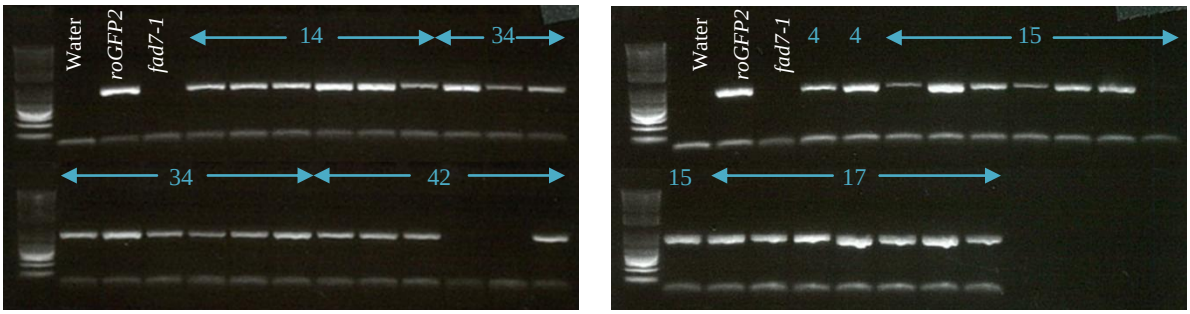

Figure 4: F3 Arabidopsis plants that expressed fluorescence were screened using *roGFP2* primers for the presence of *roGFP2* reporter gene

Table 1: Percent seed germination and percent fluorescence of different F3 lineages of *fad7-1* x *roGFP2*

F3 *fad7-1* x *roGFP2* lineage	**% germination**	**% fluorescence**
4	50	68.4
14	75	72
15	65.2	80
17	82.2	83.8
34	46.8	95
42	38	50

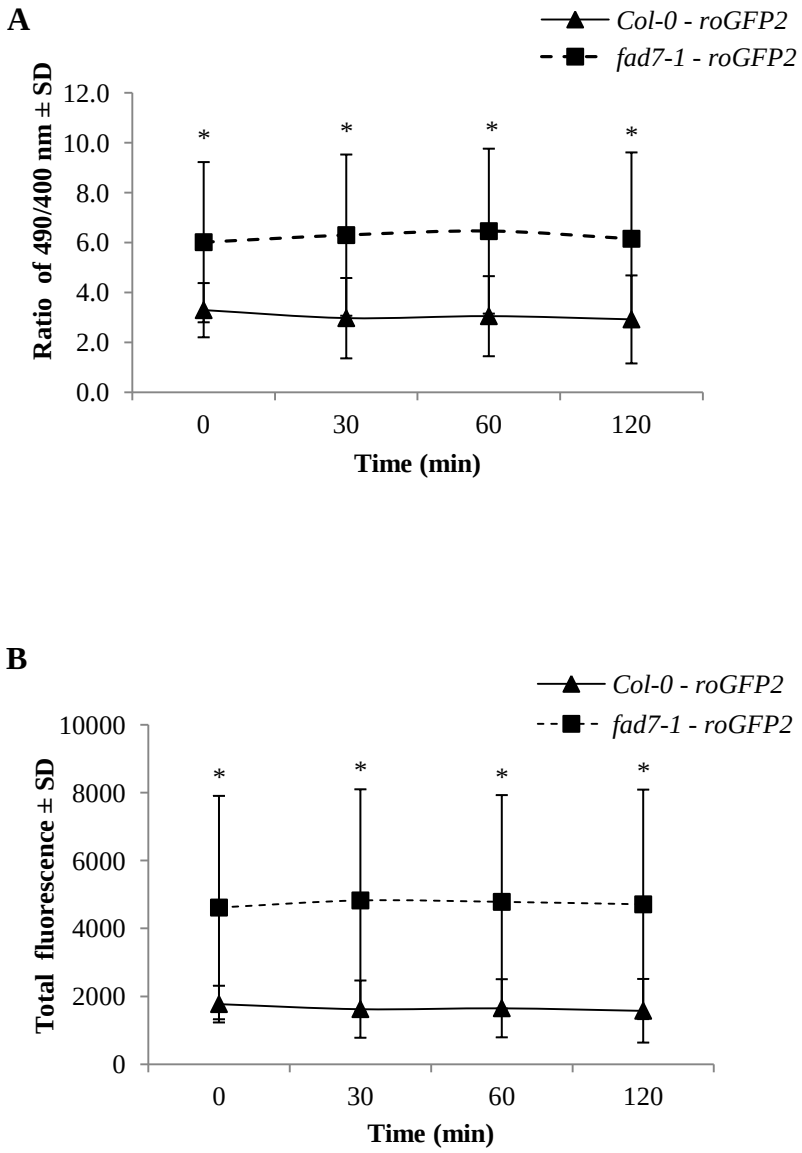

Figure 5: Fluorescent measurements from experiment 1. The ratio of 490/400 nm (A) and total fluorescence (B) were compared between *fad7-1 – roGFP2* and Col-0 – *roGFP2* Arabidopsis plants at 0, 30, 60 and 120 minutes after cutting the leaf discs. Both the ratio of 490/400 nm and total fluorescence were significantly different between *fad7-1* and Col-0 at all timepoints. Data points labeled with asterisks differed significantly between *fad7-1* and Col-0 plants. Data were analyzed by one-way ANOVA with a random block effect ($\alpha = 0.05$, $n = 20$). Error bars represent SD. In addition, both the ratio of 490/400 nm and total fluorescence did not significantly differ over time (Repeated measures analysis, $\alpha = 0.05$).

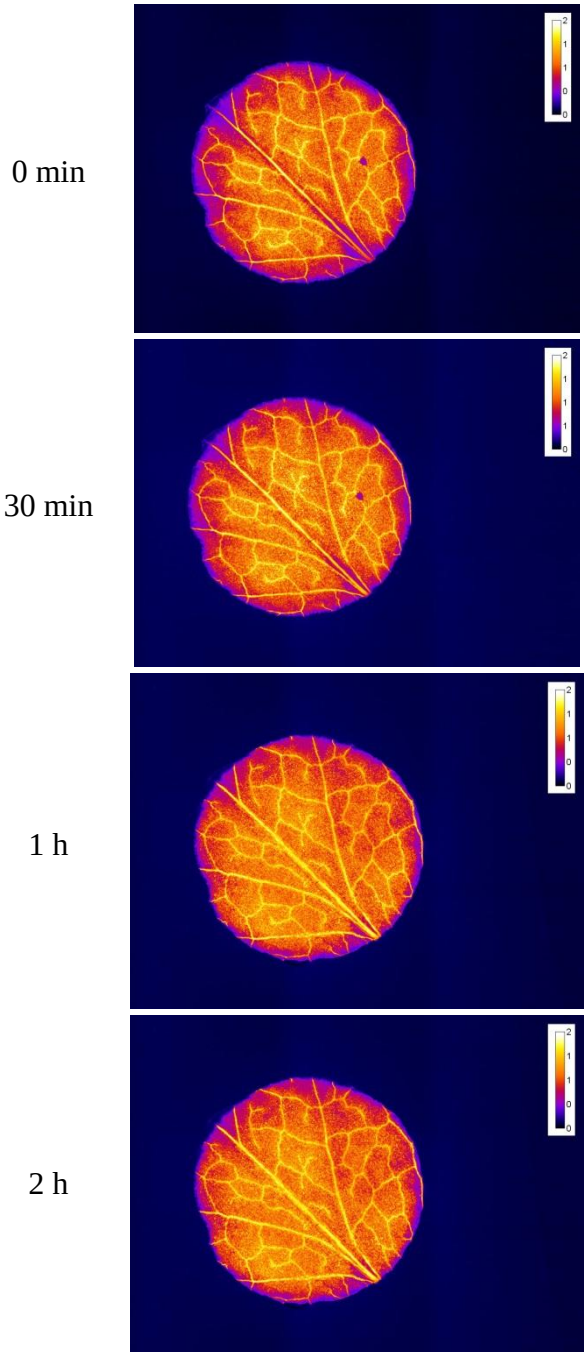

Figure 6: Ratiometric images (500/390 nm) of leaf discs of *fad7-1 – roGFP2* Arabidopsis plants showing minimal edge effects. Images were shown for a representative set of samples and six additional replicates show the same trend.

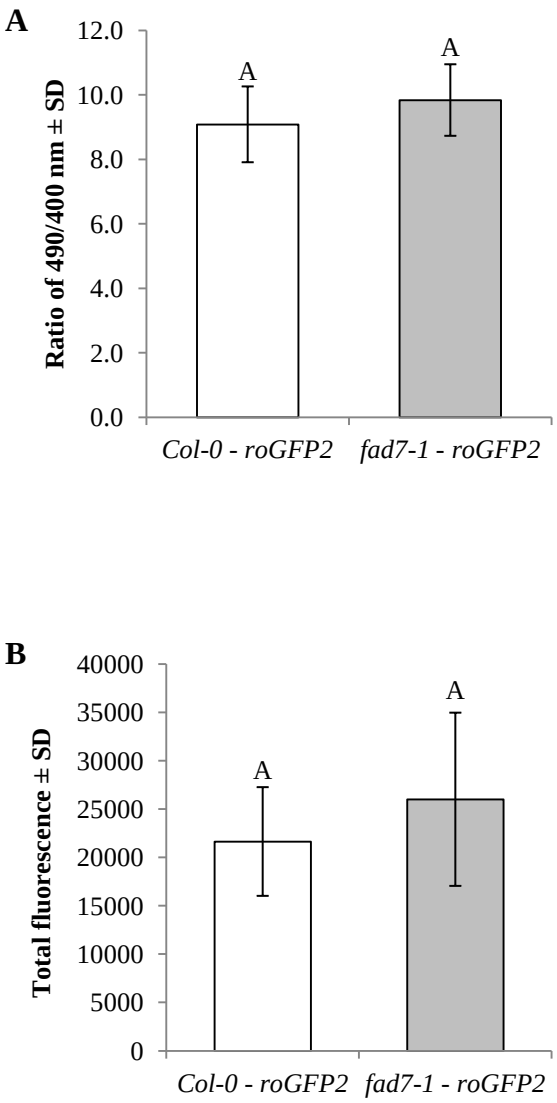

Figure 7: Comparison of basal differences in redox status in Experiment 2 using black 24-well plates. The ratio of 490/400 nm (A) and the total fluorescence (B) of *fad7-1* and Col-0 Arabidopsis plants containing *roGFP2* were compared in 60 minutes after the leaves were cut. Data were analyzed by one-way ANOVA with a random block factor (plate). Error bars represent SD. Marked pairwise comparisons denote significant differences according to paired t-tests at $\alpha = 0.05$, $n = 30$.

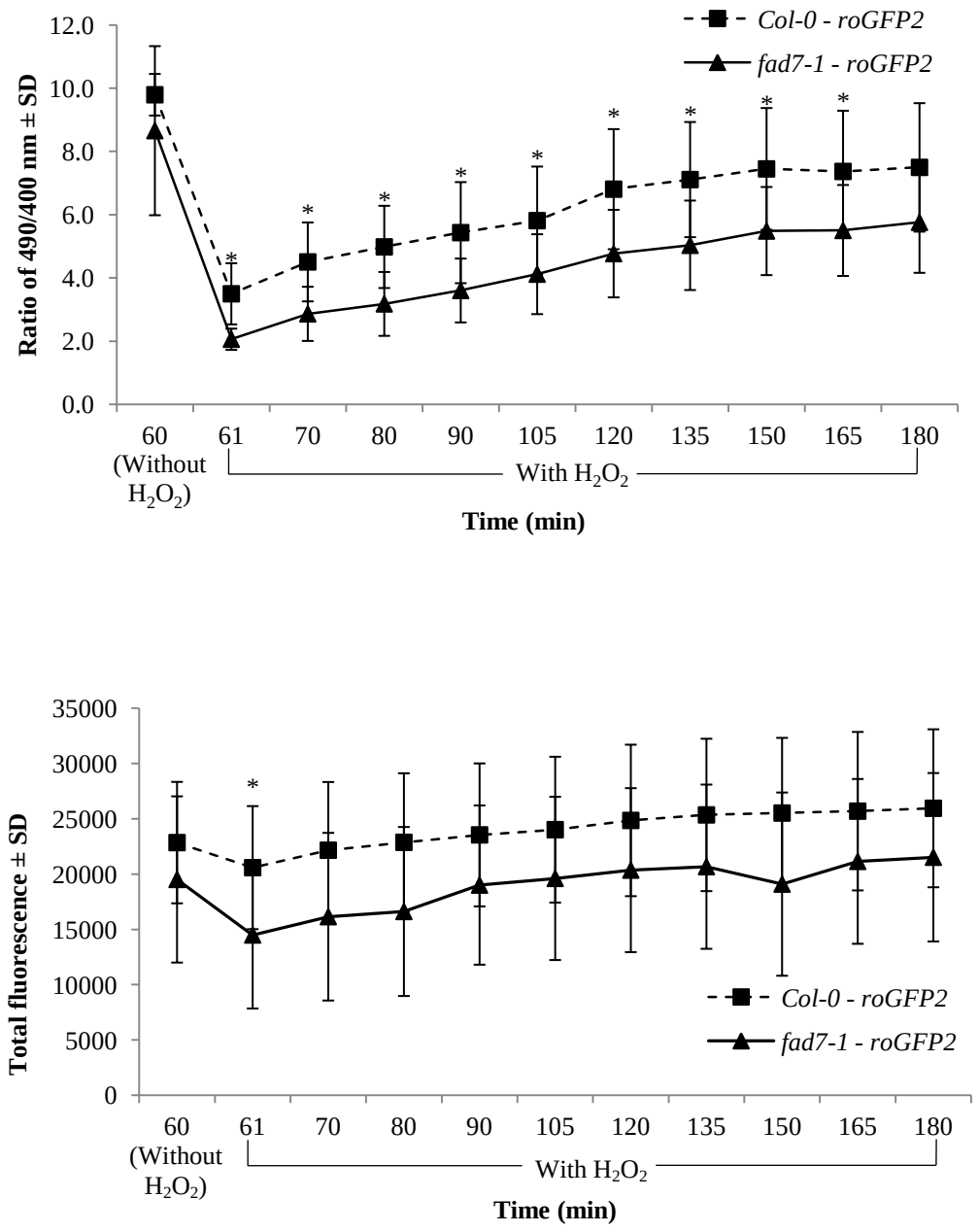

Figure 8: Redox responses to H_2O_2 in the chloroplast of Arabidopsis plants. The asterisks denote significant differences of either the ratio of 490/400 nm (A) or the total fluorescence (B) at each individual time points. Error bars represent SD.

Table 2: Test statistics of ratio of 490/400 nm and total fluorescence in response to H_2O_2 in black plates

Time (min)	**Ratio of 490/400 nm**			**Total fluorescence**		
	t - value	**df**	***P* - value**	**t - value**	**df**	***P* - value**
60	-1.24	16	0.23	-1.07	16	0.30
61	-4.21	16	0.0006	-2.11	16	0.05
70	-3.26	16	0.005	-1.84	16	0.08
80	-3.29	16	0.005	-1.90	16	0.07
90	-2.90	16	0.01	-1.41	16	0.18
105	-2.39	16	0.03	-1.34	16	0.20
120	-2.60	16	0.02	-1.34	16	0.20
135	-2.70	16	0.02	-1.39	16	0.19
150	-2.48	16	0.02	-1.80	16	0.09
165	-2.33	16	0.03	-1.32	16	0.21
180	-2.02	16	0.06	-1.27	16	0.22

References

Aller I, Rouhier N, Meyer AJ (2013) Development of roGFP2-derived redox probes for measurement of the glutathione redox potential in the cytosol of severely glutathione-deficient *rml1* seedlings. Front Plant Sci. doi: 10.3389/fpls.2013.00506

Alnasrawi AM (2015) Optimizing a luciferase-based tool for studying the effects of *fatty acid desaturase7* on singlet oxygen accumulation in *Arabidopsis thaliana*. Theses and Dissertations. 1319. http://scholarworks.uark.edu/etd/1319

Andreu V, Collados R, Testillano PS, Risueño M del C, Picorel R, Alfonso M (2007) In Situ molecular identification of the plastid ω3 Fatty Acid Desaturase FAD7 from soybean: evidence of thylakoid membrane localization. Plant Physiol **145**: 1336–1344

Apel K, Hirt H (2004) Reactive oxygen species: Metabolism, oxidative stress, and signal transduction. Annu Rev of Plant Biol **55**: 373–399

Avila CA, Arevalo-Soliz LM, Lorence A, Goggin FL (2013) Expression of α-*DIOXYGENASE 1* in tomato and Arabidopsis contributes to plant defenses against aphids. Mol Plant Microbe Interact **26**: 977–986

Bhaskar A, Chawla M, Mehta M, Parikh P, Chandra P, Bhave D, Kumar D, Carroll KS, Singh A (2014) Reengineering redox sensitive GFP to measure mycothiol redox potential of *Mycobacterium tuberculosis* during infection. PLOS Pathog **10**: e1003902

Demidchik V, Straltsova D, Medvedev SS, Pozhvanov GA, Sokolik A, Yurin V (2014) Stress-induced electrolyte leakage: the role of K+-permeable channels and involvement in programmed cell death and metabolic adjustment. J Exp Bot **65**: 1259–1270

Dietz K-J, Turkan I, Krieger-Liszkay A (2016) Redox- and reactive oxygen species-dependent signaling into and out of the photosynthesizing chloroplast. Plant Physiol **171**: 1541–1550

Dinakar C, Abhaypratap V, Yearla SR, Raghavendra AS, Padmasree K (2009) Importance of ROS and antioxidant system during the beneficial interactions of mitochondrial metabolism with photosynthetic carbon assimilation. Planta **231**: 461

Dooley CT, Dore TM, Hanson GT, Jackson WC, Remington SJ, Tsien RY (2004) Imaging dynamic redox changes in mammalian cells with green fluorescent protein indicators. J Biol Chem **279**: 22284–22293

Edwards K, Johnstone C, Thompson C (1991) A simple and rapid method for the preparation of plant genomic DNA for PCR analysis. Nucleic Acids Res **19**: 1349

Hanson GT, Aggeler R, Oglesbee D, Cannon M, Capaldi RA, Tsien RY, Remington SJ (2004) Investigating mitochondrial redox potential with redox-sensitive green fluorescent protein indicators. J Biol Chem **279**: 13044–13053

Jambunathan N (2010) Determination and detection of reactive oxygen species (ROS), lipid peroxidation, and electrolyte leakage in plants. Methods Mol Biol **639**: 292–298

Kasajima I, Ide Y, Ohkama-Ohtsu N, Hayashi H, Yoneyama T, Fujiwara T (2004) A protocol for rapid DNA extraction from *Arabidopsis thaliana* for PCR analysis. Plant Mol Biol Rep **22**: 49–52

Keren N, Gong H, Ohad I (1995) Oscillations of reaction center II-D1 protein degradation in vivo induced by repetitive light flashes. Correlation between the level of RCII-QB- and protein degradation in low light. J Biol Chem **270**: 806–814

Korbie DJ, Mattick JS (2008) Touchdown PCR for increased specificity and sensitivity in PCR amplification. Nat Protoc **3**: 1452–1456

Laloi C, Przybyla D, Apel K (2006) A genetic approach towards elucidating the biological activity of different reactive oxygen species in *Arabidopsis thaliana*. J Exp Bot **57**: 1719–1724

León P, Gregorio J, Cordoba E (2013) ABI4 and its role in chloroplast retrograde communication. Front Plant Sci. doi: 10.3389/fpls.2012.00304

Li C, Liu G, Xu C, Lee GI, Bauer P, Ling H-Q, Ganal MW, Howe GA (2003) The tomato *suppressor of prosystemin-mediated responses2* gene encodes a fatty acid desaturase required for the biosynthesis of jasmonic acid and the production of a systemic wound signal for defense gene expression. Plant Cell **15**: 1646–1661

Marks MD, Feldmann KA (1989) Trichome development in *Arabidopsis thaliana*. I. T-DNA tagging of the *GLABROUS1* gene. The Plant Cell **1**: 1043–1050

Meyer AJ, Brach T, Marty L, Kreye S, Rouhier N, Jacquot J-P, Hell R (2007) Redox-sensitive GFP in *Arabidopsis thaliana* is a quantitative biosensor for the redox potential of the cellular glutathione redox buffer. Plant J **52**: 973–986

Miller G, Suzuki N, Ciftci-Yilmaz S, Mittler R (2010) Reactive oxygen species homeostasis and signalling during drought and salinity stresses. Plant Cell Environ **33**: 453–467

Noctor G, Foyer CH (1998) Ascorbate and glutathione: keeping active oxygen under control. Annu Rev Plant Physiol Plant Mol Biol **49**: 249–279

Petrov V, Hille J, Mueller-Roeber B, Gechev TS (2015) ROS-mediated abiotic stress-induced programmed cell death in plants. Front Plant Sci. doi: 10.3389/fpls.2015.00069

Savatin DV, Gramegna G, Modesti V, Cervone F (2014) Wounding in the plant tissue: the defense of a dangerous passage. Front Plant Sci. doi: 10.3389/fpls.2014.00470

Scheibe R, Dietz K-J (2012) Reduction-oxidation network for flexible adjustment of cellular metabolism in photoautotrophic cells. Plant Cell Environ **35**: 202–216

Sharma P, Jha AB, Dubey RS, Pessarakli M (2012) Reactive oxygen species, oxidative damage, and antioxidative defense mechanism in plants under stressful conditions. J Botany doi: 10.1155/2012/217037

Suzuki N, Mittler R (2012) Reactive oxygen species-dependent wound responses in animals and plants. Free Radic Biol Med **53**: 2269–2276

Tripathy BC, Oelmüller R (2012) Reactive oxygen species generation and signaling in plants. Plant Signal Behav **7**: 1621–1633

Wallis JG, Browse J (2002) Mutants of Arabidopsis reveal many roles for membrane lipids. Prog Lipid Res **41**: 254–278

Ye Z-W, Zhang J, Townsend DM, Tew KD (2015) Oxidative stress, redox regulation and diseases of cellular differentiation. Biochim Biophys Acta **1850**: 1607–1621

Yu S-X, Feng Q-N, Xie H-T, Li S, Zhang Y (2017) Reactive oxygen species mediate tapetal programmed cell death in tobacco and tomato. BMC Plant Biol **17**: 76

Chapter V

Conclusion

Fatty Acid Desaturase7 (FAD7) is a chloroplast-localized enzyme that converts 16 and 18 carbon dienoic (two double bonds) fatty acids to trienoic (three double bonds) fatty acids. The loss of function of FAD7 in tomato (*Solanum lycopersicum*) and Arabidopsis (*Arabidopsis thaliana*) showed enhanced resistance against aphids. The FAD7 mutants used in this study are the *suppressor of prosystemin-mediated response2* (*spr2*) mutant in tomato and the *fad7-1* mutant in Arabidopsis.

Preliminary data from our laboratory suggested the genes that are associated with photosynthesis were upregulated constitutively between *spr2* and wild-type (WT) (cv. Castlemart). Also, the fatty acid hydroperoxide profiles suggested higher levels of singlet oxygen – a type of reactive oxygen species (ROS) – accumulation in *spr2* plants compared to WT plants. Therefore, to identify the factors that determine aphid resistance in FAD7 mutants, we studied 1) the effects of loss of function of FAD7 on photosynthesis of tomato in the presence and absence of potato aphids (*Macrosiphum euphorbiae*) using the *spr2* mutant; 2) the effects of *spr2* on primary metabolites; and 3) the effects of overall change in redox status in chloroplasts using *fad7-1* mutant in Arabidopsis. The results showed that *spr2* plants have enhanced carbon assimilation rates, enhanced efficiencies of light-dependent and light-independent reactions in the absence of aphids. These results showed that the enhanced overall photosynthesis in *spr2* as measured by carbon assimilation is due to enhanced efficiencies in both light-dependent and light-independent reactions. Although we observed differences in photosynthetic activity, we did not detect differences in the intermediates of the Calvin cycle, TCA cycle and glycolysis, and the end products of photosynthesis between *spr2* and WT. However, we saw more growth in *spr2*

plants compared to WT, which would suggest the enhanced photosynthesis in *spr2* plants could be transferred to growth. In addition, the abundance of glutamate was significantly greater in *spr2* than in WT plants. The increased glutamate concentration could be important in defense against aphids (Chen et al., 1997). Exogenous application of glutamate induces defense and knockout of receptors compromise resistance to more than one pest (Kan et al., 2017; Toyota et al., 2018).

We also studied whether the *spr2* mutant can maintain the enhanced photosynthetic efficiencies under potato aphid pressure. In both aphid-infested plants and uninfested controls, the efficiency of light-dependent reactions was enhanced in *spr2* plants compared to WT plants. Aphid infestation did not significantly affect the maximum efficiency of photosystem II, indicating the aphid densities used here did not have deleterious effects on photosynthesis. One day after infestation, infested plants showed significantly greater fraction of light that is directed towards photochemistry and significantly lower fraction of light that is emitted as heat, suggesting that aphid infestation triggered a short-term compensatory increase in photochemical quenching. This suggests the *spr2* plants may have enhanced overall photosynthetic efficiency in response to aphids. The increase in photosynthesis may be involved in mechanisms of defense in *spr2* plants.

Next, we studied the overall change in redox status in chloroplasts using *fad7-1* Arabidopsis plants with chloroplast-localized *roGFP2* reporter gene, which is sensitive to redox changes. When the redox status is changed, plants can signal and modify regulatory processes, which could lead to defense responses. We successfully developed a tool to measure the redox status in chloroplasts by introducing the *roGFP2* transgene into *fad7-1* background and optimize the redox status measuring technique to detect the changes in redox status in chloroplasts.

However, the statistical differences were inconclusive between multiple experiments of redox status comparisons using *fad7-1 – roGFP2* and Col-0 – *roGFP2* lines. Therefore, further experiments needs to be continued to confirm the redox status of chloroplasts in FAD7 mutants.

The enhanced photosynthesis could also be channeling energy towards secondary metabolism to produce more defensive chemicals, which could contribute to aphid resistance in *spr2* plants. Also, it is important to look at individual ROS in FAD7 mutants. So far, we have the Hyper reporter gene in *fad7-1* background, which can be used to estimate the levels of H_2O_2 in FAD7 mutants and WT plants. The redox status depends on the relative balance between ROS and antioxidants. The FAD7 mutants could potentially have more ROS, but at the same time, they could have more antioxidants. This could be a reason why one of the experiments suggested similar redox status in *fad7-1* and WT plants. Previous studies showed that *spr2* plants contain high levels of vitamin C (an antioxidant) compared to WT (Suza et al., 2010). Therefore, it would be useful to look at other antioxidants as well to study how they would contribute to the overall redox status in FAD7 mutants. In addition, the glutamate levels in *spr2* plants need further investigation, since it could be important in plant defense signaling and aphid resistance.

The *spr2* mutants also display some characteristics of tolerant plants such as enhanced photosynthetic rates and increased vegetative growth (Strauss and Agrawal, 1999; Koch et al., 2016). Tolerant plants have the ability to minimize the negative fitness effects caused by biotic and abiotic stresses. Further studies are needed to confirm the tolerance of *spr2* mutants with different densities of aphids and timings of infestations to see how these different factors affect plant fitness.

References

Chen JQ, Rahbé Y, Delobel B, Sauvion N, Guillaud J, Febvay G (1997) Melon resistance to the aphid *Aphis gossypii*: behavioural analysis and chemical correlations with nitrogenous compounds. Entomologia Experimentalis et Applicata **85**: 33–44

Kan C-C, Chung T-Y, Wu H-Y, Juo Y-A, Hsieh M-H (2017) Exogenous glutamate rapidly induces the expression of genes involved in metabolism and defense responses in rice roots. BMC Genomics. doi: 10.1186/s12864-017-3588-7

Koch KG, Chapman K, Louis J, Heng-Moss T, Sarath G (2016) Plant tolerance: A unique approach to control hemipteran pests. Front Plant Sci. doi: 10.3389/fpls.2016.01363

Strauss S, Agrawal AA (1999) The ecology and evolution of plant tolerance to herbivory. Trends Ecol Evol (Amst) **14**: 179–185

Suza WP, Avila CA, Carruthers K, Kulkarni S, Goggin FL, Lorence A (2010) Exploring the impact of wounding and jasmonates on ascorbate metabolism. Plant Physiology and Biochemistry **48**: 337–350

Toyota M, Spencer D, Sawai-Toyota S, Jiaqi W, Zhang T, Koo AJ, Howe GA, Gilroy S (2018) Glutamate triggers long-distance, calcium-based plant defense signaling. Science **361**: 1112–1115